KLF2's role in T cell trafficking and retention in lymphoid and non-lymphoid tissues

A Dissertation
SUBMITTED TO THE FACULTY OF
UNIVERSITY OF MINNESOTA
BY

Cara Noelle Skon

IN PARTIAL FULFILLMENT OF THE REQUIREMENTS
FOR THE DEGREE OF
DOCTOR OF PHILOSOPHY

Advisor: Stephen C. Jameson, PhD

July 2013

Acknowledgements

The work presented in this thesis would not have been possible without the support of my mentor Stephen Jameson. His guidance, clever wit, and sincere support for me as an individual has strengthened my abilities as a scientist. Together with Kris Hogquist, our lab meetings were always filled with insightful comments and discussion.

I would also like to acknowledge the Jamequist lab members that made the last five years enjoyable and fun. I started off with the KLF2 club: Geoff Hart, Ken Takada, and Mike Weinreich. Since then, I've not only had people to discuss science with, but also made true friendships. June-Yong Lee was my partner in crime for the last two years, providing enthusiasm and molecular expertise for this project. Past member Amy Moran always had an insightful science tidbit to offer. Janelle Olson was always supportive and encouraging, both in and outside the lab. Gretta Stritesky and Keli Holzapfel kept me laughing, bay two style. Sara Hamilton's scientific and physical strength was inspiring. Ross Fulton's publication quality figures in lab meeting and ability to stay up on literature always made me jealous. Sam Dunmire and Dare Odumade continually reminded me of the importance of human research. Yan Xing helped me with immunohistochemistry and Yu Jung Lee showed me there are limitless staining panels to try. Jie Ding and Steve P put up with my convoluted mouse typing. I will greatly miss this group of well-balanced people that do great science.

I would like to thank my above average classmates Kristin Anderson, Casey Katerdahl, Kristen Pauken, Jeff Hall, Luke Brand, Ryan Flynn, and Adam Spaulding for helping me through qualifying exams and MICaB seminars. I am amazed at how talented

and dedicated you guys are. Special thanks to Kristin Anderson for anti-CD8 protocol optimization and being my parabiosis buddy.

My thesis committee members Marc Jenkins, Dave Masopust, Chris Pennell and Matt Mescher provided critical support and feedback for keeping this project on track. With their expertise of Immunology and insightfulness, this project was broadened and enriched into its final form. Louise Shand was a godsend, always knowing what to do in any administrative predicament I found myself in. Annette Bethke helped with all my other administrative needs and Paul Champoux made my life easier by staying on top of our flow cytometry core facility.

And lastly, I would like to acknowledge my family for supporting me through this process. From hiking trips to family dinners, they have reminded me what is important in life. Bike rides with my dad and Suzanne and trips to the cabin with my mom and Brady were greatly cherished and much needed through these years of research. Conversations and excursions with my brother's Nathan and Ben reminded me of the importance of adventures and living life to the max. I am blessed to have such an amazing family to live life with. I would not have been able to accomplish this without your love and support.

Dedication

This thesis is dedicated to my mother, Barbara Lea. You have always believed in me and empowered me to follow my dreams. I am inspired by your ability to grow, question, and let life change you. Thank you for being my rock.

Abstract

The transcription factor Kruppel-like Factor 2 (KLF2) is essential for naïve T cell trafficking, yet its significance in memory T cells is unclear. This thesis investigates the significance of KLF2 expression in CD4+ and CD8+ memory T cells. Using eGFP-KLF2 reporter mice, we identified KLF2 heterogeneity in the memory phase of an immune response. In chapter one, we distinguished KLF2 expression in subsets of CD8+ memory T cells. Resident memory T cells (T_{RM}) were shown to down-regulate KLF2 in the parenchyma of non-lymphoid tissue. Using parabiosis, we identified rare circulating CD8+ memory T cells in the parenchyma of non-lymphoid tissue that have intermediate KLF2 expression. In chapter two, we investigate the relevance of the KLF2 downregulation in CD8+ T_{RM} by forcing a target of KLF2, sphingosine 1 phosphate receptor 1 (S1PR1), using retroviral transduction. We went on to show that KLF2 can be downregulated by inflammatory cytokines via the P13K/AKT pathway independent of antigen exposure. Lastly, chapter four focuses on KLF2 heterogeneity in CD4+ memory T cells showing that $KLF2^{LO}$ cells had diminished lymph node egress. In summary, this work defines KLF2 heterogeneity in memory T cells as being significant for discerning whether a cell is retained in a particular tissue or continues to traffic throughout an organism.

Table of Contents

	Page Number(s)
Acknowledgements	i-ii
Dedication	iii
Abstract	iv
List of Figures	vi-vii
Chapter 1: Introduction	1-21
Chapter 2: KLF2 and memory CD8+ T cells: KLF2's expression in lymphoid versus non- lymphoid tissue	22-51
Chapter 3: Transcriptional downregulation of S1PR1 is required for establishment of resident memory CD8+ T cells	52-90
Chapter 4: KLF2 and CD4+ T cells: Heterogeneity within lymphoid tissue effecting retention of CD4+ T cell subsets	91-130
Chapter 5: Discussion	131-138
Bibliography	139-146

List of Figures

Page Number

1-1. Lymph node architecture with trafficking molecules 9

1-2. Diagram of antigen-specific T cells after infection 13

1-3. KLF2 expression over time in T cells 18

1-4. Molecular regulation of KLF2 20

2-1. KLF2 expression in CD8+ T cells lymphoid vs non-lymphoid tissue 27

2-2. KLF2 downregulation correlates with decrease in KLF2's targets 30

2-3. KLF2 is downregulated during establishment of CD8+ T_{RM} 32

2-4. Few memory T cells migrate into NLT after parabiosis 34

2-5. Distinct $KLF2^{GFP}$ in re-circulating CD8+ memory T cells in NLT 36

2-6. Two populations arise from circulating CD8+ memory T cells in NLT 37

S2-1. CD69 vs KLF2 in parenchymal CD8+ T cells in NLT 41

S2-2. Kinetics of KLF2 downregulation in lymphoid/non-lymphoid tissue 43

S2.3. Distinct $KLF2^{GFP}$ in re-circulating CD8+ memory T cells in NLT 45

3-1. Characterization of S1PR1 retroviral transduction system 57

3-2. Forced S1PR1 does not alter proliferation in vitro 58

3-3. Forced S1PR1 prevents establishment of T_{RM} 60

3-4. Forced S1PR1 prevents early establishment of T_{RM} in NLT parenchyma 62

3-5. There is no skewing toward CD103 in S1PR1-transduced P14 in NLT 63

3-6. S1PR1-transduced effector P14 into uninfected hosts also prevents T_{RM} 65

3-7. $KLF2^{LO}$ phenotype of T_{RM} does not correlate with TCR engagement 67

3-8. Diverse cytokines induce KLF2 downregulation in CD8+ T cells *in vitro* 69

3-9. Cytokine-induced downregulation of KLF2 is dependent on P13K/AKT 71

3-10. P13K/AKT does not affect CD103 upregulation 72

3-11. Cytokine-induced downregulation of KLF2 transcriptionally is relevant 73

3-12. *In vivo* P13K inhibitor affects KLF2 and # of T_{RM} in NLT 75

3-13. Foxo1 is reduced in CD8+ T cells in non-lymphoid vs lymphoid tissue 76

3-14. Model of KLF2 downregulation in T_{RM} in NLT 77

4-1. KLF2 Heterogeneity in CD4+ memory T splenocytes 97

4-2. $KLF2^{LO}$ CD4+ memory T cells are not found in the blood 98

4-3. Decreased KLF2 is transcriptionally relevant in CD4+ memory T cells 100

4-4. KLF2 status is not transient when cultured *in vitro* 102

4-5. Unlike KLF2, CD69 levels drop to baseline after sorting 103

4-6. KLF2 status is also not transient *in vivo* 105

4-7. TLR agonists negatively affect KLF2 levels 107

4-8. IFNα/β decreases KLF2 independent of T cell responsiveness to it 108

4-9. Germ-free mice have similar percentages of CD69+ memory T cells 110

4-10. Sorted $KLF2^{LO}$ CD4+ T cells have diminished cytokine production 112

4-11. Anergic CD4+ memory-phenotype T cells are $KLF2^{LO}$ 113

4-12. Germinal center T follicular helper cells are $KLF2^{LO}$ 115

4-13. Germinal center T follicular help cells have low KLF2 transcripts 116

4-14. $KLF2^{LO}$ CD4+ memory-phenotype T cells are not egressing 118

Chapter 1

Introduction

The mammalian immune system is an intricate, complex matrix of intertwined responses to attacks from outside and within the body. It needs to be able to distinguish between self and non-self, from things that are harmful (ex. influenza) from things that are not (ex. food). It always has to be poised and ready to respond, but needs to be able to determine when a response is appropriate.

The mammalian immune system is broadly broken down into specific and non-specific responses. Non-specific responses, or innate immunity, is an evolutionarily ancient defense mechanism shared from plants to humans to distinguish self from non-self[1]. The innate immune system uses a variety of tactics to dissuade pathogens from infecting the host from barriers (skin being the most prominent in humans) and mucosal surfaces to the recognition of broad pathogen associated molecular patterns (PAMPs)[2]. PAMPs are conserved repetitive germ-line encoded molecules that are present in the majority of microbial components but not in host cells, giving the host the ability to distinguish self from non-self[3]. PAMPs are recognized by pattern recognition receptors (PRRs) found on and within innate immune cells which detect microbes[3]. When a PRR recognizes a microbial component, it triggers a cell signaling cascade leading to the activation of the NFκB pathway and production of inflammatory cytokines, predominantly IFNγ and TNFα, that activate other immune cells[3, 4]. Innate immune cells are poised to receive "danger signals" that cause them to become activated and respond. Since the innate immune system does not rely on clonal expansion of antigen-specific lymphocytes (described in detail below and referred to as a "specific" response), the innate immune response is rapid, being able to detect and eliminate pathogens within

minutes to hours of infection[1]. Most pathogens have one or more of the signature molecules that these receptors recognize, hence the majority of pathogen invasions can be dealt with by the innate immune system.

However, some pathogens cannot be controlled by the non-specific innate immune response. When this is the case, the adaptive immune response is initiated with help from essential signals delivered by the innate immune response[2]. The strength of the adaptive immune response is its antigen-specificity. While the adaptive immune response is slower to be mounted than the rapid innate immune response, its activation results in memory cells that provide long-lasting immunity from subsequent infections with the same microorganism, and is more extensively defined below. While the adaptive immune response is typically effective at clearing pathogens, it is also responsible for allergies, autoimmunity, and rejection of tissue grafts[1, 5]. Therefore, understanding how the adaptive immune system functions is significant to the development of therapeutics as well as vaccines.

Adaptive Immune Response

The adaptive immune system is composed of two classes of cells referred to as lymphocytes: B cells which make up the antibody-mediated immune response and T cells which comprise the cell-mediated immune response. One of the biggest differences between the innate and adaptive immune response is antigen-specificity. An antigen is defined as any substance that can be recognized and responded to by the adaptive immune response[1], and can vary from a pathogen to a sliver. Any one lymphocyte has the

ability to sensitively and specifically recognize only one antigen, referred to as a cell's cognate antigen, which leads to cellular activation and eventual removal of that specific antigen[1]. This specificity is the fundamental basis of the adaptive immune system, providing the ability to respond selectively to only one particular antigen. When a lymphocyte encounters its cognate antigen, the cell is able to become activated, proliferate and subsequently exert its effector functions[6, 7]. Proliferation of a lymphocyte leads to a clonal population of cells that all recognize the same antigen, providing a robust specific response that can eliminate an invading pathogen without, theoretically, harming the organism itself.

Lymphocytes are able to recognize antigen by receptors found on the surface of their cells. For B cells, the B cell receptor (BCR) recognizes intact cognate antigen that when encountered leads to the differentiation of B cells into plasma cells and memory B cells[8]. The specificity of a B cell is determined by the antigen binding site of the BCR and is randomly generated during the development of a B cell which accounts for the extensive diversity in antigens the B cells recognize[9]. Plasma cells produce antibodies that diffuse throughout the body and recognize the same cognate antigen of their B cell predecessor due to clonal expansion, leading to the eventual removal of the antigen by various mechanisms[10]. Since this thesis is focused on T lymphocytes, the remaining introduction will focus specifically on this cell type.

T cells, on the other hand, do not recognize intact antigen but instead bind to processed antigen in the form of small peptides that are "presented" to the T cell by an antigen presenting cell, or APC, in a process known as antigen presentation[11]. In every

cell, proteins are continually being synthesized and broken down. These fragmented proteins or peptides are loaded onto major histocompatibility complexes (MHC) and shuttled to the surface of the cell[12]. In this way, the peptide:MHC complexes on the surface of a cell display what is being produced and existing within a cell. When an APC engulfs or is infected by a pathogen, the pathogen gets processed into peptides inside the cell and presented on an MHC which can then be recognized by T cells. Like BCRs on B cells, T cell receptors (TCRs) are generated by the random rearrangement of gene segments that encode components of the TCR creating substantial diversity to identify almost any potential pathogen[13].

There are two different types of T cells: CD4+ helper T cells and CD8+ cytolytic T cells which recognize different types of MHCs. CD8+ T cells recognize MHC class I while CD4+ helper T cells recognize processed peptides in the context of MHC class II. All nucleated cells have MHC I but only a subset of cells, considered professional APCs, have MHC II[1]. Processed peptides that originate from engulfed or exogneous proteins are loaded onto MHC II[14]. In this way, CD4+ T cells recognize peptide:MHC II complexes from extracellular pathogens (mostly bacteria) that are phagocytosed. This is significant because as "helper" cells, one function of CD4+ T cells is to provide cytokines to activating B cells that recognize the same cognate antigen (albeit in a different form)[15].

MHC class I, on the other hand, load peptides that are derived from degraded proteins and intracellular pathogens (predominantly viruses) found in the cytosol of a cell[16]. This form of peptide: MHC I antigen presentation is recognized by CD8+ T cells which upon activation are able to directly kill infected cells by recognizing the same

peptide:MHC I complexes that initially activated the CD8+ T cell. Therefore, CD8+ T cells are known as "cytolytic" upon activation and are equipped to directly kill infected cells where as CD4+ "helper" T cells produce cytokines that help activate other cell types that eventually control an infection[17].

However, for lymphocytes to become fully activated they need to receive 3 signals[18]. The first is TCR recognition of a specific cognate antigen peptide: MHC complex on an APC as described above. The second signal is co-stimulation and is provided by co-stimulatory molecules (predominantly CD80/CD86) that become upregulated on professional APCs in the context of an infection[19, 20]. Professional APCs (dendritic cells, macrophages, and B cells) are able to express co-stimulatory molecules whose expression is triggered by cytokines produced by the innate immune system and recognized by CD28 on the T cell[21]. In this way, the adaptive immune system is only activated if the innate system has independently identified PAMPs or another danger signal and alerted the rest of the immune system through the production of inflammatory cytokines, predominantly IFNγ and TNFα[2]. The third signal leading to T cell activation are various cytokines needed for optimal differentiation and proliferation of lymphocytes[22]. When all three signals are present, a T cell becomes fully activated and is able to differentiate into an effector T cell that is capable of contributing to the elimination of an invading pathogen.

The intricately coordinated system to activate lymphocytes is crucial to the success of an immune system. Detection of all 3 signals ensures that the organism is necessarily responding to a threat and not accidentally responding to an unharmful

stimuli. Independent pathogen detection from both the innate and adaptive immune system safeguards the immune response from inappropriate activation. Tightly regulated immune responses are essential because erroneous or excessively robust activation of the adaptive immune response can have disastrous affects, leading to immunopathology[23].

Naïve T cell trafficking

Due to the exquisite specificity of T cells, any one pathogen may only have a few thousand T cells within the human body that are able to precisely recognize a processed component of the pathogen[24, 25]. Due to the shear size of a human, this provides an extremely challenging dilemma for the immune system to adequately protect the entire organism from potential pathogens.

The immune system deals with this issue by having an intricate network that channels both invading pathogens that enter peripheral organs and immune cells to the same location, called lymph nodes. Instead of having naïve T cells (T cells that have yet to encounter their cognate antigen) patrol the entire body, cells can simply migrate through a chain of lymph nodes strategically placed throughout the body. At the same time, the lymphatic system pumps interstitial fluid (the fluid that baths all peripheral organs) or lymph from peripheral organs to its draining lymph node[26]. In this way, naïve T cells are able to get exposure to most antigens that have entered the organism by circulating throughout lymph nodes and the spleen (another organ of the lymphoid system) instead of the entire body. This architectural structure is also significant for allowing T cells to come into contact with APCs, which also drain from peripheral tissues

through the lymph[27]. This is an essential step in activating adaptive cell-mediated immunity since T cells themselves cannot recognize whole pathogens, they need APCs to process antigens in the form of peptide:MHC complexes as described above before becoming activated.

Seminal work by Gowans in the 1950-1960's discovered that lymphocytes continuously re-circulate through blood, secondary-lymphoid organs (spleen and lymph nodes), and blood[28]. Lymphocytes can enter lymph nodes from the blood by migrating through high endothelial venules (HEVs) that dissect lymph nodes (Fig 1-1). HEVs are specialized post-capillary venules that contain sialyl lewis X oligosaccharides[29] on proteins collectively referred to as peripheral node addressins (PNAd). PNAds interact with L-selectin (CD62L) found on naïve T cells causing T cells to roll along HEVs[30]. CD62L-/- mice experience impaired primary T cell responses to infection primarily due to the inability to home to and be activated in lymph nodes[31, 32]. This rolling caused by CD62L is followed by subsequent tethering of naïve T cells to the HEV wall by T cell surface expression of the chemokine receptor CCR7 binding to its ligand CCL19/21 produced by endothelial cells of the HEV[33]. Binding causes a conformational change of the integrin LFA-1 found on the T cell which enables it to be able to interact with its ligand ICAM-1 on the HEV leading to T cell arrest and extravasation into the lymph node[34]. For the mesenteric lymph node and Peyer's patches, the secondary lymphoid organs of the small intestine, $\alpha 4\beta 7$ integrin on a T cell recognizes MAdCAM-1 leading to similar extravasation[35]. This process of rolling, tethering, and diapedisis allows T cells that express L-selection and CCR7 to migrate into lymph nodes via the HEVs.

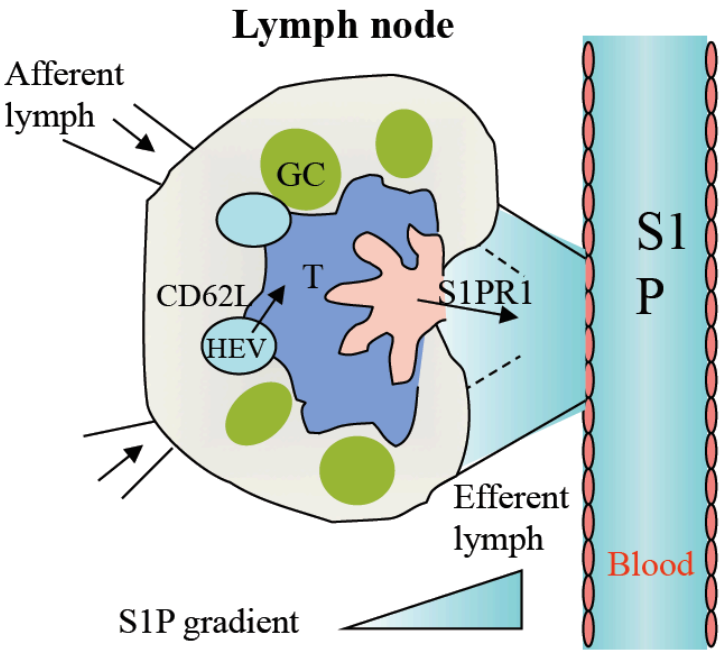

Figure 1-1. Lymph node architecture with trafficking molecules. CD62L+ T cells enter lymph nodes through high endothelial venules (HEVs) and migrate to the T cell zone (blue). Sphingosine 1-phosphate (S1P, gradient shown from white to aqua) is found in higher concentrations in the lymph and blood, allowing S1PR1+ T cells to leave the - lymph node via the efferent lymphatics.

Once a T cell enters a lymph node, it is drawn to a particular region of the node referred to as the T cell zone due to the concentrated presence of the chemokines CCL19/21, ligands for the chemokine receptor CCR7 found on naïve T cells. The architecture of the lymph node is distinguished by different zones containing condensed populations of specific lymphocytes[36]. This density of particular cell types aids in the efficiency of lymphocyte scanning. Within the T cell zone, naïve T cells are able to interact with dendritic cells and scan for their cognate antigen being presented on MHCs. If a naïve T cell encounters its specific cognate antigen on an APC, it ceases movement and starts to become activated, a process that is detailed below. However, if it does not

encounter it's cognate antigen, it is then able to exit the lymph node if it expresses another receptor called sphingosine 1 phosphate receptor 1, or S1PR1.

S1PR1 recognizes its ligand sphingosine phosphate or S1P found in high concentrations in the blood and lymph[37-39]. A naïve T cell is able to leave a lymph node by responding to the higher gradient of S1PR1 in efferent lymphatic vessels (Fig 1-1). Inhibiting S1PR1 function with the agonist FTY720 or disrupting the S1P gradient results in T cell sequestration in lymph nodes but not spleen[40-42]. In this way, naïve T cells enter lymph nodes via HEVs using L-selectin and integrins and eventually leave lymph nodes by S1PR1.

Besides the HEVs, T cells can also access the lymph node through the afferent lymphatic vessels. Lymph nodes are connected to each other via the lymphatic system with the efferent lymphatic vessel of one lymph node becoming the afferent lymphatic vessel of another lymph node[43]. This chain of lymph nodes eventually circulates T cells back to the blood via the thoradic duct and heart. Depending on which lymph node a T cell is leaving, it may migrate into the afferent lymphatic vessel of another lymph node before making it to the thoradic duct and back to the blood. A recent study showed that T cells directly injected into the afferent lymphatics of the popliteal lymph node are able to traffic to the T cell zone of the node[44]. This migration was partially dependent on the chemokine receptor CCR7, similar to studies showing the necessity of T cell's having CCR7 when migrating out of peripheral tissue and into the afferent lymphatics[45, 46].

T**rafficking after activation and memory T cell generation**

Naïve T cells migrate throughout the body by circulating between the lymphatic and cardiovascular system, patrolling lymph nodes and the spleen for their cognate antigen. During an infection, TNF and other inflammatory signals driven by the innate immune system increase the likelihood of a rare antigen-specific naïve T cell encountering its cognate antigen through increased blood flow and more promiscuous rules for lymph node entrance[47]. Lymph node homing rules undergo dynamic changes in the context of inflammation that increase the degree of interaction between naïve T cells and APCs, aiding in the activation of the adaptive immune response[47, 48].

Once encountering its cognate antigen presented on an MHC molecule in the context of co-stimulation and cytokines, a T cell becomes fully activated and differentiates into an effector T cell. In the process, activating antigen-specific T cells multiply exponentially producing a clonal army of T cells specific to the invading pathogen (Fig 1-22). This antigen-specific effector T cell population is then able to patrol the periphery of the organism to search for and fight off the specific pathogen that caused its activation. For CD8+ cytolytic T cells, this predominantly entails coming into contact with and killing infected cells displaying the antigen for which the CD8+ effector T cell is specific[1]. For CD4+ helper T cells, the extent of effector functions ranges significantly depending on the cytokines (signal 3 of the 3 signals of T cell activation) a CD4+ T cell is exposed to during activation, allowing them to help an array of immune cells during an infection[17].

After activation, an effector T cell changes the homing receptors present on the surface of the cell which in turn affects the cells trafficking patterns, allowing T cells to localize to the area of infection. L-selectin and CCR7, the molecules important for allowing T cells to enter lymph nodes, are predominantly downregulated while other homing molecules are upregulated that help effector T cells get into non-lymphoid organs. Depending on the location of T cell activation, different homing receptors are upregulated that aid that particular effector T cell in getting back to the site of activation, which is often near the site of initial infection[49]. For example, T cells activated in gastrointestinal associated lymphoid tissue (GALT) upregulate the receptors $\alpha 4\beta 7$ and CCR9, important molecules for allowing cells to home back to the small intestine[34, 50]. Likewise, T cells activated in skin lymphoid tissue upregulate E and P selectin as well as CCR4 or CCR10 which guide them back to the skin[51]. These altered homing molecules dissuade T cells from trafficking through lymph nodes and instead orchestrate movement of T cells to inflamed tissues. Altered trafficking is significant for allowing effector T cells to get to the site of infection to control and eliminate the pathogen since T cells, unlike the B cells whose antibodies can diffuse through the body with B cells trafficking to those locations, need to come in close proximity to their targets.

The clonal expansion of antigen-specific T cells is followed by clonal contraction leaving only a small population of T cells (roughly 5-10% of the peak) that survive and form the memory T cell pool (Fig 1-2). This population of memory T cells has been shown to more robustly and rapidly respond (both in terms of proliferation and effector cytokine production) to a subsequent infection with the same antigen, causing the same

pathogen to be controlled more quickly than the first exposure, often before the infected individual even experiences symptoms of being infected[1]. As such, the focus of vaccination is the generation of memory T cells without a full-blown infection, protecting an individual from a subsequent encounters with the same pathogen[52].

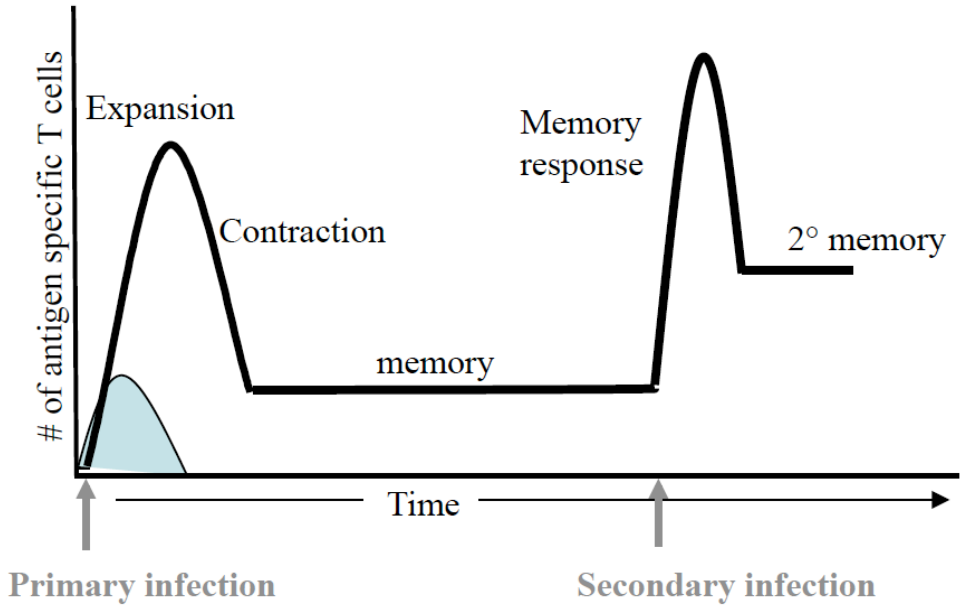

Figure 1-2. Diagram of antigen-specific T cells after primary and secondary infection. After primary infection, naïve antigen-specific T cells clonally expand to help eliminate the pathogen (blue). After pathogen clearance, the number of antigen-specific T cells contract to approximately 5-10% of the expansion peak, forming the memory pool. Upon secondary infection, memory T cells respond more rapidly and robustly.

Memory T cells that survive the contraction following the effector phase of the immune response are thought to have distinct recirculation pathways from naïve T cells[53]. Memory T cells, unlike naïve T cells, have more broad anatomical distribution[54, 55]. While naïve T cells are confined to migration through secondary lymphoid organs, memory T cells also have the capacity to enter non-lymphoid tissue. Using parabiotic mice and adoptive transfer of memory T cells, Klonowski et al. originally showed that

memory T cells are able to relocate to lymphoid and non-lymphoid tissue, although migration into the intestinal lamina propria and brain was less prominent[56]. Extensive heterogeneity in memory T cell phenotype and function have been documented[57-62], some of which has been associated with anatomical location[63].

One classic subsetting of memory T cells is based on CD62L and CCR7 expression[57]. $CD62L^{lo}$/ $CCR7^{lo}$ memory T cells (T_{EM}) are described as being more "effector"-like with rapid cytokine production or cytolytic activity after stimulation and expression of receptors that are involved in migration to inflamed tissues. On the other hand, $CD62L^{hi}$/ $CCR7^{hi}$ "central" memory cells (T_{CM}) have more proliferative capacity yet lack immediate effector function[57]. Because T_{CM} express lymph node homing receptors while T_{EM} lack these receptors, it is thought that the T_{CM} migrate similar to naïve T cells while T_{EM} migrate to non-lymphoid tissue. While attempting to clarify two different subsets within the memory compartment is informative, some have proposed that this subsetting is too simplistic and that there is actually extensive heterogeneity within the memory T cell compartment[64]. Several categories based on distinct migratory and functional characteristics have been proposed[58, 65]. A more recent subset of memory T cells are defined by a lack of circulation, instead establishing residency in non-lymphoid tissue, referred to as resident memory T cells or T_{RM} [66]. T_{RM} have been identified in the brain, skin, intestines, salivary glands and female reproductive tract[67-73].

The trafficking potential of a cell is important to the T cell's ability to contribute to the immune response to an infection[31]. A naive Ag-specific T cell needs to be able to encounter its ligand in the context of an MHC molecule to become activated. Trafficking

after activation is governed by chemokine receptors and integrins that allow T cells to access inflamed tissues and contribute to fighting off a pathogen at the site of infection. Likewise, memory T cells need to be poised in the right location to effectively control a subsequent infection from the same pathogen. In each of these stages, the trafficking pattern of a T cell is a governing factor in determining the ability of that cell to eventually control an infection. Unlike B cells that produce antibodies that can infiltrate the entire body, a CD8+ T cell needs to actually come into contact with an infected cell to be able to exert its effector function. Likewise, a CD4+ T cell needs to be in close proximity to other lymphocytes for help to be effective. Therefore, understanding the trafficking patterns of T cells is a significant component of that cell's potential to contribute to the response to subsequent infections.

Kruppel-like Factor 2

The Kruppel-like factor (KLF) family of transcription factors, including more than 15 members, are defined by having 3 zinc fingers at their carboxyl terminus that bind to GC-rich DNA sequences allowing them to exert their transcriptional regulation[74]. Kruppel-like Factor 2 (KLF2, previously known as Lung Kruppel-like Factor, LKLF) was originally isolated in 1995 using the zinc finger domain of KLF1 (erythroid kruppel-like factor)[75]. KLF2 has since been shown to be involved in vascular development and as a result KLF2 knock-out mice are embryonic lethal[74, 76]. KLF2's association with lymphocytes was discovered in 1997 by Kuo and colleagues screening for homology to KLF1, a transcription factor involved in regulating erythroid development[76]. They

reported expression of KLF2 predominantly in the lung, B cells, and single positive T cells. To circumvent the embryonic lethality of KLF2, Kuo et al used chimeric mice ($KLF2^{-/-}$ embryonic stem cells injected into blastocytes from $rag2^{-/-}$ mice) and observed a defect in peripheral T cells[76]. The few T cells in the periphery had an "activated" phenotype appearing $CD44^{hi}$, $CD69^{hi}$, $CD62L^{lo}$, and $FasL^{hi}$ suggesting that increased apoptosis is responsible for the defect in peripheral T cells. The authors concluded that KLF2 was involved in T cell quiescence as well as survival.

However, since this seminal paper was published extensive work has further dissected the role of KLF2 in lymphocytes. Our group reported in 2006 that the peripheral defect observed in chimeric $KLF2^{-/-}$ mice is not due to apoptosis, but a trafficking defect resulting in lymphocyte retention in the thymus[77]. Using fetal liver chimeras, we showed $KLF2^{-/-}$ T cells had less expression of critical trafficking molecules L-selectin (CD62L), S1PR1, and CCR7 and demonstrated that KLF2 directly binds to the promoter of SIPR1[77]. Because S1PR1 has been shown to be essential for thymic egress[39, 78], this explained the retention of thymocytes in $KLF2^{-/-}$ chimeric mice.

Indeed, KLF2's role in T cell trafficking was confirmed in 2007 when Bai et al reported that KLF2 directly activated the promoter of CD62L and S1PR1[79]. As outlined above, these key trafficking molecules allow lymphocytes to enter and subsequently exit lymph nodes. For this reason, KLF2 can be considered a regulator of naïve T cell circulation, allowing naïve T cells to circulate throughout lymph nodes and back into the blood.

A cell's ability to traffic throughout lymphoid tissues is critical to an immune response. The lymphoid tissue provide an environment whereby extremely rare ag-specific naïve T cells can encounter their cognate antigen and subsequently fight off an infection. As described above, trafficking after infection is mainly initiated by inflammation and chemokine receptors. An intriguing role for KLF2 was proposed by Sebzda et al in 2008 suggesting that KLF2 regulates naïve T cell migration by also restricting chemokine receptor expression patterns[80]. However, extensive follow-up work has refuted this hypothesis using careful exclusion of gamma-delta T cells and the use of a CD4 conditional KLF2 knock-out instead of a vav-cre model[81]. The importance of KLF2 expression on memory T cell trafficking has yet to be definitively addressed.

KLF2 has been associated with T cell quiescence since the original Kuo et al paper in 1997 that identified KLF2-/- cells as "activated" due to CD44 and CD69 expression on the few T cells found in the periphery[76]. Further research on Jurkat T cells showed that forced expression of KLF2 inhibited leukemia cell growth through the upregulation of the kinase inhibitor p21[82] and potentially decreased expression of c-Myc[83]. While forced KLF2 halted the autonomous proliferation of cancer cells, more recent studies provide evidence that KLF2 deletion does not cause proliferation defects in activated T lymphocytes, yet does result in a trafficking defect[84]. Therefore, physiological KLF2 expression appears significant for normal T cell migration, but less relevant for T cell quiescence[84].

During an infection, KLF2 expression is altered in antigen-specific T cells[76, 85, 86]. KLF2 expression has been shown to be high in naïve T cells, yet protein as well as

mRNA levels of KLF2 are drastically down-regulated after T cell activation[76, 77]. Exposing activated T cells to IL-7, IL-15, or low doses of IL-2 resulted in re-expression of KLF2 after activation while IL-12, IL-4, and high doses of IL-2 inhibited this re-expression[79, 85]. At the same time, studies have shown that bulk antigen-specific memory T cells appear KLF2^{hi} [85, 86]. Therefore, KLF2 is expressed in naïve T cells, down-regulated in activated T cells, and re-expressed in the memory T cell phase of an immune response (Fig 1-3).

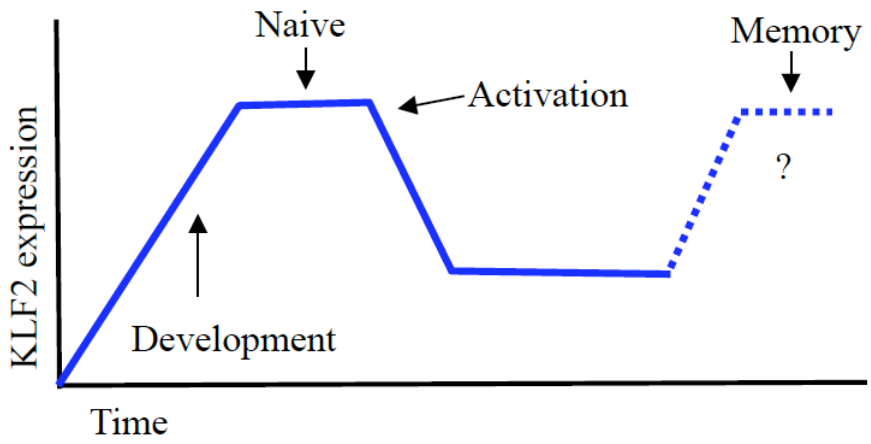

Figure 1-3. KLF2 expression over time in T cells. Developing T cells start to express KLF2 in the thymus and naïve T cells universally express KLF2. Early after activation, KLF2 is rapidly downregulated while bulk memory T cells have been shown to re-express the transcription factor.

Yet what causes KLF2 expression to vary? While the complete molecular regulation of KLF2 expression has yet to be elucidated, the role of TCR engagement and cytokine exposure is informative. In 2003 our group explored IL-7's role in KLF2 expression and showed that while IL-7 does induce expression of KLF2 after activation, it is not needed to maintain KLF2 expression in naïve T cells[87]. This suggests that KLF2 expression is regulated by a distinct mechanism in naïve versus activated T cells. An

informative paper by Sinclair et al. highlighted P13K and mTOR's role in regulation of KLF2 and SIPR1 mRNA[88]. They showed that antigen-primed CD8+ T cells exposed to high doses of IL-2 have sustained P13K signaling while exposure to IL-15 lead to low P13K signaling and KLF2 expression. This helped solidify the role of the cytokine milieu in KLF2 expression by functioning through the mTOR/PI3K signaling pathway.

In 2009, KLF2 expression was directly linked to a forkhead box transcription factor Foxo1[89]. Foxo1 is a transcription factor that is active in the nucleus during cell starvation/oxidative stress yet is de-activated in a P13K dependent manner in response to growth factors[90]. Kerdiles et al removed Foxo1 using the $Foxo1^{fl/fl}$ CD4cre system and showed a reduction in CD62L, CCR7, KLF2, and IL-7R, with direct evidence of Foxo1 binding the IL-7r promoter[89]. Further research has shown that Foxo1 directly binds to the promoter of KLF2 in human T cells[91]. Therefore, the current model for the molecular mechanism of KLF2 expression is that when mTOR signaling is initiated, via P13K pathway, Foxo1 is suppressed which in turn decreases KLF2, IL-7R, and potentially CCR7 (Fig 1-4). When Foxo1 is not translocated to the cytoplasm, predominantly when the cell is not exposed to growth conditions or proliferating, its nuclear presence causes the expression of KLF2 and IL-7R leading to the common quiescent phenotype of naïve and memory T cells.

This is in line with KLF2's downregulation during activation, a time during increased proliferation and metabolism. While KLF2's expression has been extensively characterized early after viral activation, the expression in memory T cells has been difficult to detect due to the absence of an effective anti-KLF2 antibody. While research

has shown that both the RNA[86] and protein level[85] of KLF2 has returned to naïve levels at memory phase after an infection, both these techniques required cellular lysis resulting in the inability of analyzing KLF2 expression on a per cell basis. Therefore, whether heterogeneity in KLF2 expression exists in memory T cell subsets was unknown. Addressing the potential heterogeneity of KLF2 expression at memory time points could strengthen in our understanding of T cell trafficking and function after infection.

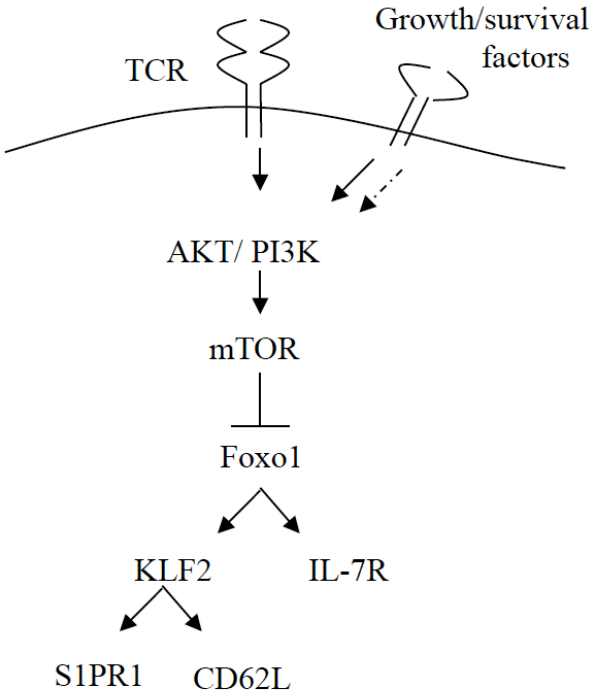

Figure 1-4. Molecular regulation of KLF2. KLF2 is regulated by the transcription factor Foxo1, which is de-activated by activity of the P13K/AKT pathway through mTOR. TCR stimulation as well as growth and survival factors have been shown to affect this pathway and thus KLF2.

KLF2 has been shown to be important for naïve T cell trafficking[77]. Its effect on memory T cell trafficking and retention have not been extensively addressed and is the central focus of this thesis.

Statement of thesis

This thesis investigates the expression of the transcription factor KLF2 in CD4+ and CD8+ T cells after activation. Our goal was to identify whether heterogeneity in KLF2 expression exists within these populations, and if so, determine whether KLF2 heterogeneity observed in memory T cell populations was functionally significant for localization of memory T cells. From previous research on KLF2 expression in lymphoid tissue[77], we hypothesized that T cells with low KLF2 expression would be retained in tissues due to the lack of trafficking molecules controlled by KLF2. Memory T cell subsets have been defined with restricted trafficking, including CD8+ resident memory T cells and CD4+ T follicular helper cells, that have also been identified as having distinct functional capabilities compared to other T cell subsets. Since T cells need to come into close proximity to their targets to be able to exert their effector functions, understanding the factors contributing to memory T cell trafficking and retention is an important component of the potential of a memory T cell. We sought to determine whether KLF2 expression is significant for the trafficking potential of an activated T cell.

We hypothesized that KLF2 would be differentially expressed in memory T cell subsets and this difference would be functionally relevant for the cells' trafficking ability and ultimate function.

Chapter 2

KLF2 and memory CD8+ T cells: KLF2's expression in lymphoid versus non-lymphoid tissue

Memory T cells, unlike naïve T cells, have the capacity to traffic and be retained in non-lymphoid tissue. The transcription factor kruppel-like factor 2 (KLF2) regulates trafficking molecules, including sphingosine 1 phosphate receptor 1 (S1PR1) and CD62L, that allow naive T cells to circulate throughout lymphoid tissues, yet its significance in memory T cells has not been extensively addressed. Using eGFP-KLF2 reporter mice, we report that almost all CD8+ memory T cells are $KLF2^{HI}$ in lymphoid tissue and blood. KLF2 expression did not directly correlate with central and effector subsets based on CD62L expression. However, we demonstrate that the vast majority of CD8+ memory T cells in the parenchyma of non-lymphoid tissues (including small intestine, salivary glands, kidney and brain) are low for KLF2 transcript and protein, as well as KLF2's targets S1PR1 and CD62L. Using parabiosis after LCMV infection, we show that the few memory CD8+ T cells that traffic into non-lymphoid tissues at a memory time point show intermediate expression for both KLF2 and CD69. Our results suggest that activated and memory CD8+ T cells enter non-lymphoid tissue expressing KLF2 and downregulate the protein after entrance as part of the profile for becoming T_{RM}.

Introduction

After activation, CD8+ T cells leave lymphoid tissue as effector cells and patrol the periphery looking for infected cells. As suggested by their name, cytolytic CD8+ T cells are able to directly kill infected cells through the perforin-mediated pathway[92]. In order to exert this effector function, the CD8+ T cell needs to come in direct contact with an infected cell. Therefore, understanding how CD8+ T cells get to inflamed sites and what factors are involved with retaining cells there once they have migrated is significant for understanding the potential a CD8+ T cell has in contributing to future immune responses to the same pathogen.

As mentioned in chapter one, one way of identifying memory T cell populations is based on CD62L expression[57]. CD62L- effector memory T cells (T_{EM}) lack access to lymph nodes through HEVs and instead are thought to patrol non-lymphoid tissue. CD62L+ central memory T cells (T_{CM}) have similar trafficking molecules as naïve T cells and are thought to remain circulating through lymphoid tissue. This way of categorizing memory T cells based on migratory patterns is particularly helpful as more diversification of memory T cell subsets become established[63].

Resident memory T cells (T_{RM}) are another recently defined population of memory T cells that reside in non-lymphoid tissue instead of continually circulating throughout the organism. Having already been defined in the brain, salivary glands, gut, skin and female reproductive tract[67-73], one universal marker of T_{RM} is CD69 expression. Often considered a marker of early activation, recent studies have shown that CD69 can also be upregulated *in vitro* by exposure to inflammatory cytokines independent of the

presence of antigen[93]. Another marker that has been identified on T_{RM} in some tissues is CD103 or αEβ7, a molecule that has been shown to aid in T_{RM} retention in the small intestine[93].

Kruppel-like factor 2 (KLF2) is a transcription factor that has been shown to bind to and activate the promoters of both L-selectin and S1PR1[77, 79]. Since L-selectin is important for lymph node access as well as being an important marker for distinguishing T_{CM} and T_{EM} populations, investigating the expression of KLF2 in these subsets seemed relevant. While research has shown that KLF2 is expressed in memory T cells[85, 86], expression of KLF2 on a per cell basis has not been documented, excluding the ability to distinguish heterogeneity within the memory T cell pool.

Addressing heterogeneity in KLF2 expression in memory T cells could shed led on the trafficking potential of CD8+ memory T cell populations. We sought to determine the KLF2 status of CD8+ memory T cell populations to elucidate whether KLF2 expression could be significant for identifying trafficking patterns of CD8+ memory T cells. Using eGFP-KLF2 reporter mice, we show that KLF2 downregulation marks T_{RM} cells in non-lymphoid tissue, while circulating CD8+ memory T cells have high expression of the transcription factor. While not directly correlating with T_{CM} and T_{EM} subsets, KLF2 expression identified rare antigen-specific T_{EM} circulating through the parenchyma of non-lymphoid tissue during the memory phase of an immune response.

Results

KLF2 is downregulated in CD8+ T cells found in non-lymphoid tissues

While KLF2 is expressed in bulk naïve and memory CD8+ T cell populations, it is unclear whether distinct memory subsets differ in KLF2 expression levels. To test this, we utilized mice in which GFP was knocked into the endogenous *Klf2* gene, creating a functional eGFP-KLF2 fusion protein ($KLF2^{GFP}$) as a reporter for KLF2 expression. The vast majority of memory-phenotype ($CD44^{HI}$) CD8+ T cells in the steady state isolated from the spleen of a $KLF2^{GFP}$ reporter mouse exhibited a $KLF2^{HI}$ phenotype (Fig 2-1a). All CD62L+ CD8+ T cells (central memory T cells) had high expression of KLF2 consistent with published studies showing that KLF2 controls the promoter of CD62L[79], yet the majority of CD62L- CD8+ T cells (effector memory T cells) also expressed KLF2. This suggests that KLF2 expression is necessary but not sufficient for CD62L expression and also shows that KLF2 expression does not differentiate central vs effector CD8+ memory T cells.

Similar with memory-phenotype CD8+ T cells, both antigen-specific polyclonal (Db/gp33 tetramer+) and monoclonal (P14 TCR transgenic) memory CD8+ T cells in lymphoid tissue >30 days after LCMV infection had high expression of KLF2 (Fig 2-1b). However, memory CD8+ T cells found in both the lamina propria and intraepithelium of the small intestine (SI) had very low expression of the transcription factor.

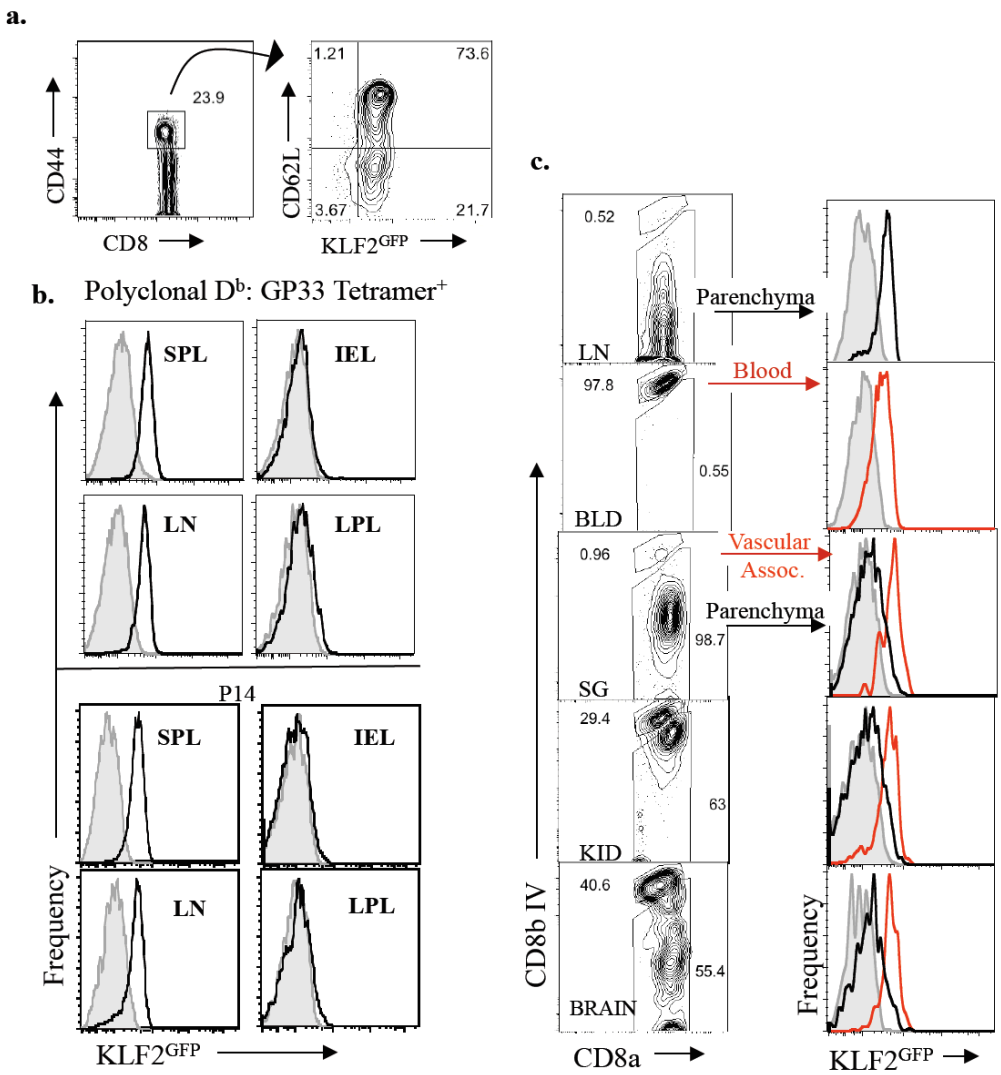

Figure 2-1. Differential KLF2 expression by memory CD8+ T cells in lymphoid and non-lymphoid tissues. (a) KLF2^{GFP} expression in splenic memory-phenotype CD8+ T cells (representative of n=9 from 3 independent experiments). (b) Expression of KLF2^{GFP} in antigen-specific CD8+ T-cells (endogenous D^{b}/gp33 tetramer^{+} or adoptively transferred P14 CD8+ T-cells) from indicated tissues, >28 days after LCMV infection. Data show KLF2^{GFP} reporter CD8+ T-cells (black) overlaid on CD8+ T cells from matched non-KLF2^{GFP}-reporter controls (grey filled), as an autofluorescence baseline. Data are representative of 6-12 animals from at least 3 independent experiments. (c) Analysis of KLF2^{GFP} expression in adoptively transferred P14 CD8+ T cells >28 days post LCMV infection. IV anti-CD8 antibody was used to distinguish P14 T cells in tissue parenchyma (black) versus vascular-associated cells (red). Data are overlaid with WT P14 CD8+ T cells (grey filled) as control (representative of n=9 from 3 independent experiments).

We extended this analysis to other non-lymphoid tissue, including the salivary gland, kidney, and brain. Because T cells found in the blood and vasculature can contaminate the population of T cells found in the tissue parenchyma of these tissues[94], we administered anti-CD8 antibody intravenously into the tail of mice before harvesting tissues. This gave us the capacity to distinguish (and exclude) vascular-associated CD8+ T cells (anti-CD8 IV positive) and those in the tissue parenchyma (anti-CD8 IV negative) (Fig 2-1c). Using this technique, we determined that memory P14 CD8+ T cells found in the blood and vasculature of non-lymphoid tissue expressed KLF2 while P14 cells in the tissue parenchyma had downregulated the transcription factor (Fig 2-1c and S2-1a). Resident memory T cells (T_{RM}) found in non-lymphoid tissue have been defined as expressing CD69[67-73] and we similarly observed an inverse relationship between KLF2 and CD69 expression (Fig 2-2a, S2-1b). This data suggests that CD8+ T cells enter non-lymphoid tissue expressing KLF2 yet downregulate the transcription factor once the cells are in the tissue parenchyma.

Low KLF2 expression may arise from active protein degradation, so we wanted to determine the transcriptional profile of parenchymal memory CD8+ T cells. More than 30 days after P14 CD8+ T cell adoptive transfer and subsequent LCMV infection, we isolated and sorted memory P14 CD8+ T cells from the spleen, salivary gland, or SI lamina propria. RNA extraction followed by RT real-time PCR analysis of sorted P14 T cells showed that along with KLF2 protein, mRNA for KLF2 was downregulated in CD8+ T cells. Consistent with this, KLF2's transcriptional targets *Sell* (encoding CD62L)

and *Edg1* (encoding S1PR1) also exhibited very low transcript levels in memory P14 in non-lymphoid tissue compared to the spleen (Fig 2-2b).

Detecting cell surface expression of S1PR1 is difficult with current reagents making it difficult to analyze S1PR1 expression in different tissues. However, both CD69+ CD8+ and CD4+ T lymph node cells appeared to have no surface S1PR1 when compared to isotype controls (Fig 2-2c). In congruence with this, previous research has shown that S1PR1 deficiency leads to surface expression of CD69[95] (due to the loss of competitive protein-protein interactions between CD69 and S1PR1) so it was possible that T_{RM} cells could be CD69+ due to low S1PR1 expression. Indeed, CD69 message was not elevated in P14 T cells in salivary gland vs spleen, with a modest increase in the SI lamina propria (Fig 2-2b). This data suggests that surface expression of CD69 on T_{RM} may be due to decreased S1PR1 caused by downregulation of KLF2.

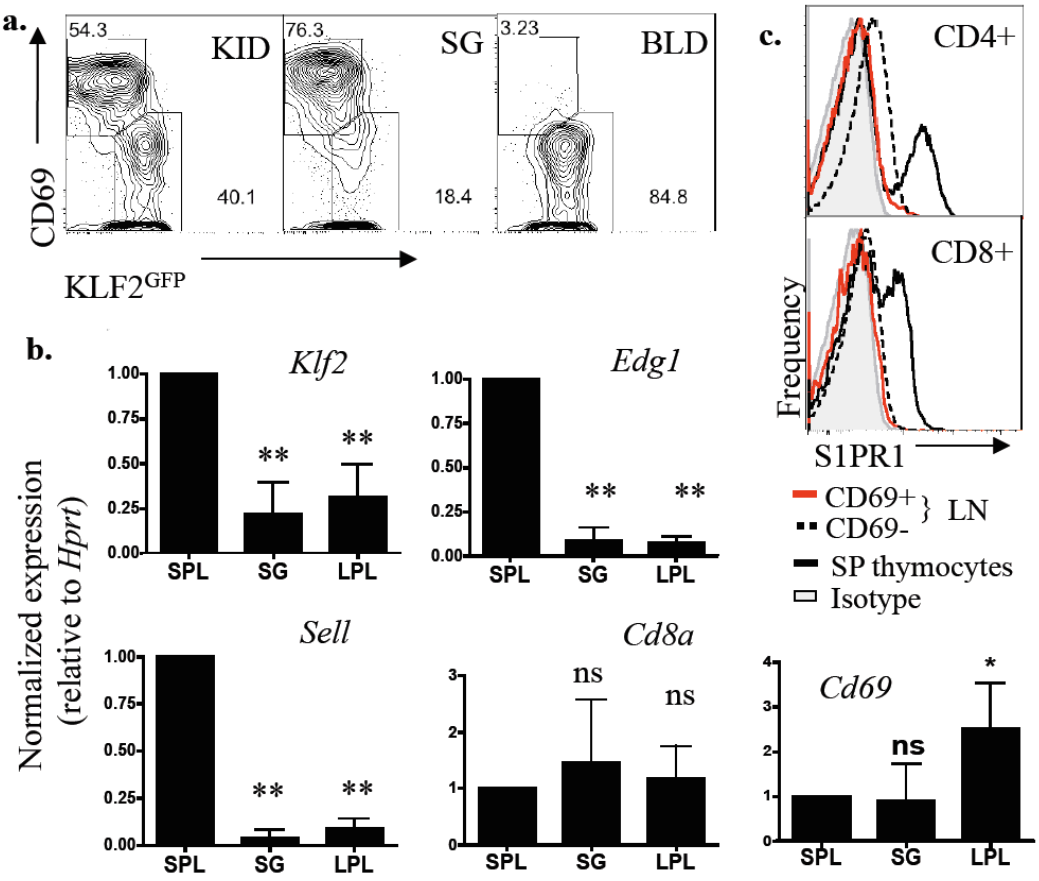

Figure 2-2. KLF2 downregulation correlates with decreased mRNA of transcriptional targets of KLF2 and increased CD69. (a) Analysis of KLF2^{GFP} expression in adoptively transferred P14 CD8+ T cells >28 days post LCMV infection. CD69 versus KLF2^{GFP} expression for indicated tissues (representative of n=9 from 3 independent experiments). (b) RNA was isolated from sorted P14 isolated from SPL, SG and LPL 30 days post LCMV and subject to RT-PCR for the indicated genes. Gene expression (relative to HPRT control) was normalized to the spleen for comparison between experiments. Compiled from four independent experiments (9-12 pooled mice each experiment), graphs show mean +/- SD. Statistical (ANOVA) significance is indicated (**, $p<0.01$; *, $p<0.05$; ns, $p>0.05$). (c) Anti-S1PR1 on SP thymocytes (black), isotype control (grey), and CD69+ (red) vs CD69-(dashed) CD4+ and CD8+ T cells in the lymph node. Representative from 3 independent experiments.

KLF2 downregulation occurs during establishment of T_{RM} in non-lymphoid tissues

KLF2 is downregulated following TCR engagement, but is re-expressed in the effector phase of a response[85, 86]. This is the same time that T_{RM} become established[96-98], so it was important to define the kinetics of KLF2 downregulation in T cells migrating to non-lymphoid tissue after infection. We adoptively transferred congenically distinct WT and $KLF2^{GFP}$ P14 T cells into mice and subsequently infected with LCMV the following day. 48 hours later, KLF2 levels dramatically declined in activated P14 T cells (Fig 2-3a), as previously shown[85, 86]. By day 5 after infection, KLF2 expression was re-expressed in the spleen, lymph nodes, and blood and remained expressed in lymphoid tissues in all further timepoints analyzed (Fig 2-3b/c, S2-2a/b).

In contrast, P14 T cells found in the parenchyma of non-lymphoid tissue had intermediate KLF2 expression at day 5 after infection and complete downregulation from day 8 onwards (Fig 2-3b/c, S2-2a/b). The downregulation of KLF2 was universally observed in parenchymal P14 T cells in all non-lymphoid tissues analyzed whereas CD103 induction was much more variable, being highly expressed in some tissues (SI lamina propria and intraepithelium) versus almost no upregulation in other tissues (brain and kidney) during this timecourse (Fig 2-3c).

The peak of T_{RM} cells in non-lymphoid tissues was day 8 after LCMV, similar with responding T cells in lymphoid tissue (Fig 2-3d). This timecourse is consistent with T_{RM} cells being establishing early after an immune response, as has previously been reported[67]. Therefore, KLF2 downregulation in responding CD8+ T cells after infection directly correlates with the timing of T_{RM} establishment. The rapid termination of KLF2

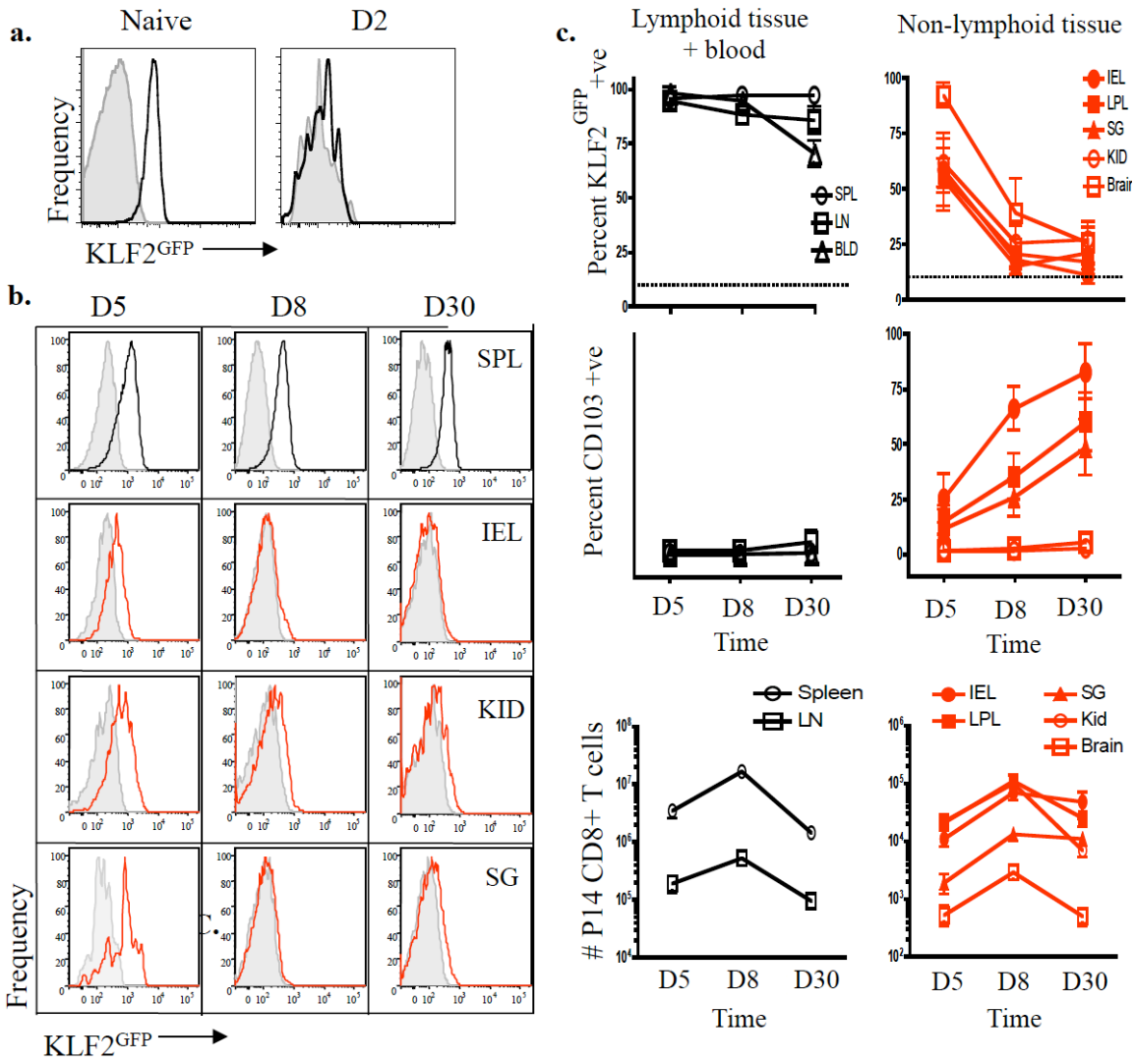

Figure 2-3. KLF2 is downregulated during establishment of CD8+ T cells in non-lymphoid tissues. WT (grey filled) and KLF2^{GFP} P14 CD8+ T cells (black or red) were adoptively co-transferred and host mice infected with LCMV. (a) KLF2^{GFP} expression by naive and 2 day activated (CD69+ve) P14 CD8+ T cells from pooled SPL/LNs (Representative from n=9 from 3 independent experiments). (b) KLF2^{GFP} expression on P14 CD8+ T cells at the indicated days following LCMV infection, in lymphoid tissues (black) and NLT (red) (representative of n=9 from 3 independent experiments). (c) Percentage of CD103+ and KLF2^{GFP}+ P14 CD8+ T cells at the indicated time points in lymphoid tissues (black lines) and NLT (red lines). Data are compiled from 3 independent experiments (n=9) and graphs show mean +/- SD. Dotted line indicates background threshold defined on WT P14 T cells. (d) Absolute number of P14 CD8+ T cells isolated from indicated tissues at specified timepoints following LCMV infection.

during the timeframe when T_{RM} are establishing (Fig 2-2b), together with the loss of trafficking molecules regulated by KLF2 (Fig 2-1e), suggests KLF2 downregulation may be significant for the establishment of T_{RM} in non-lymphoid tissue.

Distinct KLF2 expression characteristics of T_{RM} versus recirculating memory CD8+ T cells in non-lymphoid tissue

Some re-circulating memory CD8+ T cells, the classically defined effector-memory subset[57], would be expected to traffic through NLT and we sought to analyze KLF2 expression by this population compared to the non-recirculating T_{RM}. Hence, we conducted parabiosis experiments where two infection-matched mice were surgically joined at the memory phase of a LCMV infection leading to shared circulation and the ability to detect circulating memory T cells accessing non-lymphoid tissues (schemata: Fig 2-4a). In these experiments, one C57BL/6 mouse received CD45.1/2 KLF2 ^{GFP} P14 cells (and in some experiments, the other C57BL/6 mouse received CD45.1/1 WT P14 cells). We defined the mouse that originally received the KLF2^{GFP} P14 cells as being the "donor" while the mouse that acquired KLF2 ^{GFP} P14 T cells through the circulation only as the "parabiont". Both mice were infected with LCMV, and 30-65 days later the infection-matched mice were surgically joined to allow for shared circulation. A week after parabiosis mice were bled for equilibration, and either two or four weeks after surgery the parabiotic pairs were harvested and P14 T cells in various tissues analyzed.

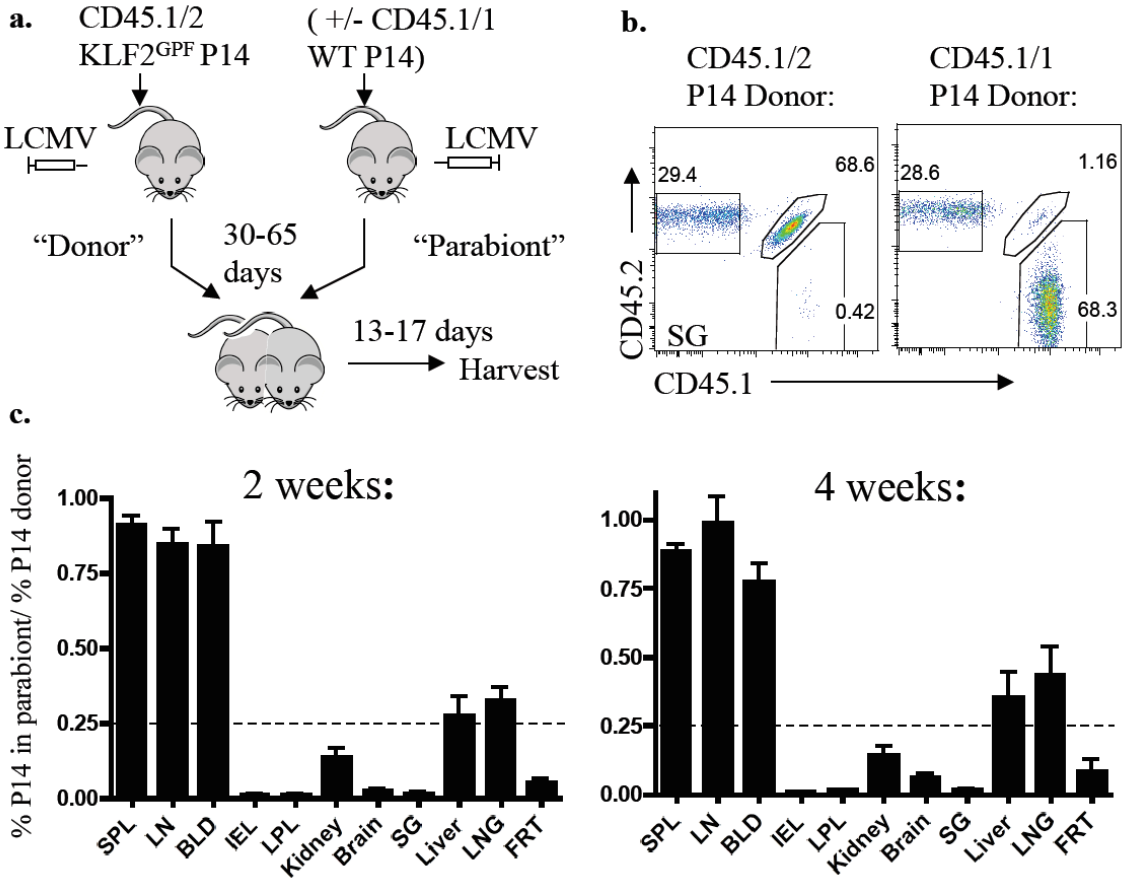

Figure 2-4. Few memory CD8+ T cells migrate into non-lymphoid tissue during the memory phase of an acute infection.

(a) Schematic for parabiosis experiments. Congenically distinct KLF2^{GFP} P14 cells were transferred into normal C57BL/6 mice, which were infected with LCMV the following day. A parallel set of mice were infected but did not receive P14 adoptive transfer (or received WT P14 as in b). At 30-65 days post-infection, pairs of transferred and non-transferred mice underwent parabiotic surgery, and 2-4 weeks after surgery, paired animals were sacrificed and tissues harvested. The mice originally receiving the KLF2^{GFP} P14 cell population is termed the "donor" while the other animal in a parabiotic pair is termed the "parabiont". (b) Representative graph of SG, equilibration typical of 5 independent experiments (involving 12 parabiotic pairs). In this experiment, both animals in the parabiotic pair had received P14 T-cells. Gated on live, non-vascular-associated CD8+ T cells. (c) Relative abundance of P14 T cells in indicated tissues of donor and parabiont 2 or 4 weeks after parabiosis. This is shown as the percent of P14 T cells among total non-vascular-associated CD8+ cells in the parabiont, divided by the percent P14 T cells among total non-vascular-associated CD8+ cells in the donor. N=6 from 2 independent experiments for each time point.

As has been reported[56, 71, 73], the KLF2 ^{GFP} P14 cells were well represented in the lymphoid tissue and blood of the parabiont yet were rare in the parenchyma of non-lymphoid tissue (Fig 2-4b/c). If trafficking into non-lymphoid tissue simply had slower kinetics than lymphoid tissue, one would expect to see an increase in P14 cell equilibration between the two animals over time at these sites. However, there was no substantial increase in parenchymal P14 cell equilibration in non-lymphoid tissue from two to four weeks after parabiosis (Fig 2-4c), confirming that very few circulating memory P14 T cells enter the parenchyma of non-lymphoid tissue during the memory phase of an immune response. This reinforces the concept that the majority of antigen-primed memory CD8+ T cells in non-lymphoid tissues are T_{RM}, but also allowed us the ability to phenotype the rare population of T_{EM} that migrate to non-lymphoid tissues during the memory phase of an immune response.

Interestingly, the few memory P14 T cells that did migrate into the non-lymphoid tissue exhibited intermediate expression of both KLF2 and CD69 (Fig 2-5a-c). This expression pattern is unique from either the P14 T cells in the vasculature of the tissue (staining positive for the anti-CD8 antibody IV) and the T_{RM} that exhibit a $KLF2^{LO}/CD69^{HI}$ phenotype. Analysis of KLF2 versus CD69 together highlighted the possibility of 2 distinct populations of circulating P14 cells being present within the parabiont: one exhibiting the $KLF2^{LO}/CD69^{HI}$ phenotype similar to T_{RM} in the host and another with more intermediate KLF2/CD69 expression ($KLF2^{INT}$) (Fig 2-6 and S2-3). Analyzing these 2 populations within the parabiont over time, there was a subtle increase in the percentage of cells exhibiting the T_{RM} level of KLF2/CD69 suggesting there may

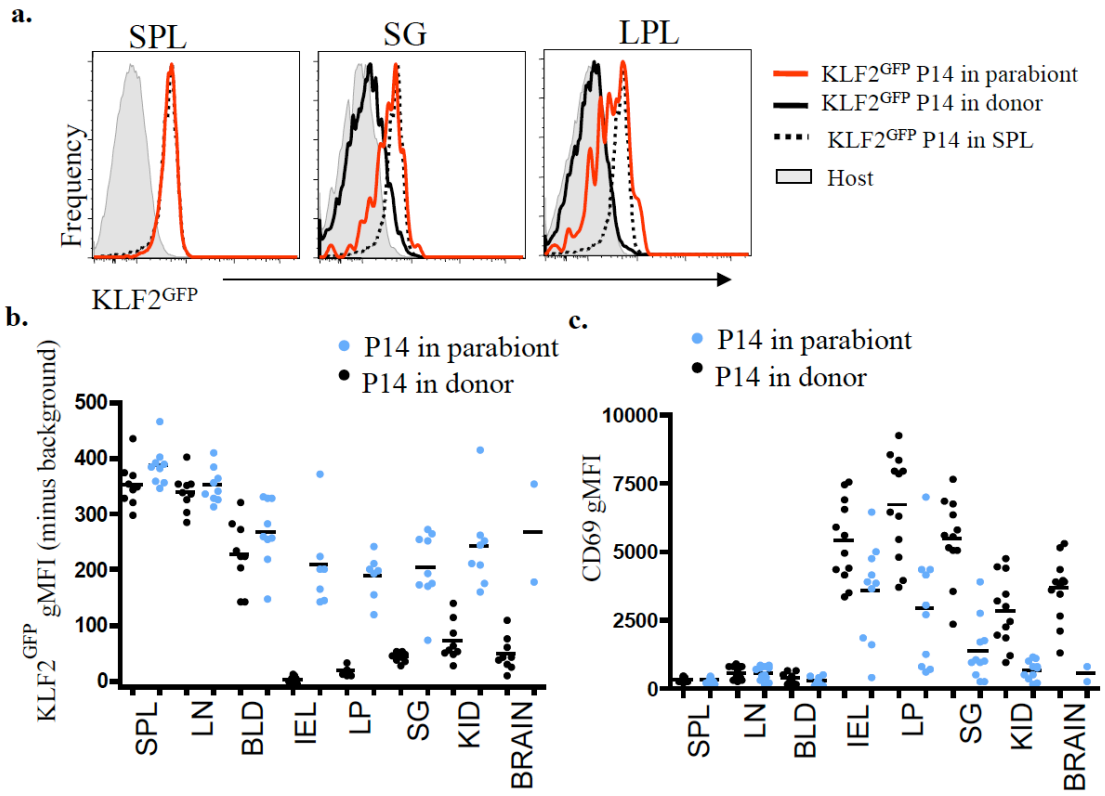

Figure 2-5. Distinct KLF2^{GFP} expression in recirculating memory CD8+ T cells in NLT. Data are from parabiosis studies (see Fig 2-4a) and are compiled from 5 independent experiments (n=12 pairs) assayed 13-17 days post surgery. (a) Histograms show live, non-vascular-associated CD8+ T cells. Black lines show KLF2^{GFP} levels in P14 cells in the donor mouse, red lines indicate P14 cells in the parabiont. Dotted lines represent P14 cells in (donor) spleen, as a reference, and grey histograms is the background control (host CD8+ T cells). (b and c) Geometric MFI (gMFI) for KLF2^{GFP} (b) or CD69 (c) on P14 cells in parabiont (blue) or donor (black) mice. In b, the background gMFI (of host CD8+ T cells) was subtracted. KLF2^{GFP} and CD69 levels are not shown when <25 P14 T cells could be detected in a tissue. Gating was on live, non-vascular-associated CD8+ P14 T cells.

be a very small replenishment of T_{RM} after an immune response has cleared (Fig 2-6 and S2-3). This strengthens the idea that full downregulation of KLF2 marks T_{RM} and the small population of KLF2^{Int} P14 observed may be re-circulating T_{EM} in non-lymphoid tissue. This is consistent with the small shoulder of potential KLF2^{INT} P14 T cells seen in some non-lymphoid tissue (Fig 2-3b and S2-2).

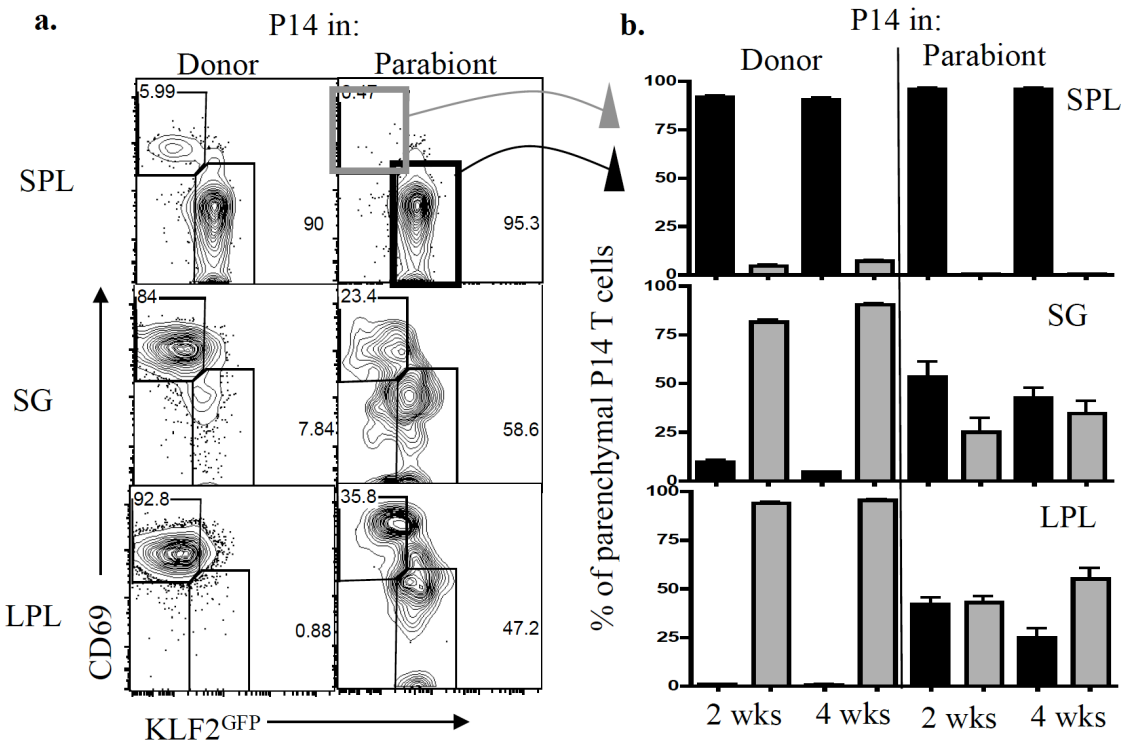

Figure 2-6. Two distinct populations arise from recirculating memory CD8+ T cells in NLT. Data are from parabiosis studies (see Fig 2-4a) and are compiled from 2 independent experiments (6=12 pairs) assayed 2-4 weeks post surgery. (a) $KFL2^{GFP}$ vs CD69 expression in parenchymal P14 cells found in the donor (left) or parabiont (right) in various non-lymphoid tissue two weeks after parabiosis. Representative of n=6 from 2 independent experiments. Gating is on $KLF2^{HI}/CD69^{LO}$ and $KFL2^{LO}/CD69^{HI}$ populations. (b) % of parenchymal P14 T cells falling in the $KLF2^{HI}/CD69^{LO}$ (black bars) and $KFL2^{LO}/CD69^{HI}$ (grey bars) gates defined in (a) either 2 or 4 weeks after parabiosis.

Discussion

This chapter outlined the expression of KLF2 in activated CD8+ T cells in both lymphoid and non-lymphoid tissue over time. We showed that while memory T cells in lymphoid tissue and blood have high expression of KLF2, CD8+ T cells that migrate to non-lymphoid tissue downregulate KLF2 at both the protein as well as transcript level. This affected transcriptional targets of KLF2, including CD62L and S1PR1, and correlated with increased CD69 on T_{RM}.

T_{RM} cells establish in non-lymphoid tissue early after infection. This was seen by the peak of T_{RM} being 8 days after LCMV infection (Fig 2-2c). Since the kinetics of KLF2 downregulation occurr at the same time as this seeding of T_{RM} (Fig 2-2b), our data suggest that KLF2 downregulation may be functionally significant for the establishment of T_{RM}. Combined with the parabiosis studies showing that very few memory T cells enter the tissue parenchyma of non-lymphoid tissue during the memory phase of an immune response, it is now clear that early events that occur in non-lymphoid tissue after systemic infection are significant for the development of establishing T_{RM}. Whether the downregulation of KLF2 and its transcriptional targets is functionally significant for the establishment of T_{RM} is at this point unclear, but is the focus of chapter 3.

From our parabiosis studies we identified two distinct populations of circulating memory T cells that appear in the parenchyma of non-lymphoid tissue: one with intermediate KLF2/CD69 expression and another with $KLF2^{LO}/CD69^{HI}$ expression similar to T_{RM}. While the percentage of the latter population slightly increases over time, it remains unclear as to whether these are two distinct populations. It may be that the

$KLF2^{LO}/CD69^{HI}$ population are circulating memory P14 T cells that have taken up residency in the non-lymphoid tissue while the P14 with intermediate expression are cells that are T_{EM} circulating through the tissue and then leaving. P14 T cells in the blood expressed KLF2 while the kinetics of KLF2 downregulation was rapid after cell entrance into non-lymphoid tissue (Fig 2-3). This fits with the idea that circulating T_{EM} that enter the parenchyma of non-lymphoid tissue would quickly start to develop a T_{RM} phenotype by being $KLF2/CD69^{INT}$. At the same time, it could also be that the two populations represent cells that have been present in the tissue for differing lengths of time; the $KLF2/CD69^{INT}$ having just entered the parenchyma of non-lymphoid tissue while the $KLF2^{LO}/CD69^{HI}$ population having been in the tissue for a more extended amount of time allowing them to develop the T_{RM} phenotype. IHC experiments could potentially decipher these differences by identifying the location of these two populations based on KLF2/CD69 expression.

P14 cells isolated from the blood during a memory timepoint after LCMV consistently experienced lower $KLF2^{GFP}$ levels than P14 in lymphoid tissue (Fig 2-1c and S2-2). The reason for this is unclear. This level of $KLF2^{GFP}$ was not as low as T_{RM} and did not correlate with an increase in CD69 expression, suggesting these cells are not recent immigrants from NLT. P14 cells associated with the vasculature in NLT (anti-CD8 antibody IV positive) also did not show lower $KLF2^{GFP}$ levels (Fig 2-1c), nor did P14 isolated from the blood 8 days after LCMV (Fig S2-2a). When T cells enter the blood and are exposed to higher concentration of their ligand S1P, S1PR1 is internalized due to ligation[96, 97]. It may be that S1PR1 internalization provides a feed forward signal that

transiently affects $KLF2^{GFP}$ protein in memory T cells, although why this would only affect T cells at the memory phase is unclear. Future studies investigating whether KLF2 transcripts are also lower in these cells combined with specific experiments addressing the affect of blood processing may shed light on why some CD8+ memory T cells are appearing lower for KLF2 protein in the blood.

This chapter outlined the KLF2 expression in CD8+ T cell populations present in various tissues over time after an infection. From this analysis, we have determined that T_{RM} cells are downregulated for both KLF2 and its transcriptional targets. The next chapter will investigate the functional significance of the downregulation of KLF2 and its targets on the establishment of T_{RM} in non-lymphoid tissue.

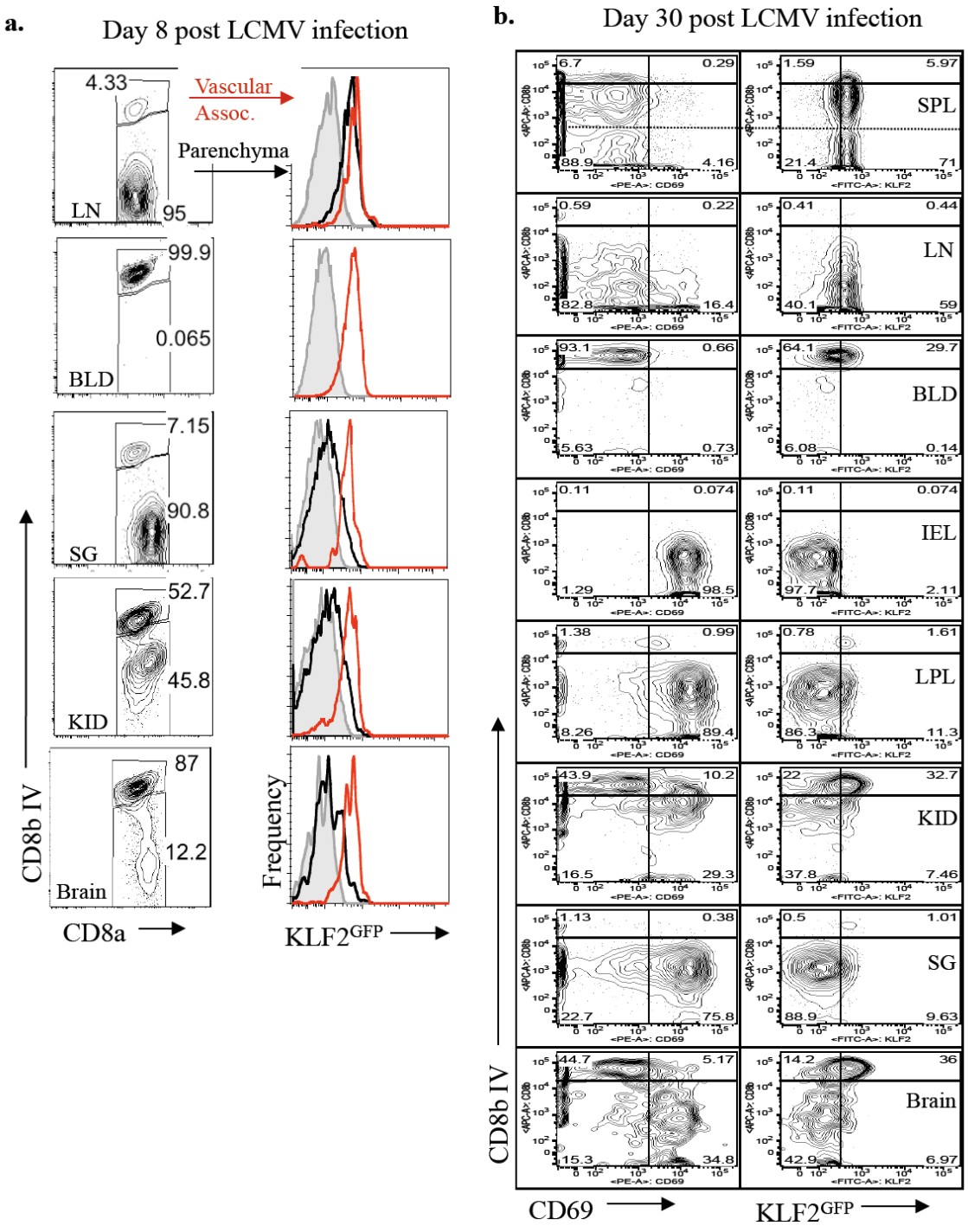
a.
Day 8 post LCMV infection
4.33
Vascular
Assoc.
Parenchyma
LN
95
99.9
0.065
BLD
7.15
90.8
SG
52.7
45.8
KID
87
12.2
Brain
CD8b IV
CD8a
Frequency
KLF2GFP
b.
Day 30 post LCMV infection
SPL
LN
BLD
IEL
LPL
KID
SG
Brain
CD8b IV
CD69
KLF2GFP

Figure S2-1. CD69 expression and KLF2 downregulation correlate with parenchymal P14 T cells in NLT. Analysis of $KLF2^{GFP}$ expression in adoptively transferred P14 cells 8 days (a) or 30 days post LCMV infection (b). (a) IV anti-CD8 antibody was used to distinguish P14 cells in tissue parenchyma (black) versus vascular-associated (red). Data are overlaid with WT P14 (grey filled) as control. Representative of n=9 from 3 independent experiments. (b) Gated on live congenically marked P14 cells isolated from different tissues. Showing CD8 IV versus CD69 (left) or $KLF2^{GFP}$ (right). Horizontal dotted line represents the seperation between red pulp and white pulp of the spleen, based on previous studies[94]. Representative of 4 independent experiments with 3 mice each.

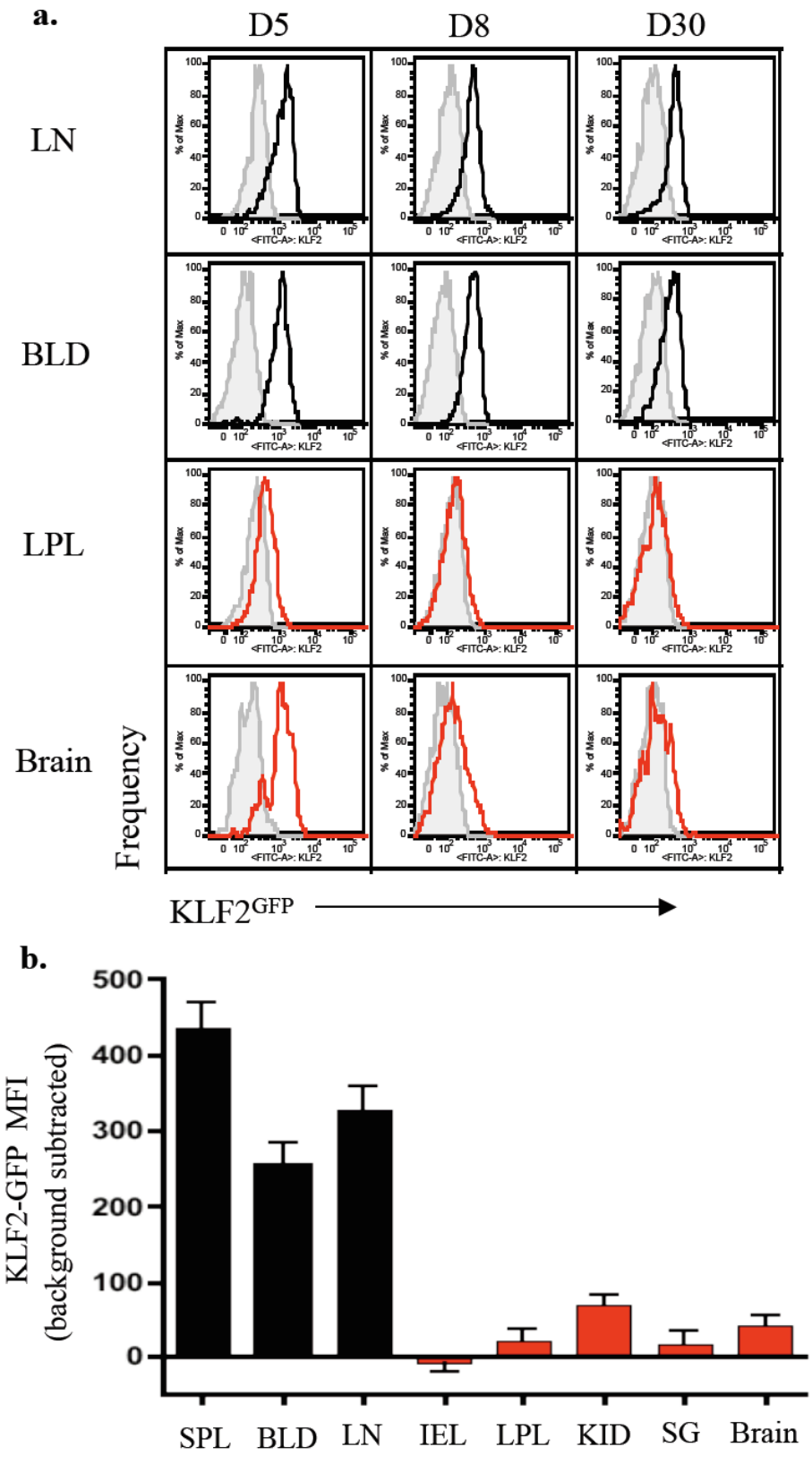
a.
D5
D8
D30
LN
BLD
LPL
Brain
Frequency
KLF2GFP
b.
KLF2-GFP MFI
(background subtracted)
500
400
300
200
100
0
SPL
BLD
LN
IEL
LPL
KID
SG
Brain

Figure S2-2. Kinetics of KLF2 downregulation in lymphoid and non-lymphoid tissues. WT (grey filled) and KLF2^{GFP} P14 cells (black or red) were adoptively co-transferred and host mice infected with LCMV. (a) KLF2^{GFP} expression on live, non-vascular-associated P14 cells at the indicated days following LCMV infection, in lymphoid tissues (black) and NLT (red) (representative of n=9 from 3 independent experiments). Cells in blood exhibit slightly lower KLF2^{GFP} levels relative to SPL/LN, especially at memory timepoints, for unclear reasons. (b) GFP MFI from KLF2^{GFP} P14 isolated from various tissues 30 days post LCMV infection. GFP MFI from WT P14 cells was subtracted from KLF2^{GFP} MFI to eliminate background variability from tissue to tissue (this graph was compiled from 2 independent, representative experiments; n=6).

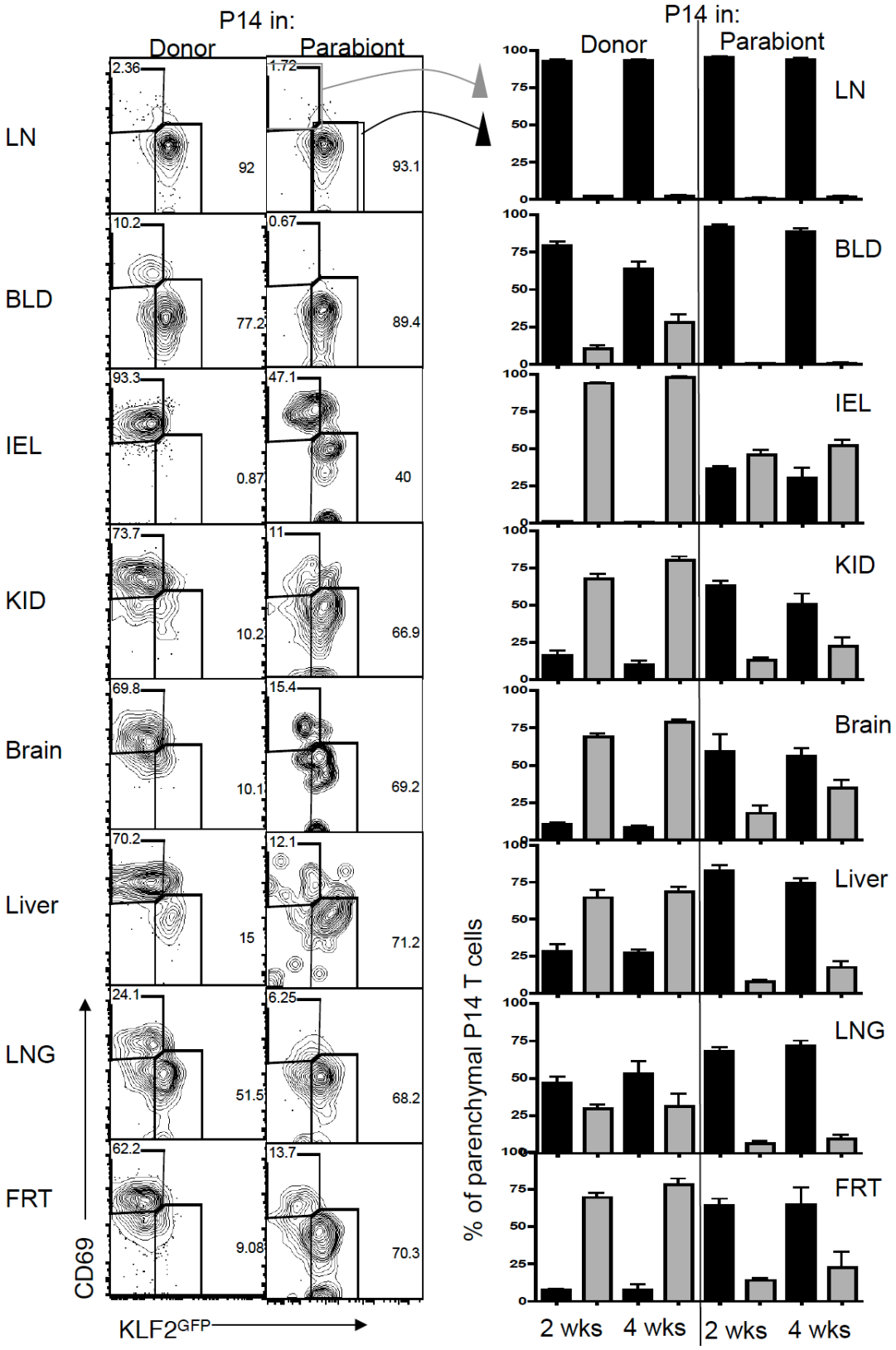
P14 in:
Donor
Parabiont
LN
BLD
IEL
KID
Brain
Liver
LNG
FRT
2.36
92
1.72
93.1
10.2
77.2
0.67
89.4
93.3
0.87
47.1
40
73.7
10.2
11
66.9
69.8
10.1
15.4
69.2
70.2
15
12.1
71.2
24.1
51.5
6.25
68.2
62.2
9.08
13.7
70.3
CD69
KLF2GFP
% of parenchymal P14 T cells
100
75
50
25
0
2 wks
4 wks
2 wks
4 wks

Figure S2-3. Two distinct populations arise from recirculating memory CD8+ T cells in NLT. Data are from parabiosis studies (see Fig 2-4a) and are assayed 2-4 weeks post surgery. (a) $KFL2^{GFP}$ vs CD69 expression in parenchymal P14 cells found in the donor (left) or parabiont (right) in various non-lymphoid tissue two weeks after parabiosis. Representative of n=6 from 2 independent experiments. Gating is on $KLF2^{HI}/CD69^{LO}$ and $KLF2^{LO}/CD69^{HI}$ populations. (b) % of parenchymal P14 T cells falling in the $KLF2^{HI}/CD69^{LO}$ (black bars) and $KLF2^{LO}/CD69^{HI}$ (grey bars) gates defined in (a) either 2 or 4 weeks after parabiosis. N=6 from 2 independent experiments for each time point.

Materials and methods

Mice.

C57BL/6 and CD45.1 congenic B6 mice were purchased from the National Cancer Institute and used at 6-8 weeks of age. $KLF2^{GFP}$ reporter mice were described earlier[81] and were crossed to P14 TCR transgenic mice (specific for the $H\text{-}2D^b$ restricted LCMV $gp_{33\text{-}41}$ epitope [KAVYNFATC]). For adoptive co-transfer studies, combinations of CD45.2, CD45.1 and CD45.1/CD45.2 mice were used for donor and host strains, to allow for discrimination of each donor population versus host cells. Animals were maintained under specific pathogen-free conditions at the University of Minnesota, and all experimental procedures were approved by the Institutional Animal Care and Use Committee.

Adoptive transfer and infections.

Splenocytes were prepared from $KLF2^{GFP}$ P14 and congenic wild type P14 mice. The cell populations were mixed 1:1 and 25,000-45,000 CD8+ T cells were transferred into recipient B6 mice, which were infected the next day with $2x10^5$ PFU LCMV (Armstrong strain), via ip injection. Mice were maintained under BSL-2 housing and, at indicated times following infection, were sacrificed for analysis.

In vivo anti-CD8 antibody IV and lymphocyte isolation.

In order to label cells in the circulation, mice were injected with fluorchrome conjugated anti-CD8 antibodies (via the tail vein), as previously described[94]. At 2.5

minutes (min) following antibody injection, mice were bled and 30 seconds later mice were sacrificed. Heart perfusion, using 10ml of cold PBS was performed (in some experiments this step was eliminated) and tissues were harvested and lymphocytes isolated as described[93, 94]. Briefly, lymph nodes were mashed to achieve a single cell suspension, while the salivary glands, kidney, brain, and spleen were mashed and incubated at 37^{o}C with 100U/ml collagenase type I (Worthington Biochemical Corporation), 10% FBS, $MgCl_2$/$CaCl_2$, HEPES/L-glumatime RPMI solution (45 min shaking at 450 rpm). For the small intestine, Peyer's patches were dissected out and the remaining tissue cut longitudinally and then into 1cm pieces. These were rinsed and incubated with 15.4mg/ml dithioerythritol in HBSS/HEPES bicarbonate buffer for 30 min (37^{o}C at 450 rpm) to extract IELs. The remaining pieces were additionally incubated with the collagenase solution and conditions as listed above, to isolate LPL. All tissues were then subjected to a 44/67% percoll gradient (2,000rpm at 20^{o}C for 20 min) to isolate lymphocytes.

Cellular gating strategy and calculation of absolute numbers in non-lymphoid tissue.

For analysis of P14 CD8+ T cells in all tissues, the gating strategy included: live, singlet CD8+ lymphocytes, non-vascular-associated (stained negative for IV administered anti-CD8b)[94], with respective congenic markers. Absolute numbers of P14 cells in Figure 2-3d is compiled from 6 independent experiments (including KLF2^{GFP} P14 and empty-vector transduced P14 from Fig 3-3e), n=15-21.

Flow cytometry and antibodies.

Single-cell suspensions were prepared and cells were resuspended at 3-6x10^7 cells/ml in FACS buffer (1% FBS, 0.1% sodium azide) and stained in 100ul. Isolated lymphocytes in all experiments were incubated with LIVE/DEAD Fixable Aqua Dead Cell Stain Kit (Invitrogen) for 15 min at 4°C to detect dying cells before staining with a cell surface antibody staining cocktail. For detection of S1PR1, cells were stained with 2ug unconjugated anti-S1PR1 antibody (R and D systems) or 0.5 ug isotype control in 50uL for 30 minutes at 4°C. After washing, 1:400 anti-rat PE (Jackson Research) was incubated for 20 min on ice followed by blocking with normal rat serum (0.5ul/100ul) for 15 at 4°C and lastly a 20 minute normal surface stain with the remaining antibodies. All additional fluorochome-conjugated antibodies were purchased from eBioscience, BD BioScience, R&D Systems, or BioLegend. Cells were analyzed using a BD Pharmingen LSR II flow cytometer and data analyzed using FlowJo (TreeStar) software.

Quantitative RT PCR.

Congenically marked WT and KLF2^{GFP} P14 were co-transferred into C57BL/6 mice and infected with LCMV the following day. At 28-36 days post LCMV infection, spleen, salivary glands and small intestine LPL were isolated and P14 CD8+ T cells were sorted on a FACS Aria (Becton Dickinson) based on congenic markers. RNA was isolated using the RNeasy microkit (Qiagen) and reverse transcription was performed (qScript cDNA synthesis kit, Quanta Biosciences). Expression levels of genes were

determined using the ABI 7700 sequence detection system and amplification was detected using the SYBR Green PCR Master Mix (Applied Biosystems). Cycle threshold values were normalized to a control gene (HPRT or GAPDH) to determine relative quantitative gene expression levels with the P14 from the spleen (Fig 2-2e) set at 1.

Gene:	Forward:	Reverse:
KLF2	ACCAACTGCGGCAAGACCTA	CATCCTTCCCAGTTGCAATGA
S1PR1	GTGTAGACCCAGAGTCCTGCG	AGCTTTTCCTTGGCTGGAGAG
CD62L	CTAATTTCCCCTCGCTCATTCAT	GCATTAGCTTCTGTGCTGAATTGA
CD69	TGGTCCTCATCACGTCCTTAATAA	TCCAACTTCTCGTACAAGCCTG
CD8a	AAGAAAATGGACGCCGAACTT	AAGCCATATAGACAACGAAGGTG
HPRT	CATTATGCCGAGGATTTGGAA	CACACAGAGGGCCACAATGT
GAPDH	TGGCCTACATGGCCTCCA	TCCCTAGGCCCCTCCTGTTAT

Parabiosis.

Congenically marked KLF2^{GFP} P14 T cells were transferred into C57BL/6 mice. The following day, the animals were infected ip with LCMV and 30-65 days later, mice underwent parabiotic surgery following the schematic described in Figure 2-4a. Procedures were as described previously[56]: Briefly, mice were anesthetized with ketamine, flank hair removed using nair and the skin cleaned using betadine. A lateral incision was made on each mouse from knee to elbow. Mice were joined with a continuous sub-cuticular suture on both the dorsal and ventral sides, with mattress and cruciate sutures joining the skin layer. Mattress sutures just under the armpit and knee were made to secure the parabiosed mice together. At 7-9 days post surgery mice were bled to ensure equlibration and 13-17 days post surgery tissues were harvested from both mice. The number of non-vascular-associated P14 memory T cells was calculated in "donor" and "parabiont" (see Fig 2-4a). A minimum threshold of 25 events was applied

for calculation of P14 T-cell KLF2^{GFP} and CD69 MFI.

Statistical analysis.

Data were analyzed using Prism software (GraphPad). For standard data sets Student's t-test was used (with Welch's correction utilized when variances were different), while normalized data was analyzed using ANOVA. For values that differed by >10-fold, values were $\log_{10}$ transformed prior to t-test analysis. Asterisks indicate obtained p-values, with *** meaning $p<0.001$; **, $p<0.01$; *, $p<0.05$, while "ns" indicates $p>0.05$.

Chapter 3

Transcriptional downregulation of S1PR1 is required for establishment of resident memory CD8+ T cells

Recently a new subset of CD8+ memory T cells termed resident memory or T_{RM} have been defined that stay embedded in non-lymphoid tissue instead of re-circulating throughout the organism. T_{RM} have been shown to mount a more rapid response upon localized secondary infection compared to T_{CM}, highlighting the significance of having frontline CD8+ T cells in tissues during infection with a pathogen. However, the defining transcriptional basis for T_{RM} has not been determined. In the previous chapter we demonstrated that T_{RM} have low expression for the transcription factor KLF2. In this chapter we show that forced expression of KLF2's transcriptional target S1PR1 dampens the establishment of T_{RM} in non-lymphoid tissue. Cytokines inducing T_{RM} phenotype (TGF-β, IL-33 and TNF) provoked KLF2 downregulation, in a P13K/AKT dependent pathway, suggesting the local environment of non-lymphoid tissue can regulate KLF2 expression. Hence KLF2 and S1PR1 regulation provides a switch, dictating whether CD8+ T cells join the recirculating memory population, or commit to tissue residency.

Introduction

During an immune response, antigen-specific T cells undergo massive clonal expansion, contribute to antigen clearance and then generate a memory population capable of more rapid and efficient recall responses. An important feature of memory T cells is their altered trafficking capacity which allows them (but not naïve T cells) to survey non-lymphoid tissue[53, 56]. Indeed, it has become clear that a subset of memory CD8+ T cells, T_{RM}, do not re-circulate through the body, but are instead maintained in diverse non-lymphoid tissue (including the small intestine, brain, salivary glands, skin, and female reproductive tract)[67-73]. T_{RM} have been shown to provide superior protection (compared to circulating memory cells) against local secondary infections[69-73, 98], and T_{RM} are now recognized as critical sentinels for protective immunity[99-102].

However, an essential and unresolved question is the mechanism through which T_{RM} residency becomes established[99-102]. For some non-lymphoid tissues, T_{RM} expression of CD103 (or its ligand, E-cadherin) contribute to T_{RM} maintenance[69, 93]. However, these molecules are not expressed by T_{RM} in all non-lymphoid tisue[93] suggesting such interactions do not constitute a universal mechanism for T_{RM} retention. Indeed, while CD103 is required for maintenance of T_{RM} in the small intestinal intraepithelial lymphocyte (IEL) population, it is not necessary for establishment of the lamina propria lymphocyte (LPL) population in the same tissue[93].

A more consistent marker for T_{RM} populations from multiple NLT is expression of CD69[93, 101]. CD69 upregulation is often correlated with T cell receptor (TCR)

stimulation – yet foreign antigen persistence is dispensable for establishment and/or maintenance of T_{RM} in various NLT[72, 93]. Hence the factors that promote residency of T_{RM} remain ill-defined, and nothing is known about the transcriptional regulation that distinguishes cells committing to the recirculating versus resident populations.

Kruppel-like factor 2 (KLF2) is a zinc-finger transcription factor that directly promotes expression of the genes for sphingosine-1 phosphate receptor 1 (S1PR1) and L-selectin, two molecules that are critical for naïve T cell recirculation[77, 79]. S1PR1, through detection of its ligand S1P in the blood and lymph, is essential for naïve lymphocytes to access the circulatory system from lymph nodes and thymus[38]. Consequently, deficiency in KLF2[77] or S1PR1[38] causes retention of naïve T cells in lymphoid tissues. TCR stimulation induces rapid loss of KLF2 (and S1PR1), providing a mechanism for initial retention of activated T cells in lymphoid tissues, while these molecules are re-expressed in memory CD8+ T cells isolated from lymphoid tissues[38, 85, 86, 96]. In chapter two we showed that CD8+ T_{RM} in non-lymphoid tissue are characterized by low expression of KLF2 and S1PR1. In this chapter we show that transcriptional downregulation of S1PR1 is critical for the establishment of this resident memory pool.

Results

Establishing a model to force S1PR1: Retroviral transduction

Although we could correlate downregulation of KLF2 with the establishment of T_{RM} in chapter two, the mechanistic importance of this change was unclear. To test the functional significance of the downregulation of KLF2 and its transcriptional targets in T_{RM} establishment, we needed to establish a model to force the expression of these molecules. Previous research has suggested that KLF2 is a quiescent factor for naïve T cells[82, 83, 103]. Therefore, we were hesitant to force KLF2 due to the possibility of proliferation defects complicating the interpretation of results. Of KLF2's targets, S1PR1 was a good candidate for regulating T_{RM} retention due to its already documented role in T cell egress from lymphoid tissues[38, 96]. Hence we developed a model to force S1PR1 in activated T cells.

We generated a retroviral vector containing a Flag-S1PR1 cassette driven by the murine stem cell virus (MSCV) promoter, an internal ribosomal entry site, and thy1.1 as a transduction marker (Fig 3-1a). An identical vector lacking the Flag-S1PR1 cassette ("empty vector") was used as a control to verify that results seen using the S1PR1 vector were specific to S1PR1, and served as a control in all subsequent experiments (Fig 3-1a). Retroviral transduction of activated P14 cells subsequently cultured *in vitro* resulted in expression of thy1.1 with both empty and S1PR1 vectors while only S1PR1 transduced cells stained positive for an anti-flag antibody, suggesting the flag-S1PR1 was specifically expressed on the surface of S1PR1 transduced cells (Fig 3-1b). At the same time, thy1.1+ S1PR1 transduced cells had diminished surface CD69 expression not seen

in empty transduced P14 cells. Given the antagonistic interaction between CD69 and S1PR1[95], these data suggest functional S1PR1 protein was being expressed in our retroviral transduction system.

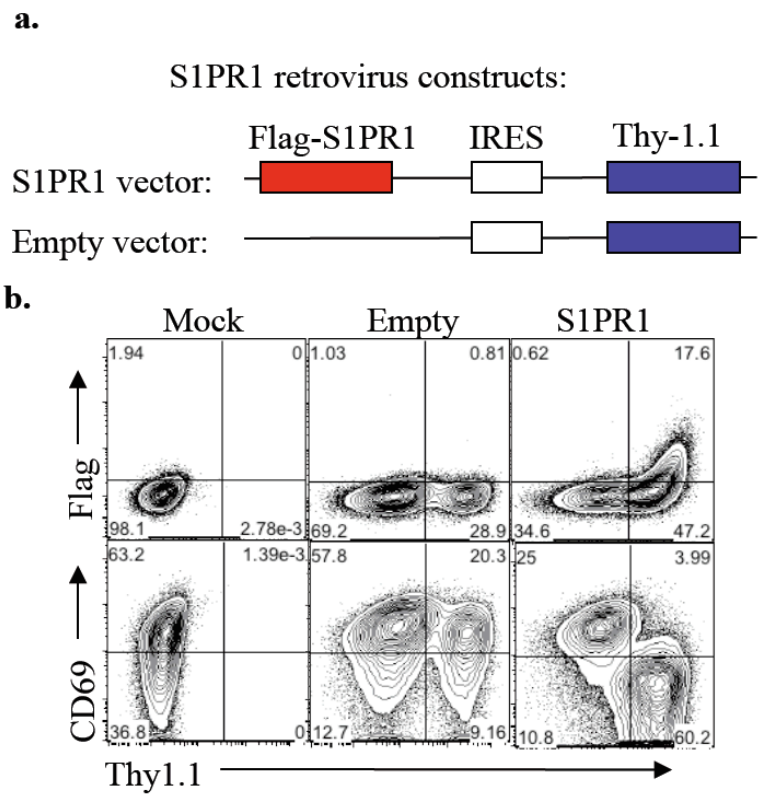

Figure 3-1. Characterization of the retroviral transduction system used for forced S1PR1 expression. (A) Retroviral construct for transduction containing the S1PR1 cassette (top) or the empty vector (bottom). (B) Mock, empty or S1PR1-transduced P14 cells incubated *in vitro* for 2 days with 10 ng/ml hIL-2 and 250 nM gp33 peptide. Cells were stained for Thy-1.1 (the transduction marker) and for CD69 or the Flag-epitope (which was cloned into the N-terminus of the retroviral S1PR1). Expression of the retroviral S1PR1 is indicated by cell surface Flag-epitope staining, and loss of staining for CD69 (which competes with S1PR1 for surface expression). Gated on live CD8 + cells.

A potential caveat from this approach arises from studies involving S1PR1 transgenic mice which suggested that forced S1PR1 impairs T cell expansion after TCR activation[104]. However, this effect was not seen in our retroviral studies since the percent

transduction of S1PR1 vs empty transduced CD8+ T cells was constant *in vitro* over time and showed no diminishing of thy1.1+ cells (Fig 3-2a). Likewise, the total number of cells in culture was comparable between S1PR1, empty, and mock transduced cells suggesting that proliferation was not affected with forcing S1PR1 (Fig 3-2b).

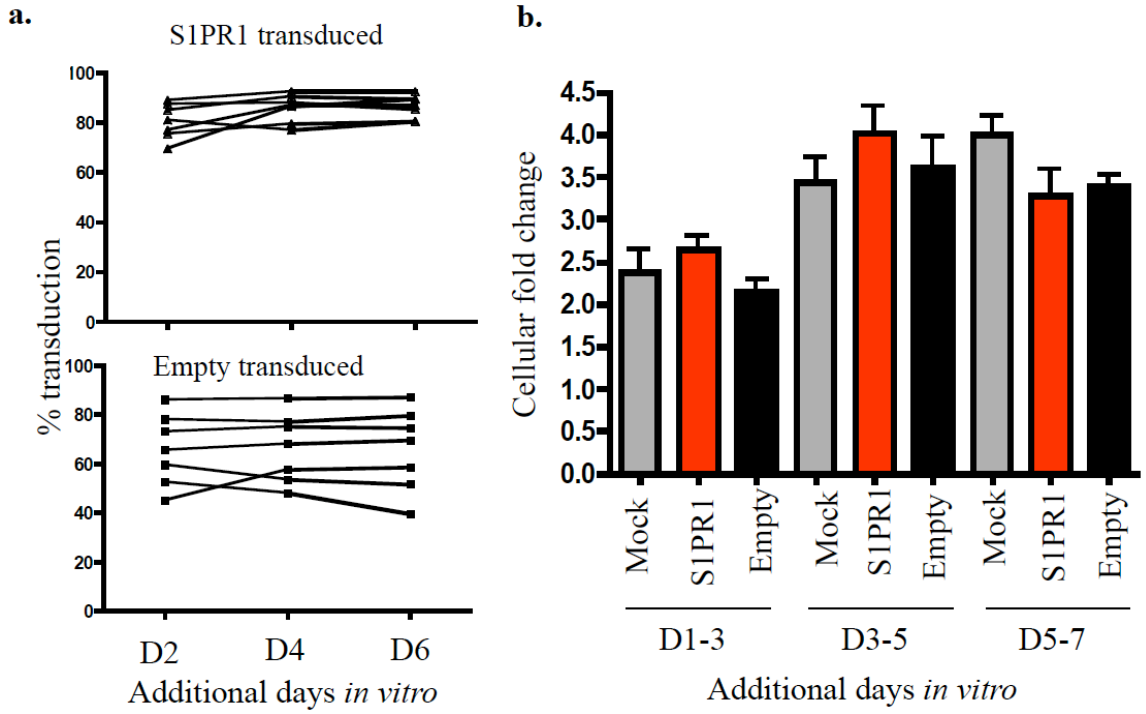

Figure 3-2. S1PR1 retroviral transduction does not alter proliferation over time in vitro. (a) Transduction efficiency of live S1PR1 (top) and empty (bottom) transduced P14 cells cultured *in vitro* for additional days with 20ng/ml hIL-2. Each line is from an independent experiments (n=7). (b) Mock (grey), S1PR1 (red), and empty (black) transduced P14 cells were cultured *in vitro* for additional days as in (a). Data show the fold-change in live cell numbers over 2 day increments. Data were compiled from at least 3 independent experiments (n=5-8). Note that proliferation is not impaired in the S1PR1 transduced population (relative to mock or empty transduced) (b), and that there is no selective disadvantage of S1PR1 transduced cells for expansion (a). Virus was constructed with help from June Yong Lee.

This gave us a model to address the significance of KLF2 and S1PR1 downregulation in T_{RM} by forcing S1PR1 in activated T cells.

Forced expression of S1PR1 in CD8+ T cells inhibits establishment of T_{RM}

We next wanted to explore how forced S1PR1 expression would affect T_{RM} residency. We retrovirally transduced activated congenically distinct P14 T cells with either the S1PR1 or empty vector, transferred these cells into uninfected recipients, and subsequently infected the animals with LCMV the following day. Analysis of animals during the memory phase of the response determined that while the frequency of empty vs S1PR1 transduced P14 cells was comparable in lymphoid tissue, the percent of S1PR1 transduced P14 cells was noticeably decreased in the parenchyma of non-lymphoid tissue relative to empty transduced P14 cells (Fig 3-3a).

To normalize between experiments, we calculated the percent transduction in each tissue relative to the spleen of each animal (Fig 3-3b). The percent of S1PR1 transduced P14 relative to the spleen was significantly diminished in the salivary glands, kidney, and small intestine LPL and IEL, while this result was not seen with empty transduced P14 cells (Fig 3-3c). This demonstrated that while forcing S1PR1 had little impact on lymphoid tissue, it had a profound affect on the representation of P14 cells in non-lymphoid tissue. Similarly, while the absolute number of S1PR1 and empty transduced P14 was comparable in lymphoid tissue, the number of S1PR1 transduced P14 cells was considerably lower in non-lymphoid tissue compared to empty transduced cells (Fig 3-3d/e).

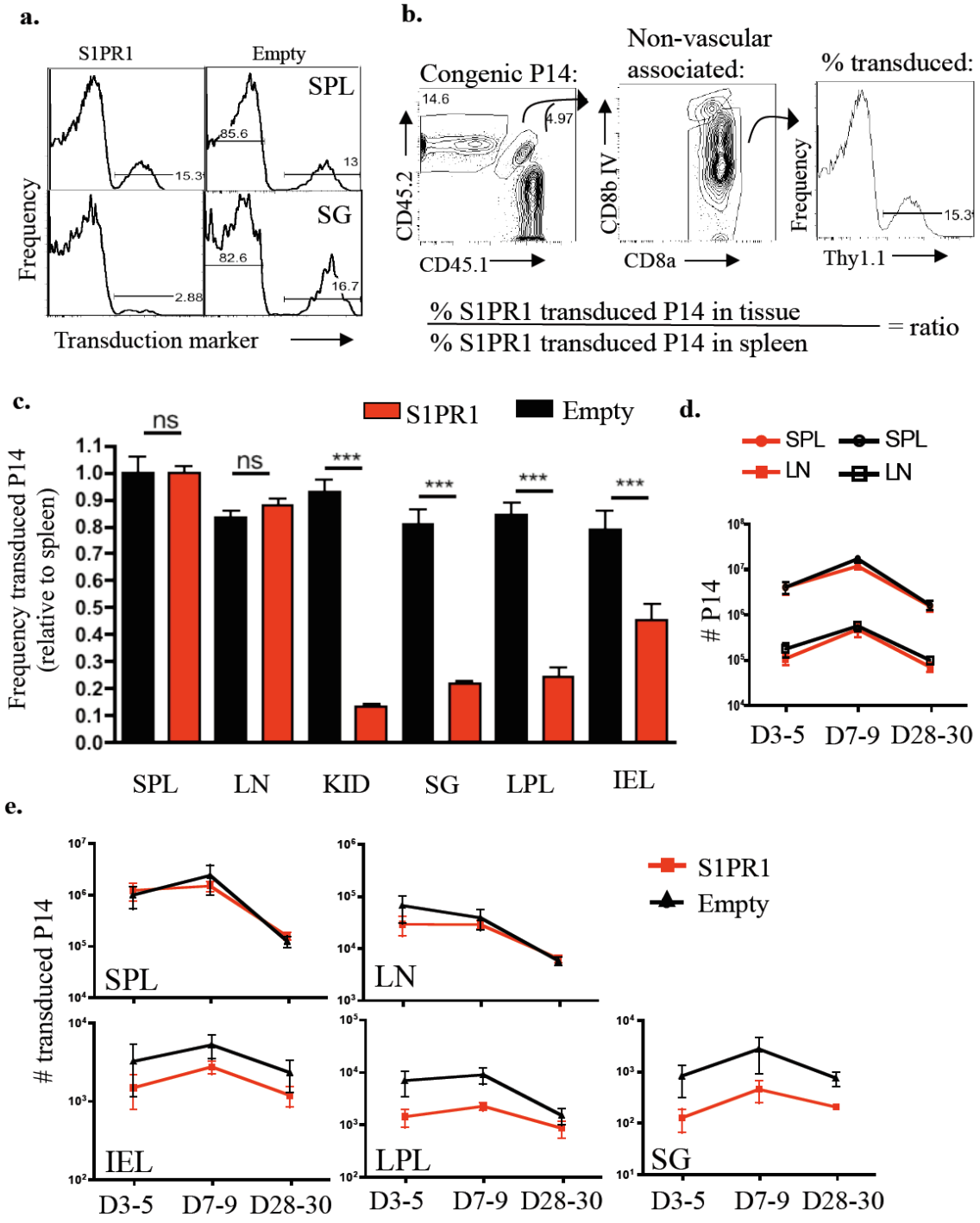
a.
S1PR1
Empty
SPL
SG
Frequency
85.6
15.3
13
82.6
2.88
16.7
Transduction marker
b.
Congenic P14:
Non-vascular associated:
% transduced:
14.6
4.97
CD45.2
CD45.1
CD8b IV
CD8a
Frequency
15.3
Thy1.1
% S1PR1 transduced P14 in tissue
% S1PR1 transduced P14 in spleen
= ratio
c.
S1PR1
Empty
Frequency transduced P14 (relative to spleen)
ns
ns
***
***
***
***
SPL
LN
KID
SG
LPL
IEL
d.
SPL
SPL
LN
LN
P14
D3-5
D7-9
D28-30
e.
S1PR1
Empty
transduced P14
SPL
LN
IEL
LPL
SG
D3-5
D7-9
D28-30

Figure 3-3. Forced S1PR1 prevents establishment of T_{RM}. Activated P14 CD8+ T cells were transduced with retroviral vectors encoding S1PR1 and the transduction marker Thy-1.1 (S1PR1) or Thy-1.1 alone (Empty). Congenically distinct P14 S1PR1 and empty-vector transduced cells were co-transferred into recipients subsequently infected with LCMV. (a) Representative graphs (n=12 from 4 independent experiments) showing the frequency of P14 CD8+ T cells transduced with S1PR1 and empty vectors isolated from SPL and SG, >30 days post LCMV. (b) Gating strategy for calculating % transduction per tissue and equation for calculating normalized transduction relative to the SPL. Adoptively co-transferred P14 cells were identified using congenic markers, non-vascular-associated cells were detected using CD8b IV administration, and percent transduction was calculated using the Thy1.1 marker. (c) Percent transduction of empty (black) and S1PR1 (red) transduced P14 CD8+ T cells in the parenchyma of the indicated tissues 28-60 days post LCMV. Data are normalized to the percent transduction for the spleen from the same animal. (d) Number of total non-vascular-associated P14 T cells from SPL and LN that underwent S1PR1 (red) or empty (black) transduction prior to adoptive transfer. The date ranges are the times of sacrifice following *in vivo* LCMV infection. (e) Number of transduced, non-vascular-associated P14 T cells for empty (black) or S1PR1 (red) vectors in indicated tissues within the time ranges following LCMV infection *in vivo*. (b-c) Data are compiled from 4 independent experiments (n=9-15). Graphs show mean +/- SEM for 11-18 samples per group, compiled from at least 4 independent experiments. Statistical significance is indicated (***, $p<0.001$; ns, $p>0.05$).

This result was observed in the parenchyma of non-lymphoid tissue but not the corresponding vascular-associated P14 cells, ruling out the effects of tissue processing on these results (Fig 3-4a). Analyzing the percent transduction relative to the spleen at earlier timepoints revealed that forcing S1PR1 had an impact on P14 cells very early on in the immune response during the time when T_{RM} were developing (Fig 3-4b). This is consistent with S1PR1 downregulation being important for the seeding of non-lymphoid tissue during the establishment of T_{RM} early after infection (Fig 2-3c).

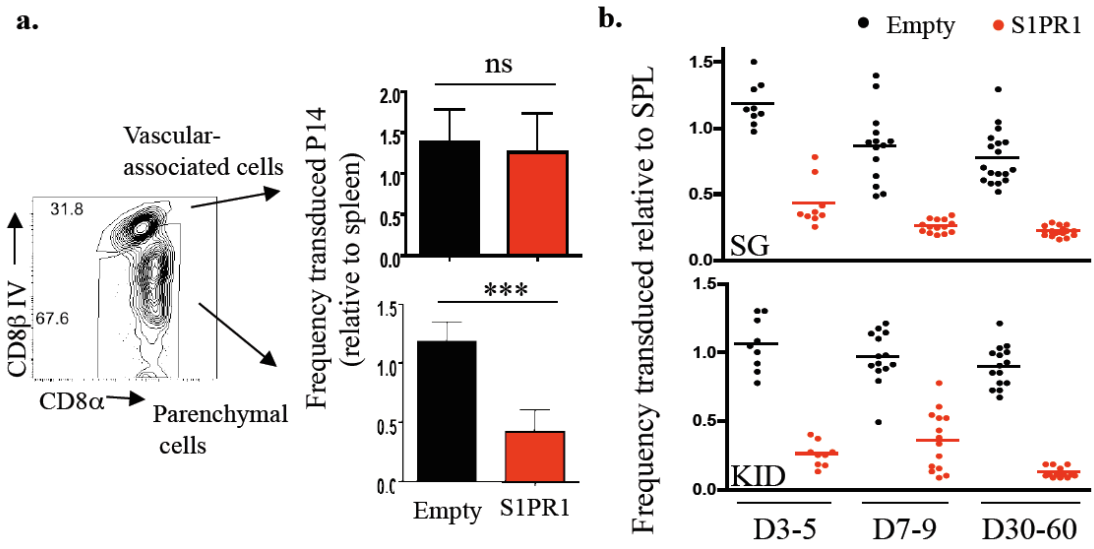

Figure 3-4. Forced S1PR1 prevents establishment of T_{RM} early after infection and is specific to the parenchyma of non-lymphoid tissue. As in Figure 3-3, activated P14 CD8+ T cells were transduced with retroviral vectors encoding S1PR1 and the transduction marker Thy-1.1 (S1PR1) or Thy-1.1 alone (Empty). Congenically distinct P14 S1PR1 and empty-vector transduced cells were co-transferred into recipients subsequently infected with LCMV. (a) Relative transduction for S1PR1 (red) or Empty vector (black) transduced P14 CD8+ T cells present in vascular-associated (top) versus tissue parenchyma (bottom) of the SG 5 days after LCMV infection. Bar graph is compiled from 3 independent experiments (n=9). (b) Percent transduction relative to spleen of empty (black) vs S1PR1 (red) transduced P14 cells days post LCMV at indicated time points in KID and SG. N=9-18 from at least 3 independent experiments. Similar timecourse trends were observed for other NLT (data not shown). In all panels, analysis gated on live P14 CD8+ T cells, and (except panel a) with exclusion of vascular-associated cells.

The few remaining S1PR1 transduced P14 in non-lymphoid tissue do not skew towards being CD103+

The frequency of S1PR1 transduced P14 in the small intestine IEL compartment relative to the spleen, while still significant, was much more variable compared to other tissues (Fig 3-5a vs 3-4b). Since previous research has shown that CD103 expression is significant for the retention of T_{RM} in the small intestine IEL but not LPL[93], we

considered whether upregulation of CD103 might override S1PR1 in promoting tissue residency. If this were the case, we would see a skewing toward CD103+ transduced P14 cells within the small compartment of S1PR1 transduced P14 that remained in the IEL. However, CD103 profiles were not altered when forcing S1PR1 arguing against this model (Fig 3-5b).

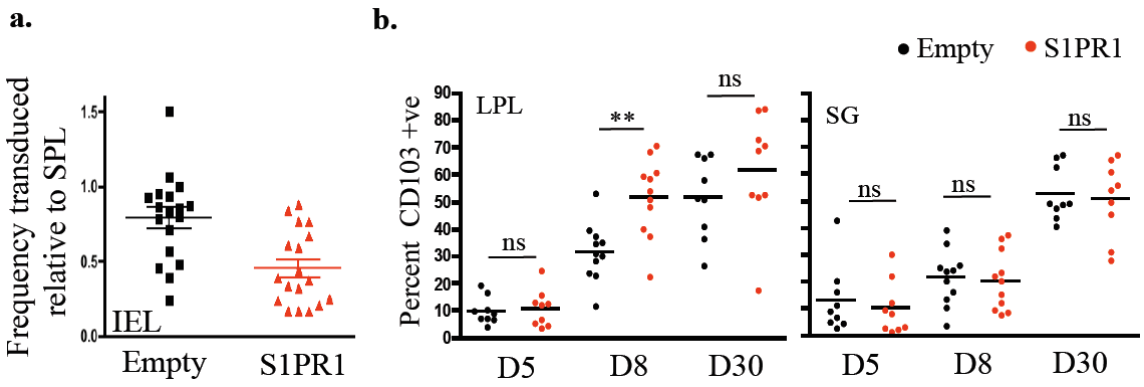

Figure 3-5. Compared to empty-transduced P14 cells, there is no skewing toward CD103 expression on the few S1PR1-tranduced P14 cells that remain in non-lymphoid tissue. (a) Shows percent transduction (relative to spleen) of empty (black) and S1PR1 (red) vector-transduced P14 cells in the parenchyma of IEL 28-60 days post LCMV. The frequency of S1PR1 transduced cells was more variable in the IEL versus other NLT (see Fig 3-4b). N=15-18 from at least 5 independent experiments. (b) The percentage of CD103+ P14 cells transduced by empty (black) or S1PR1 (red) vectors in the indicated tissue parenchyma isolated at 5, 8 and 30 days post LCMV infection (n=9 from 3 independent experiments). (a-b) Gated on live, non-vascular-associated CD8+ P14 T cells.

Differences in T cell priming location do not account for S1PR1 effects seen while treatment with FTY720 significantly diminishes the affects of forcing S1PR1 on T_{RM}

It was possible that forcing S1PR1 in activated T cells resulted in initial altered trafficking after adoptive cellular transfer *in vivo*. If this were the case, S1PR1 vs empty transduced P14 cells may be activated in different locations leading to differing activation and differentiation profiles. To eliminate this possibility, we allowed activated S1PR1

and empty transduced P14 to remain cultured *in vitro* as the cells developed into effector T cells. Transduced effector T cells were then transferred into uninfected recipients which remained uninfected. This allowed us to distinguish whether differences in initial T cell priming were governing the noticeable decrease in representation of S1PR1 transduced P14 in non-lymphoid tissue. While transfer into uninfected hosts did compromise the magnitude of cells getting into non-lymphoid tissue (data not shown), eliminating the *in vivo* priming step of T cell activation still resulted in decreased percentages of S1PR1 transduced P14 cells in the salivary gland and small intestine LPL relative to the spleen (Fig 3-6, vehicle only samples). Notably, there was not a decrease in the representation of S1PR1 transduced P14 cells in the small intestine IEL compartment with this experimental approach (Fig 3-6). This is consistent with the variability observed in the small intestine IEL in general (Fig 3-5a) and suggests that establishment of residency in the small intestine IEL may be more complex than other tissues.

We next tested how FTY720 treatment, a drug that blocks S1PR1 function, influenced trafficking of effector S1PR1 transduced P14 T cells. Administration of FTY720 4 days after cellular transfer blunted the effect caused by forced S1PR1 expression analyzed 24 hours later in the salivary glands and small intestine LPL (Fig 3-6). With this analysis, the frequency of transduced P14 cells is relative to the spleen of each respective condition, with the spleen being normalized to the untreated samples. This data suggests that surface S1PR1 is significant for causing diminished T_{RM} formation when forcing S1PR1, suggesting inhibition of S1PR1 signaling permits T_{RM} generation.

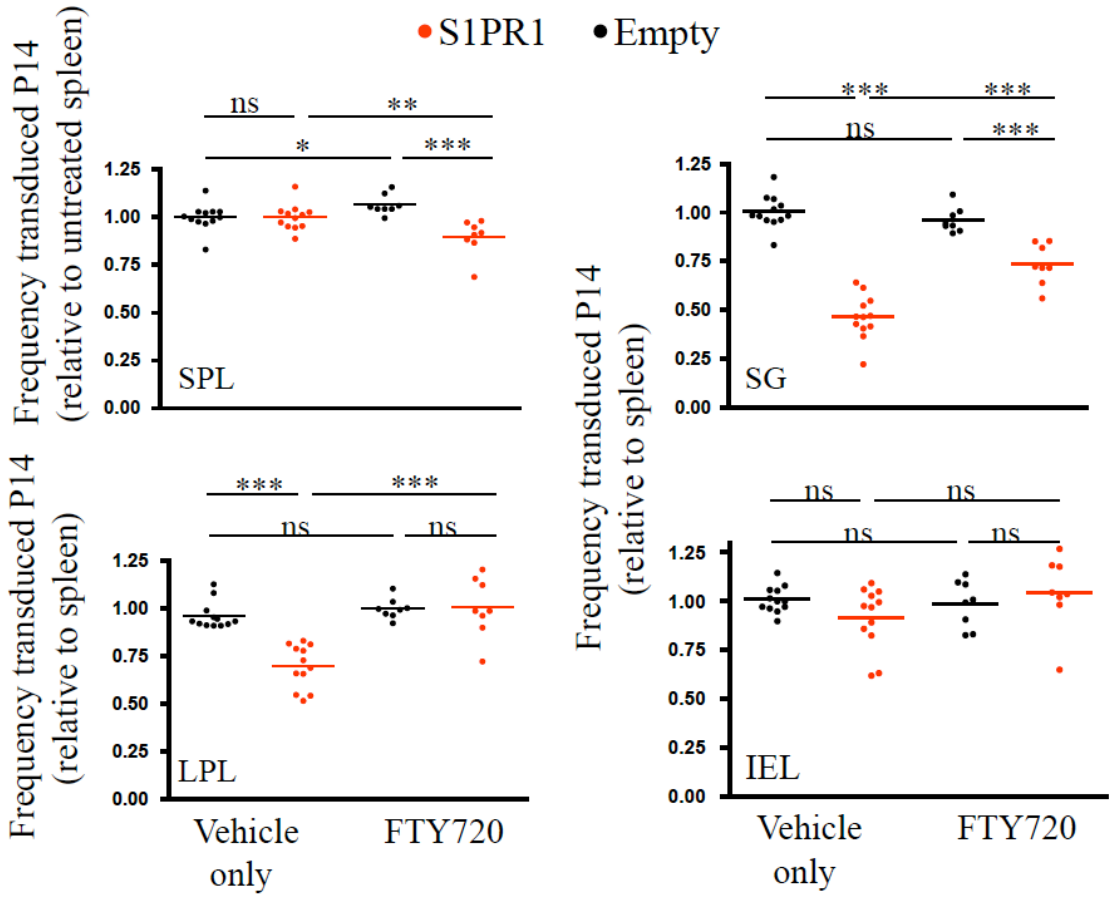

Figure 3-6. Forced S1PR1 also prevents establishment of T_{RM} from transduced effector P14 cells transferred into uninfected hosts that is dependent on S1PR1 signalling. Transduced effector P14 cells were transferred into uninfected recepients and treated with vehicle alone (n=12 from 4 independent experiments) or 1mg/kg FTY720 (n=8 from 3 independent experiments) starting at day 4. Cells were harvested at Day 5 after transfer. Relative percent transduction of S1PR1 (red) or empty (black) transduced P14 cells normalized to the spleen from the same animal. There is a trend for reduced frequency of S1PR1 transduced cells in the small intestine IEL, but this was highly variable and not stastically significant. In all panels, analysis gated on live P14 CD8+ T cells with exclusion of vascular-associated cells.

KLF2 downregulation is not a consequence of sustained TCR stimulation

The loss of KLF2 during T_{RM} generation shown in chapter 2 indicates a basis for impaired S1PR1 expression, but what signals induce downregulation of KLF2 in non-lymphoid tissue? TCR stimulation is well known to terminate KLF2 expression[76, 85]. Even though our system involved an acute infection (the LCMV armstrong strain), it was possible that sustained TCR stimulation was driving down KLF2 levels.

To test this possibility, we first investigated whether KLF2 was still down-regulated in a condition where no cognate antigen was present. To do this, we transferred *in vitro* generated effector $KLF2^{GFP}$ P14 T cells into uninfected hosts (similar to Fig 3-6), and monitored $KLF2^{GFP}$ expression 12-15 day later. While the migration of P14 T cells into non-lymphoid tissue was less efficient in uninfected hosts compared to after infection (data not shown), we observed similar patterns of KLF2 expression with lymphoid P14 cells exhibiting a $KLF2^{HI}$ phenotype while $KLF2^{GFP}$ levels in non-lymphoid tissues were low (Fig 3-7a vs 2-3). This demonstrates that engagement with specific foreign peptide/MHC ligands is not required for the downregulation of KLF2 in CD8+ T cells developing into T_{RM} in non-lymphoid tissue.

It was possible, however, that TCR engagement with other cross-reactive foreign peptides (ex. commensal microbes) or even self-peptide/MHC could drive down KLF2 expression in non-lymphoid tissue. To investigate this, we used $Nur77^{GFP}$ transgenic mice, which sensitively report TCR stimulation[105]. Naïve $Nur77^{GFP}$ P14 T cells were adoptively transferred into mice and subsequently infected with LCMV (or not, for the uninfected controls). 30 days later, $Nur77^{GFP}$ levels in memory P14 T cells were

comparable to naïve levels in most non-lymphoid tissue (small intestine IEL, salivary glands, and kidney) (Fig 3-7b). Systemic gp33-41 peptide given 8 hours before harvest confirmed that the Nur77^{GFP} reporter was functional. We did observe modest (yet reproducible) increases in Nur77^{GFP} expression in cells isolated from the small intestine LPL for unclear reasons. With the possible exception of the small intestine LPL, this showed that basal TCR stimulation between P14 cells in lymphoid and non-lymphoid

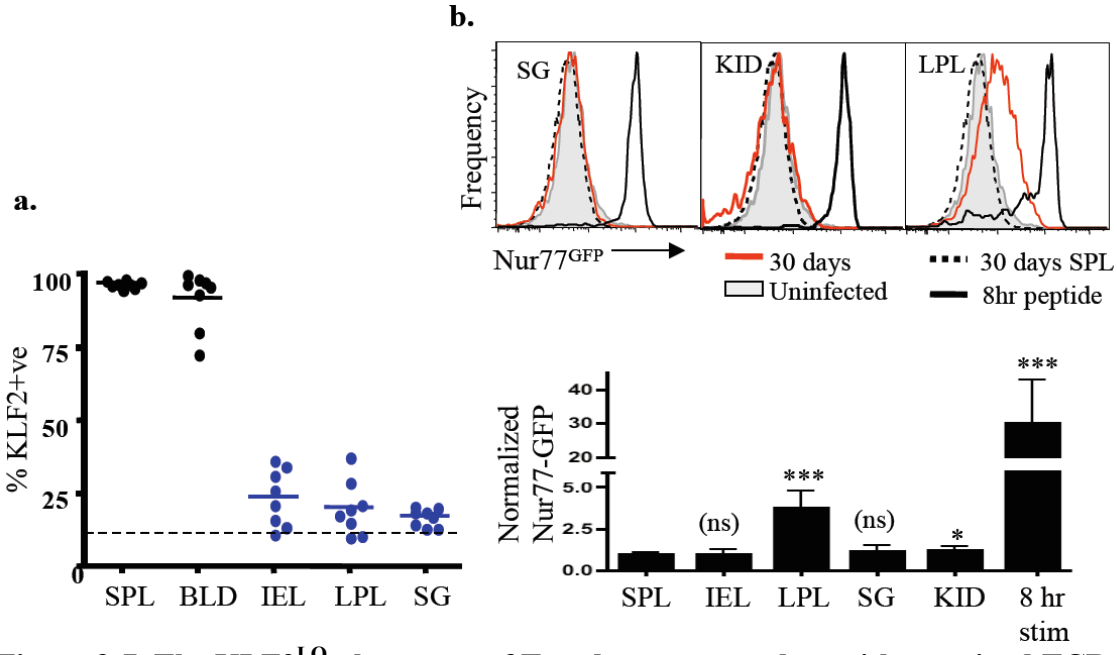

Figure 3-7. The KLF2^{LO} phenotype of T_{RM} does not correlate with sustained TCR engagement. (a) 1x10^6 *in vitro* activated effector KLF2^{GFP} P14 splenocytes were transferred into uninfected hosts and 12-15 days later the KLF2^{GFP} status of live non-vascular-associated P14 cells in lymphoid tissue (black) and non-lymphoid tissue (blue) were analyzed. N=8 from 3 independent experiments**.** Dotted line indicates threshold defined as KLF2-ve based on WT P14 cells being defined as 90% KLF2-ve (similar to Fig 2-3c). (b) To evaluate TCR activation status of CD8+ T cells in NLT, Nur77^{GFP} P14 CD8+ T cells were transferred into C57BL/6 and either infected with LCMV or left uninfected (grey-filled). Thirty days after infection, Nur77^{GFP} expression in P14 T cells isolated from tissue parenchyma of indicated NLT (red) was compared to cells from spleen (dotted line). Black lines indicate Nur77^{GFP} expression in mice injected with gp33-44 peptide 8 hours before harvest. Bar graph shows Nur77^{GFP} expression as mean +/- SD, normalized to spleen for each group. Data are compiled from 4 independent experiments (n=11-12). Statistical analysis is relative to spleen.

tissue is comparable. Taken together, these data suggest that cognate antigen is not the universal mechanism of KLF2 downregulation in CD8+ T cells establishing residency in non-lymphoid tissue.

Cytokines induced KLF2 downregulation *in vitro*

Cytokines have also been shown to affect KLF2 expression[79, 85, 88]. A recent study demonstrated that particular cytokine combinations, specifically TGF-β paired with other inflammatory cytokines, could drive the T_{RM} phenotype *in vitro*[93]. Therefore, we wanted to determine whether these T_{RM} inducing cytokines were also driving down KLF2 expression. With a similar experimental design as the Masopust group, we transferred congenically distinct $KLF2^{GFP}$ and WT P14 cells into mice and infected them with LCMV the following day. 4.5 days later, we harvested the spleen and exposed bulk splenocytes to different cytokine mileus *in vitro* for 40 hours.

Compared to cultures not receiving additional cytokines, pair-wise combinations of TGF-β, IL-33, and TNFα all significantly down-regulated KLF2 protein 40hrs later (Fig 3-8a). The addition of all three inflammatory cytokines resulted in the most pronounced downregulation of KLF2, suggesting a synergistic affect when multiple cytokines were present. IL-6 and TGF-β resulted less KLF2 downregulation (Fig 3-8a), consistent with this combination not driving the T_{RM} phenotype in previous studies[93] and suggesting that not all cytokine combinations will drive down KLF2 protein. KLF2 downregulation was sequential over time indicating that transcriptional regulation may

also be involved instead of or along with translational regulation of KLF2 protein (Fig 3-8b).

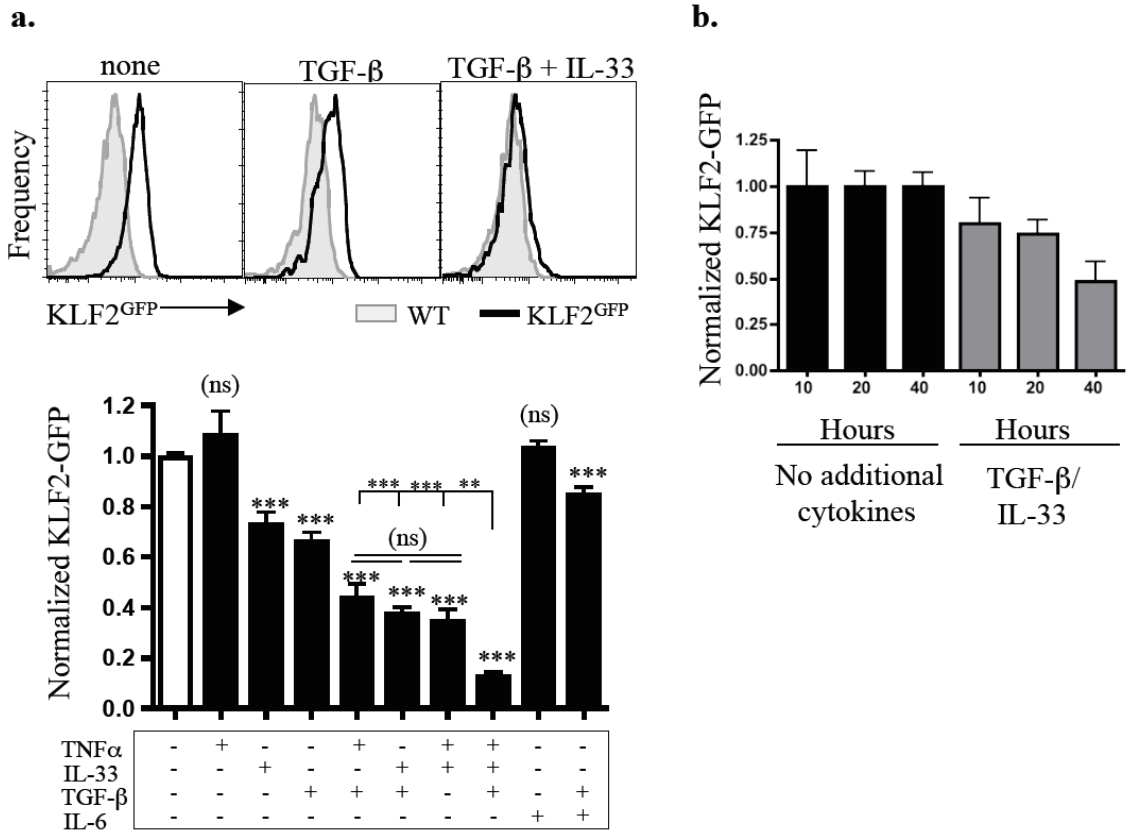

Figure 3-8. Diverse cytokines induce KLF2 downregulation in activated CD8+ T cells *in vitro*. (a-b) WT (grey) and KLF2^{GFP} (black) P14 CD8+ T cells were co-transferred and activated for 4.5 days *in vivo* with LCMV, and then cultured with indicated cytokines. (a) Splenocytes were cultured for 40 hrs *ex vivo*. Histograms show representative examples, while the bar graph indicates compiled data (from at least 4 experiments; n=11-18), normalized on cells cultured with no added cytokines. Data show mean +/- SEM, with statistical analysis relative to the no cytokine group. (b) Spenocytes were exposed to TGF-β and IL-33 (grey) or no additional cytokines (black) (set as one) for 10-40 hours *ex vivo* (n=11-13 from at least 4 independent experiments).

Cytokine induced KLF2 downregulation is dependent on the P13K/AKT pathway

KLF2 is induced by the Foxo1 transcription factor and Foxo1 has been shown to be negatively regulated by the P13K/AKT pathway[89-91]. While TGF-β signaling is

primarily through the smad pathway, it has been shown to activate P13K/AKT in some situations[106]. Therefore, we wanted to determine whether cytokine-induced downregulation of KLF2 was also P13K/AKT pathway dependent.

D4.5 bulk splenocytes were exposed to TGF-β /IL-33 or no additional cytokines *in vitro* as in Figure 3-8 with or without the presence of either the P13K inhibitor LY294002 or the AKT inhibitor AKTi. When P13K/AKT inhibitors were present during *in vitro* culture, there no longer was a decrease in KLF2 protein caused by TGF-β /IL-33 (Fig 3-9a/b). Similar results were seen using *in vitro* activated P14 T cells, eliminating the possibility of the cytokines or inhibitors functioning through a cell type other than CD8+ T cells (Fig 3-9c). This suggests that downregulation of KLF2 caused by T_{RM}-inducing cytokines is functioning through the P13K/AKT pathway.

While cytokine-induced downregulation of KLF2 was P13K/AKT dependent, the upregulation of CD103 in the same culture was not dependent on this pathway (Fig 3-10). This indicates that the signals causing downregulation of KLF2 and upregulation of CD103 are not identical.

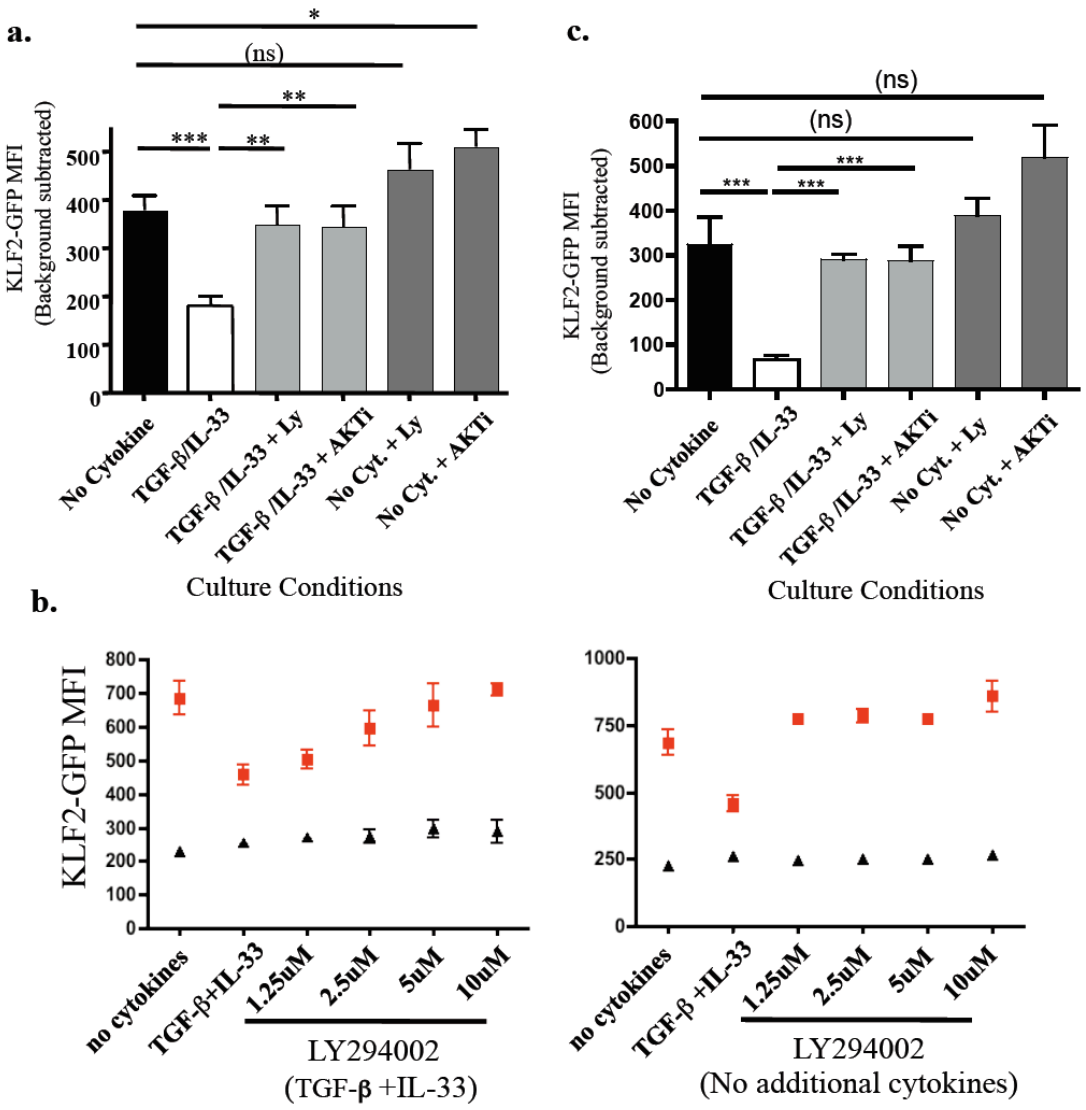

Figure 3-9. Cytokine-induced downregulation of KLF2 is dependent on the P13K/AKT pathway (a-b) WT (grey) and KLF2^{GFP} (black) P14 CD8+ T cells were co-transferred and activated for 4.5 days *in vivo* with LCMV, and then cultured with indicated cytokines with or without addition of either LY294002 or AKTi, to inhibit PI3K and AKT, respectively. (a) LY294002 (10uM) or AKTi (1uM) concentrations. (n=11-12 from 4 independent experiments). (b) Splenocytes were exposed to TGF-β and IL-33 (left) or no additional cytokines (right) in the presence of varying dilutions of the LY294002 PI3K inhibitor for 40 hrs *ex vivo* (representative graph from 4 independent experiments (n=8)). Graph shows KLF2^{GFP} mean flourescent intensity of P14 cells. (c) WT and KLF2^{GFP} P14 CD8+ T cells were activated *in vitro* for 48 hours and then cultured with cytokines and inhibitors as in a. Experiments in part c were conducted by graduate student June Yong Lee.

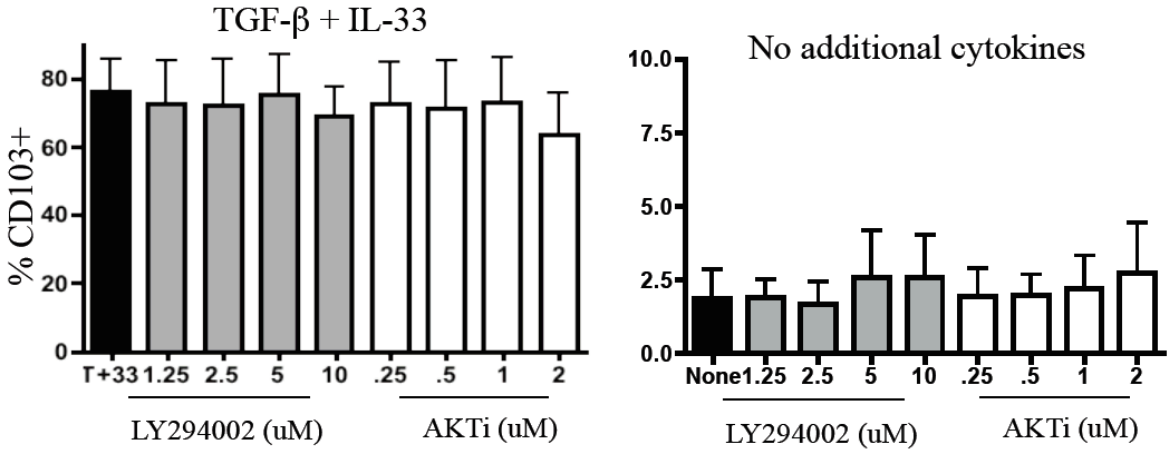

Figure 3-10. While the P13K/AKT pathway affects cytokine-induced downregulation of KLF2, it does not affect the upregulation of CD103. WT (grey) and $KLF2^{GFP}$ (black) P14 CD8+ T cells were co-transferred and activated for 4.5 days *in vivo* with LCMV, and then cultured with indicated cytokines with or without addition of either LY294002 or AKTi, as in Figure 3-9. Percentage of CD103+ P14 cells from cultures in (Fig 3-9b) and similar cultures using AKTi (Akt inhibitor). Data are compiled from 4 independent experiments (n=12).

We next wanted to determine the mechanism of cytokine-induced downregulation of KLF2. We sorted *in vitro* activated CD8+ T cells 40 hours after *in vitro* cytokine culture as in Figure 3-9c and performed RT real-time PCR. Along with KLF2 protein, KLF2 mRNA was also lower in TGF-β/IL-33 cultures relative to no additional cytokine levels (Fig 3-11). The transcripts for KLF2's targets S1PR1 (*edg1*) and CD62L (*sell*) were also negatively affected suggesting the downregulation of KLF2 was functionally significant for transcriptional regulation (Fig 3-11). The downregulation of KLF2, CD62L, and S1PR1 transcripts was negatively affected by blocking AKT suggesting transcriptional regulation of KLF2 was also dependent on the P13K/AKT pathway (Fig 3-11). Hence, TGF-β and IL-33, in a P13K/AKT dependent fashion, induce changes in

gene expression similar to those observed in T_{RM}. Whether these cytokines directly activate the P13K/AKT pathway or act through intermediate factors is, however, unclear.

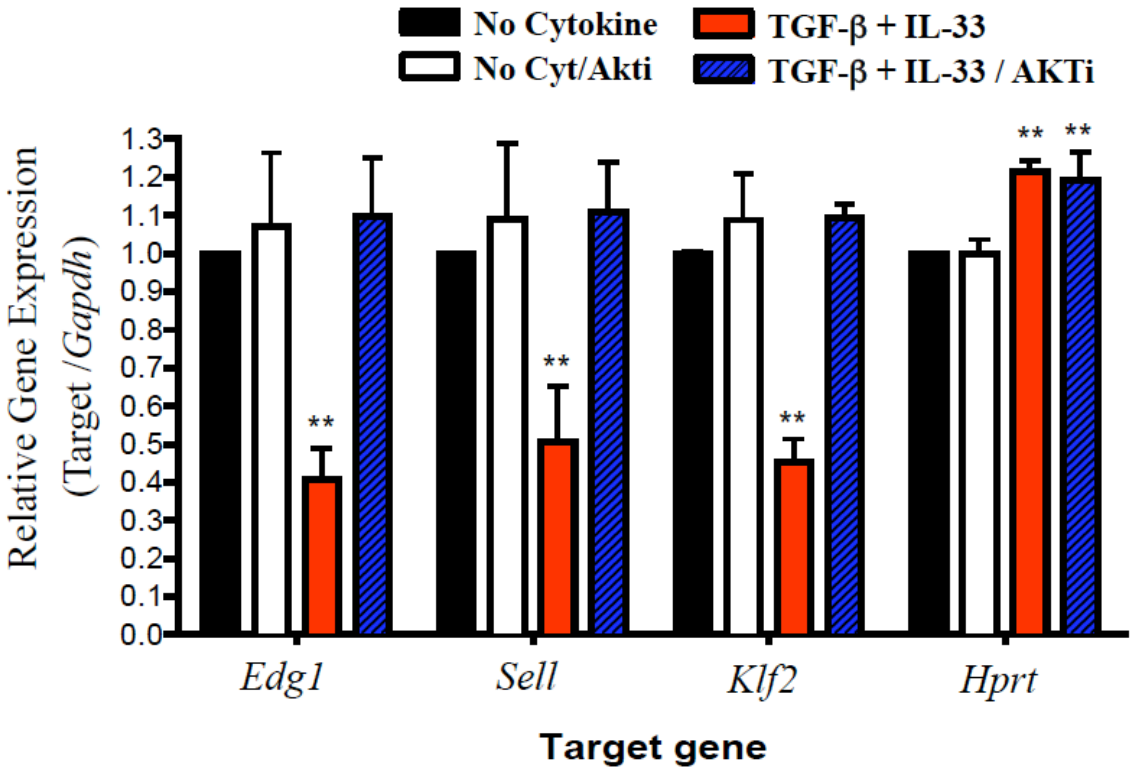

Figure 3-11. Cytokine-induced downregulation of KLF2 via the P13K/AKT pathway is transcriptionally relevant for KLF2 targets S1PR1 and CD62L. WT and $KLF2^{GFP}$ P14 CD8+ T cells were activated *in vitro* for 48 hours and then cultured with cytokines and AKTi (1uM) for 40 hrs *ex vivo* as in Figure 3-9. Bar graph shows shows indicated gene expression determined by RT-PCR of sorted P14 CD8+ T cells. Data are compiled from 4 independent experiments.

Global administration of a P13K inhibitor *in vivo* negatively affects T_{RM} formation and Foxo1 is downregulated in T_{RM} *in vivo*

Lastly, we investigated whether affecting P13K *in vivo* would also affect KLF2 levels and the formation of T_{RM}. We adoptively transferred $KLF2^{GFP}$ and WT P14 mice, infected them with LCMV, and 4 days later globally administered LY294002. 24 hours

after LY294002 treatment we observed a significant increase in the $KLF2^{GFP}$ MFI in P14 cells receiving the P13K inhibitor versus the vehicle only in the small intestine LPL and salivary glands, with a similar trend in the small intestine IEL (Fig 3-12a). Along with this, the absolute numbers of parenchymal P14 T cells was significantly lower in animals receiving LY294002 compared to vehicle only controls (Fig 3-12b). This is consistent with the P13K/AKT pathway being important for the downregulation of KLF2 and the establishment of T_{RM}. However, it is worth noting that systemic P13K inhibition will have diverse affects on other cell types and may complicate interpretations of this data.

Since Foxo1 is dependent on the P13K/AKT pathway, we lastly wanted to determine whether foxo1 itself was also affected in T_{RM} *in vivo*. While phosphorylation of Foxo1 results in nuclear exclusion of the transcription factor, studies have also shown that P13K/AKT signaling can elicit Foxo1 protein degradation[107]. We found that memory P14 T cells in the salivary glands had significantly lower Foxo1 protein compared to memory P14 T cells in the spleen (Fig 3-13), consistent with the induction of this pathway in T_{RM} in non-lymphoid tissue *in vivo*.

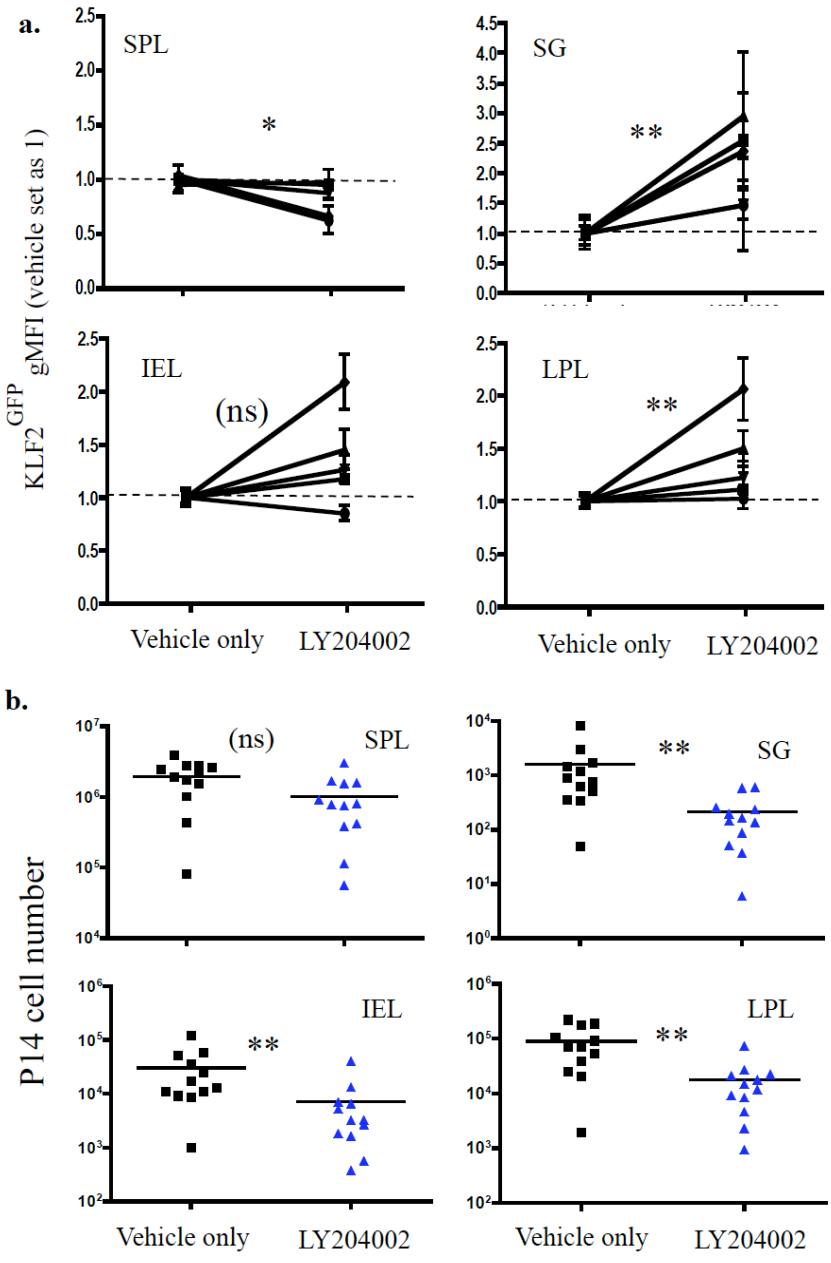

Figure 3-12. *In vivo* administration of the PI3K inhibitor LY294002 leads to upregulation of KLF2 and decreased P14 CD8+ T cell numbers in the SG and LPL
(a-b) WT and KLF2^{GFP} P14 CD8+ T cells were co-transferred into C57BL/6 which were then infected with LCMV. Four days post infection, 50mg/kg LY294002 or vehicle only was administered IP every 12 hours for 24 hours. Cells were harvested on day 5 post infection. N=12 from 5 independent experiments. (a) KLF2^{GFP} gMFI (minus WT gMFI) was calculated and analyzed with vehicle only set as 1. (b) Total live non-vascular-associated P14 cells was determined for tissues indicated. Statistical analysis for (a) used ANOVA, while (b) used Student's t-test.

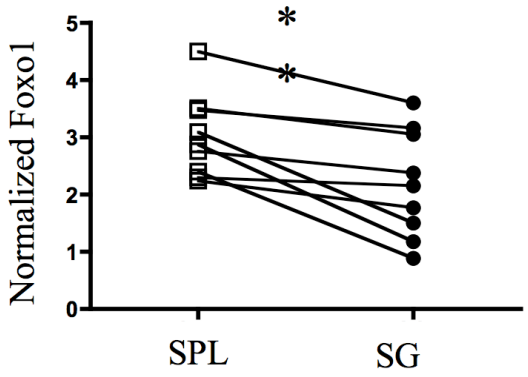

Figure 3-13. Foxo1 expression is reduced in memory P14 CD8+ T cells from NLT versus lymphoid sites. P14 cells were isolated from SPL and SG, 30-60 days post LCMV and stained for intracellular Foxo1 protein (n=9 from 3 independent experiments). Data are normalized on isotype control and gated on live P14 CD8+ T cells. Statistical analysis used Student's t-test.

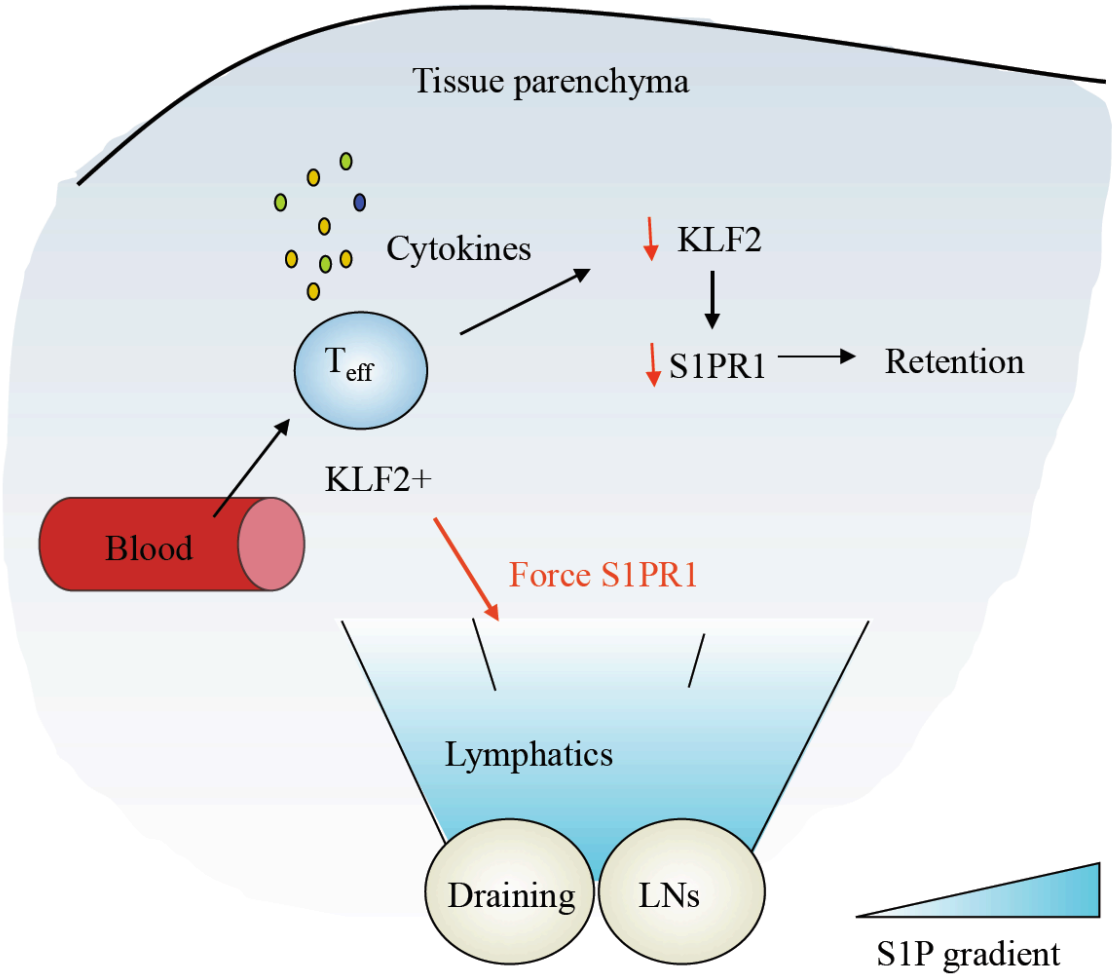

Figure 3-14. Model of KLF2 downregulation in T_{RM} in non-lymphoid tissue. KLF2+ T cells enter non-lymphoid tissue from the blood. Local inflammatory cytokines converging on the P13K/AKT pathway cause the downregulation of KLF2 and its target S1PR1 leading to cell retention. Forcing S1PR1 results T cell egress from non-lymphoid tissue.

Discussion

In this chapter we investigated the functional significance of the downregulation of KLF2 and its transcriptional targets. Using a retroviral transduction model, we show that forced expression of S1PR1 prevents the establishment of T_{RM} in non-lymphoid tissue. Additionally, we determined that cytokines that have been shown to induce the T_{RM} phenotype *in vitro* also downregulate KLF2, in a P13K/AKT dependent fashion. These data suggest that the local cytokine mileu in non-lymphoid tissue can drive down KLF2. In turn, KLF2's target S1PR1 is downregulated which retains T cells in non-lymphoid tissue allowing them to adopt the T_{RM} phenotype (Fig 3-14).

Pairwise combinations of the inflammatory cytokines IL-33, TNFα, and TGF-β all resulted in KLF2 downregulation *in vitro*. As such, while it would be informative to identify the main essential cytokines that affect KFL2 downregulation *in vivo*, the fact that multiple cytokines can yield these same results *in vitro* suggests that multiple cytokines may all be able to drive down KLF2 *in vivo*. Therefore, single, double, or even triple cytokine KO experiments may not yield fruitful results in determining the exact cytokines responsible for KLF2 downregulation *in vivo*. Likewise, it may be that different cytokines are important in different non-lymphoid tissue. The more essential point is that an array of different cytokines are all able to converge on the same pathway, P13K/AKT, to drive down KLF2.

Interestingly, while cultures with TGF-β/IL-33 drive down KLF2 and upregulate CD103 *in vitro*, only KLF2 downregulation was affected by P13K/AKT inhibition (Fig 3-9 and 3-10). This suggests that the signals that govern KLF2 downregulation and

CD103 upregulation are not identical. TGF-β responsiveness has been shown to be necessary for the induction of CD103 on CD8+ T cells in the small intestine intraepithelial cells *in vivo*[93]. It may be that in CD8+ T cells in the small intestine IEL and perhaps various other non-lymphoid tissue, TGF-β signalling results in CD103 upregulation through the more classically defined SMAD-associated pathway than the P13K/AKT pathway[108]. Although it is worth pointing out that CD103 is not induced on all NLT (Fig 2-3c).

Along with this, transferring effector KLF2^{GFP} P14 T cells into uninfected hosts caused a similar decrease in KLF2^{GFP} in all NLT (Fig 3-7a), mirroring experiments involving infection (Fig 2-1). At the same time, transferring effector S1PR1 transduced P14 T cells into uninfected hosts yielded a similar decrease in the representation of S1PR1 transduced P14 T cells in most tissues, but not the small intestine IEL (Fig 3-6). We did not perform a detailed analysis of the kinetics of KLF2 downregulation using the no infection system, although the limited experiments we did conduct suggested that the downregulation of KLF2 was slower when the hosts were uninfected (data not shown). It may be that additional signals are needed for the establishment of T_{RM} in small intestine IEL compared to other tissues, and these additional signals may also affect CD103 induction. Since the small intestine IEL T_{RM} upregulate CD103 the quickest compared to all other non-lymphoid tissue analyzed (Fig 2-3c), in situations where KLF2 downregulation is slower (lack of infection) the upregulation of CD103 in the SI IEL may be more important for retention than the decrease in S1PR1. This would explain why forced S1PR1 was significant for decreasing T_{RM} in the SI IEL in a model of infection,

but not in our uninfected system. Further experiments detailing the kinetics of KLF2 downregulation and CD103 upregulation in the context of no infection could determine whether this hypothesis is accurate.

Based on S1PR1's established role in lymph node egress[38, 96], it seems most probable that the mechanism that leads to reduced T_{RM} in NLT during our forced S1PR1 experiments is tissue egress. However, while global survival defects are not seen *in vitro* or in S1PR1-transduced P14 in lymphoid tissue *in vivo*, it is formally possible that selective survival is significant for CD8+ T cells that migrate to NLT. Experiments using Bim KO P14 could distinguish whether this is a possibility. At the same time, proliferation defects isolated to NLT could account for the percentage discrepancy between S1PR1 and empty transduced P14. While this is unlikely considering no other studies have identified S1PR1 having an affect on proliferation, experiments transferring CFSE labeled S1PR1 and empty transduced P14 into uninfected hosts could address this issue. Alternatively, establishing a model to selectively label P14 that have trafficked to a non-lymphoid tissue could enable us to detect S1PR1-transduced P14 that have egressed from a NLT. This could be done using Kaede transgenic mice whose cells contain a photoconvertible fluorescent protein, allowing us to monitor T_{RM} by exposing a NLT to violet light[109].

Experiments using global P13K inhibition resulted in dampened KLF2 downregulation and fewer P14 in non-lymphoid tissue. Since P13K inhibition will act on many cell types, it's unclear whether the results shown were due to the inhibitor acting directly on P14 cells or through another cell type. It is also not clear as to whether the

decrease in P14 cells found in NLT is due to tissue egress vs survival. Since an affect was observed only 24 hours after inhibitor administration, it seems unlikely that the downregulation of KLF2 affecting S1PR1 would happen so quickly. It may be that P14 that migrate into NLT need to receive a P13K signal to remain alive, although at this time we do not have direct evidence to support this.

We also conducted experiments using treatment of FTY720, which affects the function of S1PR1. However, while FTY720 is a functional antagonist of S1PR1, it is an agonist for the receptor causing it to be internalized, blocking its ability to function. This means that forced S1PR1 transduced T cells that are exposed to FTY720 will receive a strong S1PR1 signal. We did notice in experiments using FTY720 that there was a global affect on S1PR1 transduced P14 T cells that was not observed in just the non-lymphoid tissue. This can be seen when comparing the frequency of S1PR1 vs empty transduced P14 in the spleen of FTY720 treated mice (Fig 3-6, upper left). There was a significant decrease in the frequency of S1PR1 transduced P14 cells suggesting that FTY720 selectively causes death in transduced P14 independent of whether they are located in lymphoid or non-lymphoid tissue. It may be that the strong signal elicited by FTY720 treatment in cells experiencing additional surface S1PR1 results in cellular death, making interpretation of these FTY720 experiments more complicated. However, because treatment of FTY720 lead to an increase in the normalized frequency of P14 cells in the non-lymphoid tissue, inhibiting S1PR1 function does still seem to affect T_{RM} retention above and beyond global affects in S1PR1 transduced P14 observed. Forcing S1PR1 then administering FTY720, which is a functional antagonist but agonistly stimulates the cells,

may promote cell death. At the same time, it is surprising that cell numbers would be effected with only 24 hours of treatment with FTY720. It would be advantageous to do follow-up experiments looking more closely at the cellular affect of FTY720. While data trends with what we would expect from other experiments, enhanced signaling may complicate the ability to fully interpret these data.

While cognate antigen and/or peptide: MHC driven signals did not appear to be the main driver of KLF2 downregulation in P14 migrating to non-lymphoid tissue in general, the small intestine lamina propria T_{RM} cells had different outcomes. Both CD69 levels (Fig 2-2b) and $Nur77^{GFP}$ levels (Fig 3-7b) were elevated in the small intestine lamina propria T_{RM} compared to other tissues. It seems unlikely that cognate antigen would persist after an acute LCMV infection and be isolated solely in the small intestine lamina propria, but based on the data presented this cannot be ruled out. Considering the processing time for lamina propria cell isolation is longer, careful control experiments could be done to determine whether processing factors are involved in complicating these data. Likewise, co-culturing naïve Nur77 P14 with the infected lamina propria tissue at memory time points could be informative.

This chapter identified the functional significance of the downregulation of S1PR1 and KLF2 for the development of T_{RM} in non-lymphoid tissue. It is already clear that CD8+ T_{RM} play a critical role as a first line of defense against local infection[69-72, 99-102]. Our data suggest that induced downregulation of KLF2 or S1PR1 could be used as a method to efficiently populate or enhance the formation of T_{RM} during vaccination. T_{RM} may also contribute to pathological conditions, such as fixed drug eruptions in the

skin[99, 101]. Hence, our studies indicate potential therapeutic targets through which generation of resident memory CD8+ T cells could be promoted or reversed.

S1PR1 expression is firmly established as being critical for lymphocyte recirculation – our data indicate that the immune system co-opts regulation of this pathway to dictate residency of T_{RM} cells. Furthermore, these studies argue that expression of KLF2 constitutes a defining transcription factor of recirculating versus resident memory CD8+ T cells. There has been considerable advancement in relating functional characteristics of T cell subsets to key transcriptional regulators[110-112]: Our work suggests another dimension in this system, whereby control of T cell recirculation through regulated KLF2 expression determines tissue distribution characteristics of T cell subsets – and hence dictates how effector functions are deployed during recall responses.

Materials and methods

Mice.

C57BL/6 and CD45.1 congenic B6 mice were purchased from the National Cancer Institute and used at 6-8 weeks of age. KLF2^{GFP} and Nur77^{GFP} reporter mice were described earlier[81, 105] and were crossed to P14 TCR transgenic mice (specific for the H-2D^{b} restricted LCMV gp_{33-41} epitope [KAVYNFATC]). For adoptive co-transfer studies, combinations of CD45.2, CD45.1 and CD45.1/CD45.2 mice were used for donor and host strains, to allow for discrimination of each donor population versus host cells. Animals were maintained under specific pathogen-free conditions at the University of Minnesota, and all experimental procedures were approved by the Institutional Animal Care and Use Committee.

Adoptive transfer and infections.

Splenocytes were prepared from KLF2^{GFP} (or Nur77^{GFP}) P14 and congenic wild type P14 mice. The cell populations were mixed 1:1 and 25,000-45,000 CD8+ T cells were transferred into recipient B6 mice, which were infected the next day with $2x10^{5}$ PFU LCMV (Armstrong strain), via ip injection. Mice were maintained under BSL-2 housing and, at indicated times following infection, were sacrificed for analysis.

In vivo anti-CD8 antibody IV and lymphocyte isolation.

In order to label cells in the circulation, mice were injected with fluorchrome conjugated anti-CD8 antibodies (via the tail vein), as previously described[94]. At 2.5

minutes (min) following antibody injection, mice were bled and 30 seconds later mice were sacrificed. Heart perfusion, using 10ml of cold PBS was performed (in some experiments this step was eliminated) and tissues were harvested and lymphocytes isolated as described[93, 94]. Briefly, lymph nodes were mashed to achieve a single cell suspension, while the salivary glands, kidney, brain, and spleen were mashed and incubated at 37°C with 100U/ml collagenase type I (Worthington Biochemical Corporation), 10% FBS, $MgCl_2/CaCl_2$, HEPES/L-glumatime RPMI solution (45 min shaking at 450 rpm). For the small intestine, Peyer's patches were dissected out and the remaining tissue cut longitudinally and then into 1cm pieces. These were rinsed and incubated with 15.4mg/ml dithioerythritol in HBSS/HEPES bicarbonate buffer for 30 min (37°C at 450 rpm) to extract IELs. The remaining pieces were additionally incubated with the collagenase solution and conditions as listed above, to isolate LPL. All tissues were then subjected to a 44/67% percoll gradient (2,000rpm at 20°C for 20 min) to isolate lymphocytes.

Cellular gating strategy for non-lymphoid tissue.

For analysis of P14 CD8+ T cells in all tissues, the gating strategy included: live, singlet CD8+ lymphocytes, non-vascular-associated (stained negative for IV administered anti-CD8b)[94], with respective congenic markers.

Flow cytometry and antibodies.

Single-cell suspensions were prepared and cells were resuspended at 3-6x10^7

cells/ml in FACS buffer (1% FBS, 0.1% sodium azide) and stained in 100ul. Isolated lymphocytes in all experiments were incubated with LIVE/DEAD Fixable Aqua Dead Cell Stain Kit (Invitrogen) for 15 min at 4°C to detect dying cells before staining with a cell surface antibody staining cocktail. For detection of Foxo1 protein, lymphocytes were isolated from salivary glands and spleens of adoptively transferred P14 mice infected 30-60 days previously with LCMV. After surface staining, cells were fixed with a fix/perm solution (eBioscience) for 45 min at 4°C. Cells were then stained with anti-Foxo1 (Cell signaling clone c29H4) or rabbit IgG isotype control (Cell signaling) at 75-150ng/test for 45 min at 4°C. This was followed by a secondary donkey anti-rabbit PE antibody (Immunoresearch) for 30 min on ice. All additional fluorochome-conjugated antibodies were purchased from eBioscience, BD BioScience, R&D Systems, or BioLegend. Cells were analyzed using a BD Pharmingen LSR II flow cytometer and data analyzed using FlowJo (TreeStar) software.

Retroviral construct generation.

To generate the S1PR1 expressing retrovirus vector (MiT-S1PR1), a BglII/NotI fragment including FLAG-tagged mouse S1PR1 was amplified from a MSCV-S1PR1-hCD4 vector[95, 113] (a gift from Jason Cyster, University of California, San Francisco, San Francisco, CA) and was subsequently subcloned into the retroviral vector, MSCV-IRES-Thy1.1 (MiT) which was kindly provided from Jianzhu Chen (Massachusetts Institute of Technology, Cambridge, MA)[79]. MiT-S1PR1 and the retroviral packaging vector, pCL-Eco were co-transfected into 293T cells with Lipofectamine 2000 (Life Technology).

Supernatants were collected at 48 hrs after transfection.

Retroviral transduction and calculations.

P14 CD8+ T cells were activated either *in vivo* or *in vitro* prior to retroviral transduction. For *in vivo* activation, P14 mice were infected iv with $1x10^6$ LCMV (Armstrong). *In vitro* activation involved culture of $2\text{-}3x10^6$ bulk P14 splenocytes with either plate-bound anti-CD3 (2mg/ml) and soluble anti-CD28 (0.5mg/ml) per well of a 24-well plate, or with 250nM $gp_{33\text{-}41}$ peptide. At 24 hrs post activation, $3\text{-}6x10^6$ activated splenocytes were incubated per well of a 24-well tissue culture plate with 10mg/ml polybrene and 20ng/ml hIL-2 and incubated at 37°C for 30 min. After centrifugation at 1500rpm for 5 min, the culture media was removed and 1 ml of S1PR1 or empty retroviral supernatant was added to each well including 10mg/ml polybrene and 20ng/ml IL-2. Spin infection (2500rpm for 90 min at room temperature in a table top centrifuge) was followed by a 1 hr 37°C incubation to rest the cells before co-transferring 25,000-50,000 congenically marked S1PR1 and empty transduced P14 cells into congenic hosts, which were infected with LCMV the following day.

In some experiments, retronectin was used to enhance transduction efficiency by coating 6 well plates with 25mg/ml retronectin followed by a 2,000g spin of 4 ml retrovirus onto the plate for 90 min at 4°C. Virus supernatant was aspirated off and $6x10^6$ activated P14 splenocytes and 20ng/ml hIL-2 were added to the plate and incubated for 30 min at 37°C. The plates were then spun at 600g for 30 min at room temperature, and cells injected into congenically marked hosts, which were LCMV

infected as above. At 3-60 days post transfer, mice were treated with anti-CD8 antibody iv (as described above) and lymphocytes were harvested from indicated tissues. Percent transduction of live non-vascular-associated P14 cells was calculated, based on the Thy-1.1 marker. For normalization, the percent transduction for P14 CD8+ T-cells within a given tissue was normalized to the percent transduction found in the spleen of the same animal (Fig 3-3b).

To characterize transduction efficiency and monitor proliferation, after transduction splenocytes were set at $1x10^6$ cells in 2ml complete media/well in a 24 well plate with 10-20ng/ml hIL-2. Every 2 days, live cells were counted and re-set at $1x10^6$ cells in 2ml/well and replenished with new media containing hIL-2. Transduction efficiency over time was also monitored. Some experiments included 250nm gp_{33-41} peptide for the first 2 days after transduction.

***In vitro* activated Effector P14 transfer into uninfected hosts.**

For analysis of KLF2 expression in *in vitro* activated effector P14 cells transferred into uninfected hosts, $KLF2^{GFP}$ and WT P14 were activated *in vitro* with gp_{33-41} peptide for 24 hours and then cultured for 2 additional days *in vitro* with 20ng/ml hIL-2. $1x10^6$ splenocytes were transferred into uninfected hosts and 12-15 days later the $KLF2^{GFP}$ status of cells in different tissues were analyzed.

Ex vivo cytokine and inhibitors assay.

WT and KLF2^{GFP} P14 CD8+ T cells were co-transferred into C57BL/6 mice and infected with LCMV the following day. At 4.5 days post infection, bulk splenocytes were harvested and added to 96 well flat bottom plates at 700,000 cells/well in 200uL complete RPMI media, in the presence of the cytokines TGF-β (10ng/ml), IL-33 (100ng/ml), IL-6 (100ng/ml), IL-15 (20ng/ml), and/or TNFα (125ng/ml) in the indicated combinations, similar to previous studies [114]. In some experiments, the Akt inhibitor AKTi (0.25-2uM, Millipore) or the PI3K inhibitor LY294002 (1.25-10uM, Millipore) were also included from the beginning of the culture period. At 10-40 hrs of culture, cells were stained with appropriate antibodies and analyzed by flow cytometry.

In vitro cytokine and inhibitors assay and RNA isolation.

WT and KLF2^{GFP} P14 splenocytes ($5x10^6$ cells/ml) were primed *in vitro* culture in a 10 cm cell culture dish with 250nM gp_{33-41} peptide for 48 hrs. Activated WT and KLF2^{GFP} P14 splenocytes were mixed 1:1 and $2x10^5$ cells of the mixed splenocytes were cultured in 96-well flat bottom plates, with no additional cytokines or with TGF-β (10ng/ml) and IL-33 (100ng/ml), in the presence or absence of LY294002 (10mM) or AKTi (1mM) inhibitors for 48 hrs. Cells were analyzed by flow cytometry, or, to determine gene expression changes, live P14 CD8+ T cells were sorted using a FACS aria (BD Biosciences) (gating on live, CD3+, CD8+ events), and quantitative RT PCR was performed with the primers indicated above.

***In vivo* LY294002 administration.**

Cogenically distinct WT and KLF2^{GFP} P14 CD8+ Tcells (25,000-50,000 cells of each type) were co-transferred into C57BL/6 and infected with LCMV. Four days post infection, 50mg/kg LY294002 (LC Laboratories) in 50ml DMSO or 50ml DMSO only as a vehicle control was administered ip every 12 hours for 24 hours. On day 5, tissues were harvested and KLF2^{GFP} levels and cell counts determined.

Statistical analysis.

Data were analyzed using Prism software (GraphPad). For standard data sets Student's t-test was used (with Welch's correction utilized when variances were different), while normalized data was analyzed using ANOVA. For values that differed by >10-fold, values were $\log_{10}$ transformed prior to t-test analysis. Asterisks indicate obtained p-values, with *** meaning $p<0.001$; **, $p<0.01$; *, $p<0.05$, while "ns" indicates $p>0.05$.

Chapter 4

KLF2 and CD4+ T cells: Heterogeneity within lymphoid tissue effecting retention of CD4+ T cell subsets

CD4+ T cells, when compared to cytolytic CD8+ T cells, exhibit more diverse effector functions and as such have been defined as having significantly more heterogeneity. In this chapter, we identified another contributor to CD4+ T cell heterogeneity by identifying a subset of CD4+ memory T cells that remain $KLF2^{LO}$ in lymphoid organs. The downregulation of KLF2 in this population was not transient as KLF2 transcript was also decreased along with targets of KLF2 S1PR1 and CD62L. Likewise, CD4+ memory T cells sorted on $KLF2^{GFP}$ expression predominantly maintained their KLF2 status both *in vitro* and *in vivo*. Commensal bacteria did not appear to be responsible for this population yet TLR agonists were shown to negatively affect $KLF2^{GFP}$ levels. $KLF2^{LO}$ CD4+ memory T cells had diminished IFNγ/IL-2 production compared to their $KFL2^{HI}$ counterparts. Consistent with this, both anergic CD4+ memory-phenotype and germinal center follicular helper T cells were found to be $KLF2^{LO}$ yet did not comprise the entire $KLF2^{LO}$ population. While being absent in the blood, we demonstrated that $KLF2^{LO}$ CD4+ memory-phenotype T cells are not egressing from lymph nodes. Taken together, these data identify another factor in CD4+ T cell heterogeneity that overlays with already defined subsets of CD4+ T cells, determining that KLF2 status is a relevant distinction for a CD4+ T cell both in terms of a cell's transcriptional profile as well as trafficking potential.

Introduction

During activation, CD4+ T cells polarize into subsets capable of secreting different effector cytokines depending on the type of cytokines present during activation[115, 116]. Exposure to IFNγ and IL-12 during activation leads to Th1 cells that help macrophages control intracellular pathogens by the release of IFNγ[117, 118]. The presence of IL-4 during activation drives Th2 development whose effector cytokines help active responding B cells[119] while Th17 cells (from exposure to TGF-β and IL-6) help fight of parasitic infection through IL-17 generation[120]. T regs, another subset of effector CD4+ T cells driven by the presence of TGF-β during activation, are an important regulatory cell that helps dampen an immune response through secretion of TGF-β and IL-10[121]. Each CD4+ T cell is defined by a specific transcription factor that drives the profile of each cell subset while dissuading the development of the other subsets, encouraging the development of one differentiation pathway while inhibiting the other[122].

CD4+ effector T cells are able to cater their effector functions to the pathogen at hand due to their ability to be influenced by cytokines present during their activation. As such, CD4+ T cells are notorious for having significantly more diversity than CD8+ T cells[115]. On top of the canonical CD4+ Th1, Th2, and Th17 effector cells, T follicular helper cells (T_{FH}) have been defined by the presence of the transcription factor BCL-6 and the expression of IL-21[123-125]. T_{FH} have high expression of PD-1, CXCR5, SAP, and ICOS[126]. Germinal center T_{FH}, which have the highest expression of PD-1 and CXCR5, have been shown to localize within the germinal center of lymphoid tissue, providing help to activating B cells[126]. Unlike the other classically defined CD4+ T cell subsets, T_{FH}

cells are associated with a specific location: within the B cell follicles of lymphoid tissue and specifically the germinal centers in the case of germinal center T_{FH}. The plasticity of the CD4+ T cell subsets and there relationship with T_{FH} cells is highly debated in terms of whether T_{FH} are a unique subset or fall within the already defined subsets (Th1 T_{FH} vs Th2 T_{FH}, etc)[127], particularly with location being a defining factor for T_{FH}.

Besides the classical helper T cell subsets, CD4+ T cells can also be characterized as being anergic. Anergic T cells are defined by a lack of responsiveness to antigen, both in terms of cytokine production as well as proliferation[128]. Recently, FR4 and CD73 have been identified as markers on anergic T cells[129]. Using these markers, it is possible to distinguish cells that have undergone peripheral tolerance.

As described in previous chapters, the transcription factor KLF2 has been shown to be important for regulating trafficking molecules associated with entry and egress of lymphoid tissue. CD69, while considered a marker of early activation, has also been shown to directly correlate with the downregulation of KLF2 in CD8+ memory T cells found in either lymphoid or non-lymphoid tissue (Fig 2-2a and S2-1b). While the precise mechanism that drives CD69 expression is still elusive, Shiow et al determined that treatment with the IFNα/β inducer Poly(I:C), a toll-like receptor 3 ligand, causes transient CD69 induction and lymphocyte circulation cessation[113]. Therefore, in the context of inflammation, CD69 is upregulated by inflammatory molecules. Extensive work by Jason Cyster's lab has demonstrated that CD69 interacts with and inhibits the function of S1PR1, causing the protein complex to be internalized from the surface of the cell[95, 96, 113]. Therefore, cells that are low for S1PR1 have surface CD69 due to basal

expression of the CD69 molecule[96]. As in T_{RM}, cells that are low for KLF2 and subsequently S1PR1 may have surface CD69 due to the lack of S1PR1. In other contexts, like TCR stimulation, CD69 message itself is turned on while KLF2 protein and RNA are decreased[130-132]. In this situation, cells are $CD69^{HI}$ not simply because KLF2 is low, but also because CD69 mRNA is being upregulated. Therefore, depending on the situation, CD69 upregulation is not always dependent on KLF2 downregulation.

Considering KLF2 heterogeneity was significant for the trafficking of CD8+ T cells, we wanted to investigate KLF2 expression in CD4+ T cell subsets. While KLF2 heterogeneity did not directly correlate with a defined CD4+ T cell subset like it did with CD8+ T_{RM}, we determined that a population of $KLF2^{LO}$ CD4+ memory-phenotype T cells did exist in lymphoid tissue. This population of $KLF2^{LO}$ cells correlated with a distinct phenotype and a lack of lymph node egress. Therefore, KLF2 status in CD4+ memory T cells provides a way of distinguishing whether a CD4+ T cell has the capacity to circulate or is retained in a lymphoid tissue.

Results

Unlike CD8+ memory T cells, CD4+ memory T cells exhibit considerable KLF2 heterogeneity in lymphoid tissue

While we had defined a functional role for KLF2 and its targets in a subset of CD8+ memory T cells, we also wanted to investigate heterogeneity in CD4+ memory T cells to distinguish whether KLF2 expression is also relevant for CD4+ T cell subsets. Therefore, we analyzed $KLF2^{GFP}$ reporter mice in the steady state to observe the KLF2 status of CD4+ memory-phenotype T cells. For CD4+ T cells, memory-phenotype T cells were defined as being $CD44^{HI}$ and CD25 (or gitr) negative to exclude T regs from analysis. Unlike CD8+ memory-phenotype T cells, we observed considerable heterogeneity in CD4+ memory-phenotype T splenocytes (Fig 4-1a). This trend was consistent when looking at the antigen-specific polyclonal response of CD4+ memory T cells ($I\text{-}A^b$:GP66-80 tetramer+) after LCMV infection (Fig 4-1a). Likewise, monoclonal smarta TCR transgenic CD4+ T cells specific to an LCMV epitope also exhibited heterogeneity in KLF2 expression during the memory phase of the immune response (Fig 4-1b). Taken together, while the percentages of $KLF2^{LO}$ T cells within the $CD44^{HI}$ population was the most robust, both antigen-specific polyclonal and monoclonal CD4+ memory T cells had a significant percentage of $KLF2^{LO}$ cells that were predominantly absent in CD8+ memory T cells (Fig 4-1c).

While we had already determined that KLF2 did not correlate with central and effector CD8+ memory T cells based on CD62L expression in chapter 2 (Fig 2-1a), CD4+ memory-phenotype T cells had three distinct subsets of cells based on CD62L and

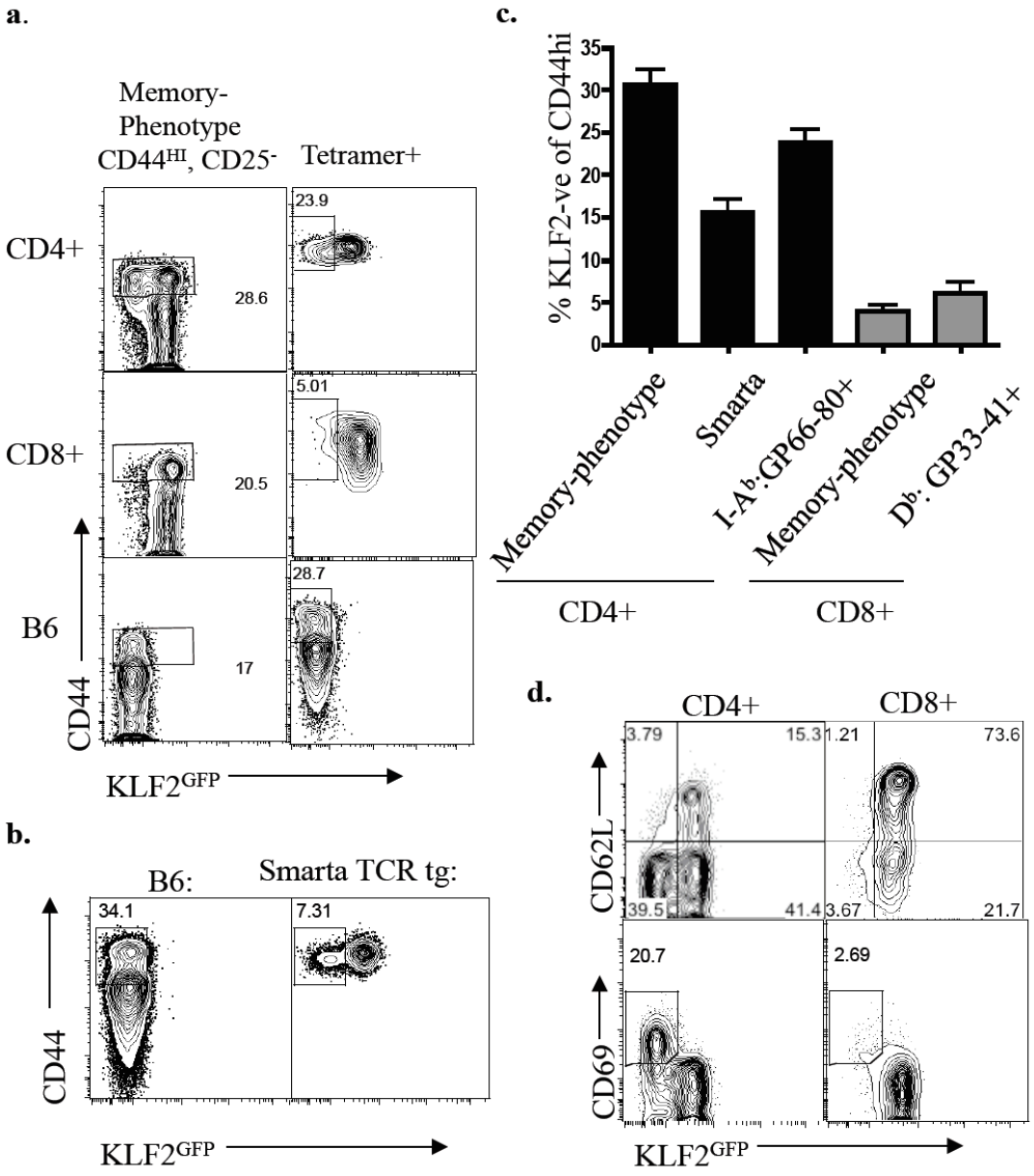

Figure 4-1. KLF2 heterogeneity is observed in CD4+ memory T cells found in the spleen. (a) Left panel is gated on memory-phenotype ($CD44^{HI}$, CD25-) CD4+ (top) or CD8+ (middle) T cells in $KLF2^{GFP}$ reporter mice. Right panel is gating on I-Ab: GP66-80+ CD4+(top) or D^b:GP33-41+ CD8+ (middle) memory T cells >30 days after LCMV infection of $KLF2^{GFP}$ reporter mice compared to B6 controls (bottom). (b) 25,000 smarta $KLF2^{GFP}$ TCR transgenic CD4+ splenocytes were adoptively transferred into B6 mice and subsequently infected with LCMV. Gating on congenically distinct smarta mice >30 days after infection. (c) Quantification of the percent KLF2-negative within the $CD44^{HI}$ pool data in a and b. (d) CD62L and CD69 expression versus $KLF2^{GFP}$ in memory-phenotype CD8+ and CD4+ T cells in the steady state of $KLF2^{GFP}$ reporter mice.

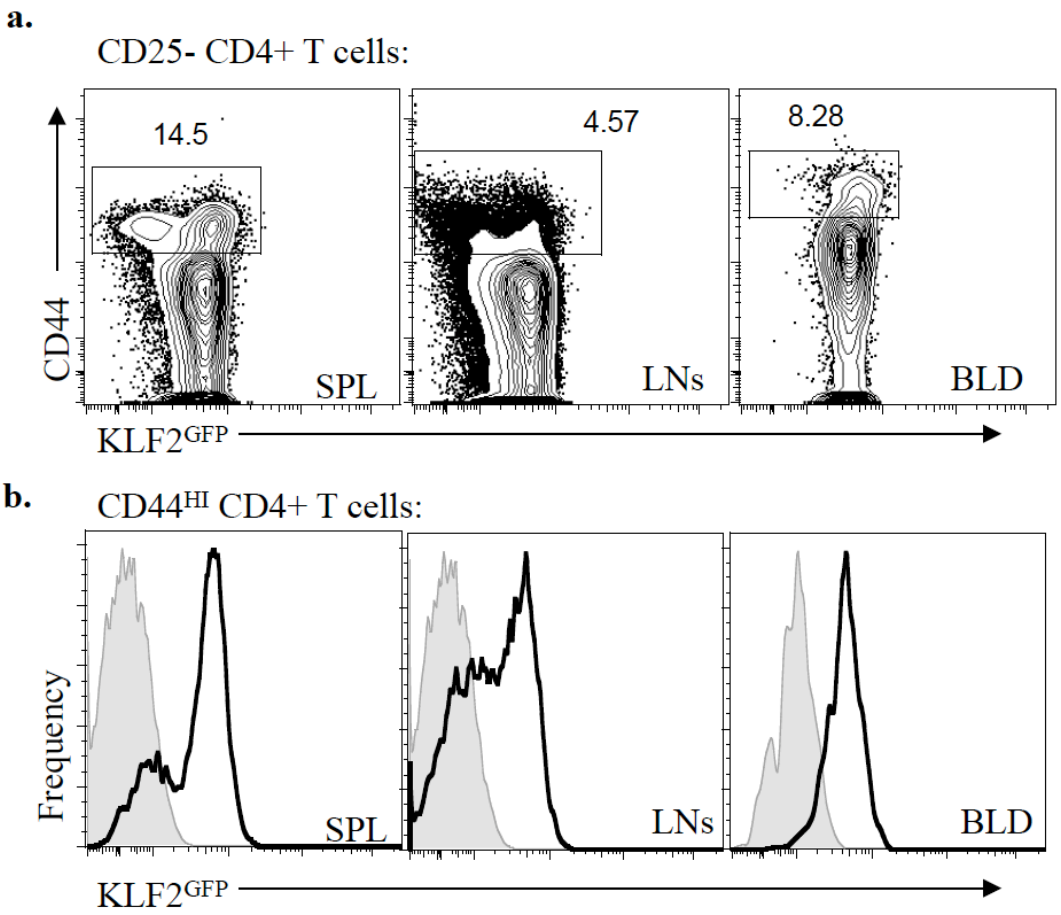

Figure 4-2. KLF2^{LO} CD4+ memory-phenotype T cells are present in lymphoid tissue but absent in blood. (a-b) Expression of KLF2^{GFP} in CD25- CD4+ T cells (a) or CD44^{HI} CD25- CD4+ T cells (b) in the steady state of KLF2^{GFP} reporter mice in the spleen, lymph nodes, and blood. (a) KLF2^{GFP} vs CD44. (b) memory-phenotype CD4+ T cells in KLF2^{GFP} reporter mice in various tissues (black) versus a WT control (grey).

KLF2 expression (Fig 4-1d). CD62L^{HI} cells, or CD4+ central memory T cells, had high expression of KLF2 while CD62L^{LO} CD4+ T cells (effector memory T cells) contained both a KLF2^{LO} and KLF2^{HI} subset (Fig 4-1d). This suggested that similar to CD8+ memory T cells, KLF2 also does not distinguish CD4+ central and effector memory T cells yet does highlight a unique population of CD4+ KLF2^{LO} T cells not seen in CD8+ memory T cell lymphoid compartment. Similar to CD8+ T_{RM} found in non-lymphoid tissue (Fig 2-2a), low KLF2 expression in CD4+ memory T cells correlated with an

increase in CD69 expression (Fig 4-1d). $KLF2^{LO}$ CD4+ memory-phenotype T cells were present in both the spleen and lymph node of intact $KLF2^{GFP}$ reporter mice, yet were notably absent from the blood (Fig 4-2).

Differential KLF2 expression in CD4+ memory-phenotype T cells correlates with KLF2 targets' protein and mRNA levels

We next wanted to determine other characteristics of this newly defined $KLF2^{LO}$ CD4+ memory-phenotype T cell population. To do so, we gated on either $KLF2^{LO}$ or $KLF2^{HI}$ CD4+ memory-phenotype T cells in the steady state of $KLF2^{GFP}$ reporter mice (or naïve CD4+ T cells) and identified other molecules that correlated with KLF2 downregulation (Fig 4-3a). While surface expression of CD62L and CCR7 were lower in memory-phenotype subsets compared to CD4+ naïve T cells in general, $KLF2^{LO}$ cells exhibited lower levels of these molecules than $KLF2^{HI}$ CD4+ memory-phenotype T cells (Fig 4-3b). Interestingly, $KLF2^{LO}$ CD4+ memory-phenotype T cells were also lower for the IL-7 receptor. This is consistent with a cell that has decreased nuclear Foxo1, as Foxo1 has been shown to control both the KLF2 and IL-7 receptor locus (Fig 1-4)[89].

To discern whether the downregulation of KLF2 protein was transient, we sorted each population (as shown in Fig 4-3a) to isolate RNA from each subset of CD4+ T cells. Reverse transcription real time PCR analysis determined that KLF2 transcripts were significantly lower in $KLF2^{LO}$ cells compared to $KLF2^{HI}$ CD4+ memory-phenotype T cells when normalized to CD4+ naïve T cells (Fig 4-3c). This suggested that the downregulation in KLF2 protein was a more permanent transcriptional downregulation

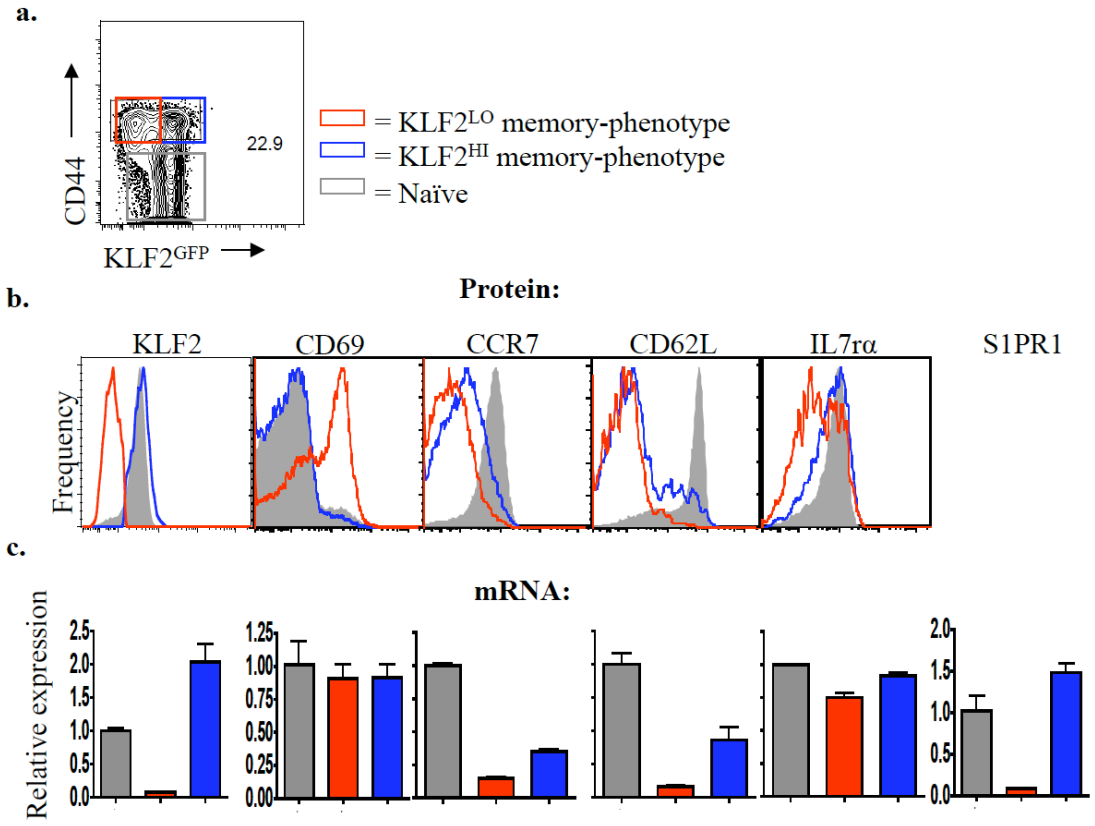

Figure 4-3. KLF2 mRNA is also lower in KLF2^{LO} CD4+ memory-phenotype T cells and correlates with the downregulation of other trafficking transcripts. (a) Gating strategy for identifying KLF2^{HI} (blue), KLF2^{LO} (red) memory-phenotype, and naïve CD4+ T cells in KLF2^{GFP} reporter mice. (b) Surface expression of trafficking molecules in the three population defined in (a). (c) RNA from sorted KLF2^{LO} and KLF2^{HI} memory-phenotype CD4+ T cells (as well as naïve CD4+ T cells) was extracted and analyzed for molecules in b. Expression is relative to HPRT and naïve CD4+ T cell expression is set as 1.

than transient post-translational regulation at the protein level. mRNA levels of CD62L, CCR7, and IL-7 receptor all had the same trends as those observed when analyzing protein surface expression (Fig 4-3b/c). Transcripts for CD62L and S1PR1 were lower in KLF2^{LO} versus KLF2^{HI} CD4+ memory-phenotype T cells consist with what would be expected of a cell having low levels of KLF2 at both the protein and mRNA level (Fig 4-3c). While surface CD69 expression was elevated in KLF2^{LO} CD4+ memory-phenotype

T cells compared to KLF2^{HI} cells, CD69 message was comparable between the two subsets (Fig 4-3b/c). Considering this expression profile is similar to CD8+ T_{RM} (Fig 2-2b), this may suggest that signals other than TCR stimulation are driving down KLF2 expression in this CD4+ memory-phenotype T cell subset.

KLF2 downregulation in CD4+ memory T cells is not transient

While both KLF2 protein and mRNA were significantly declined in KLF2^{LO} versus KLF2^{HI} CD4+ memory-phenotype T cells, it was unclear how stable these populations were. Therefore, we sought to determine whether KLF2 levels would remain distinct after sorting CD4+ memory T cells based on KLF2^{GFP} levels.

KLF2^{GFP} reporter mice were infected with LCMV and >30 days later CD44^{HI} CD4+ memory T cells were sorted into either KLF2^{LO} or KLF2^{HI} populations, as well as naïve CD4+ T cells as a control. Each sorted population was co-cultured with congenically distinct bulk splenocytes *in vitro* and KLF2 levels were monitored over time. Both KLF2^{HI} bulk CD4+ memory T cells and antigen-specific IA^{b}:GP66-81 tetramer+ T cells remained KLF2^{GFP} high over time, similar with CD4+ naïve T cells (Fig 4-4). Sorted KLF2^{LO} bulk CD4+ memory T cells and antigen-specific IA^{b}:GP66-81 tetramer+ T cells exhibited more intermediate levels of KLF2 24 hours after *in vitro* culture, yet the majority of the CD4+ memory T cells remained KLF2^{LO} after 3 days of *in vitro* culture (Fig 4-4). These data suggest KLF2^{HI} expression in CD4+ memory T cells is sustainable. While KLF2^{LO} expression in CD4+ memory T cells is less stable, the

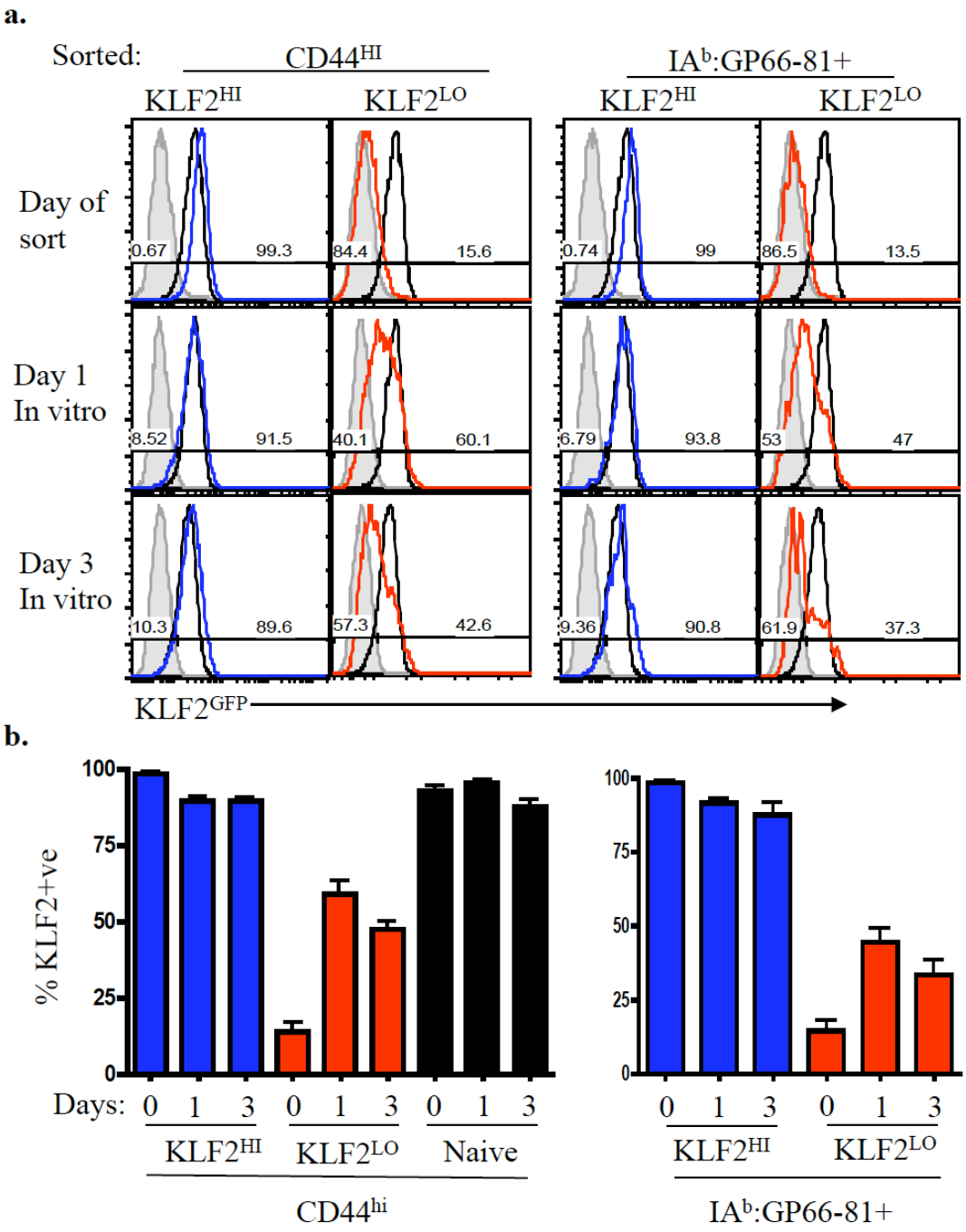

Figure 4-4. CD4+ memory T cells sorted on KLF2 expression predominantly maintain their KLF2 status when culture *in vitro*. (a-b) $KLF2^{GFP}$ reporter mice were infected with LCMV and >30 days later $CD44^{HI}$ $KLF2^{HI}$ (blue) and $KLF2^{LO}$ (red) CD4+ memory T cells or naïve T cells (black) were sorted and cultured *in vitro* with bulk uninfected splenocytes. (a) Histograms of $KLF2^{GFP}$ over time gating on CD44hi (left) or I-A^b: GP66-80+ (right) CD4+ T cells compared to a WT control (grey). (b) Quantification of the percent KLF2-positive cells from (a).

majority of sorted cells remain low for KLF2 over time suggesting this population is not transient, at least not *in vitro*.

We also monitored CD69 expression in these sorted populations over time. Interestingly, while the KLF2^{GFP} MFI of the sorted KLF2^{LO} and KLF2^{HI} CD4+ memory T cells remain distinct, the CD69 MFI of KLF2^{LO} CD4+ memory T cells and antigen-specific IAb:GP66-81 tetramer+ T cells decreased to baseline after 3 days of *in vitro* culture (Fig 4-5). This would suggest that the factors driving down KLF2 in KLF2^{LO} CD4+ T cells may not be identical as the signals causing high CD69 surface expression.

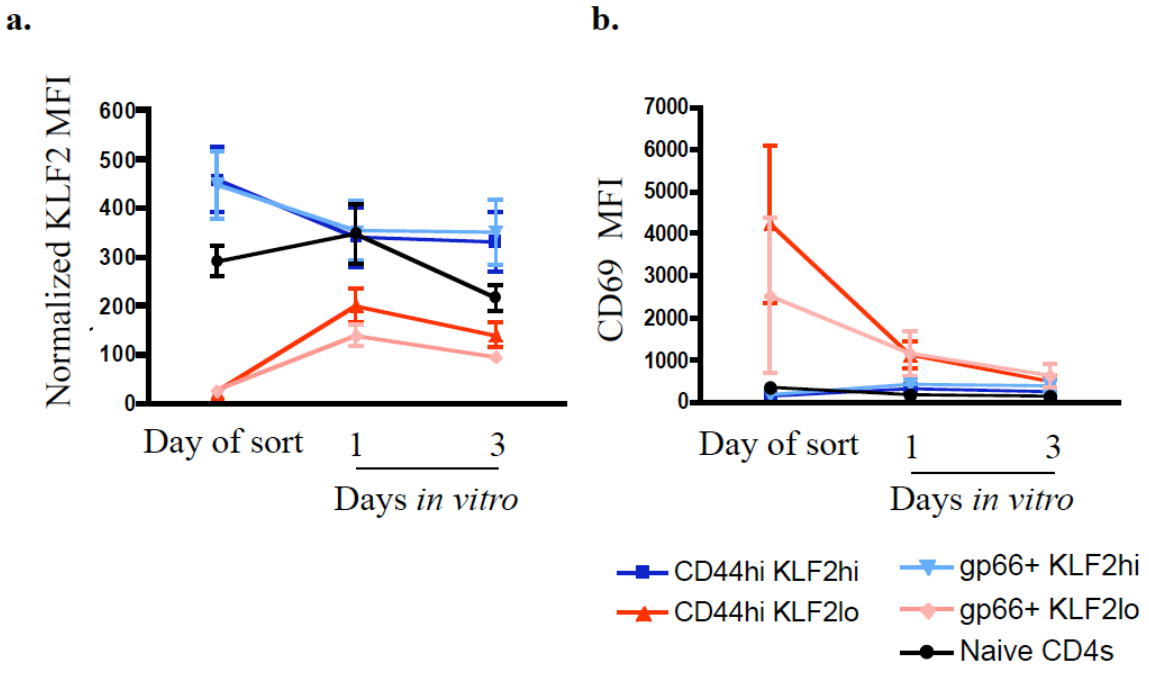

Figure 4-5. While CD4+ memory T cells sorted on KLF2 expression maintain distinct levels of KLF2, CD69 levels in sorted KLF2^{LO} cells drop to baseline when cultured *in vitro* (a) Normalized KLF2^{GFP} MFI (WT baseline subtracted) and CD69 MFI (b) of sorted KLF2^{HI} (blue and light blue) and KLF2^{LO} memory T cells (red and pink) described in Figure 4-4 compared with sorted naïve CD4+ T cells (black).

Since signals driving low KLF2 expression may not be present during *in vitro* culture, we also sought to determine whether KLF2 status remains constant when sorted CD4+ memory T cells are returned to an *in vivo* setting. For these experiments, CD4+ memory-phenotype T cells from $KLF2^{GFP}$ reporter mice were sorted on KLF2 expression and adoptively transferred back into uninfected mice and $KLF2^{GFP}$ levels were monitored. Seven days later, $KLF2^{GFP}$ levels still trended with being $KLF2^{LO}$ and $KLF2^{HI}$ in each sorted population (Fig 4-6a). When quantifying the percentage of $KLF2^{GFP}$ low and high CD4+ memory-phenotype T cells, $KLF2^{LO}$ percentages remained comparable between cells immediately after sorting and 7 days *in vivo* (Fig 4-6b). Since the sorting purity for $KLF2^{LO}$ cells was less pure, it was difficult to distinguish whether some $KLF2^{HI}$ cells arose from the sorted $KLF2^{LO}$ population.

Interestingly, unlike data from the *in vitro* set-up (Fig 4-4a), sorted $KLF2^{HI}$ CD4+ memory-phenotype T cells did develop a shoulder of $KLF2^{LO}$ cells upon return to an *in vivo* setting. This suggests *in vivo* factors may be involved in the development of $KLF2^{LO}$ CD4+ T cells from $KLF2^{HI}$ cells. It is worth noting that there is not a sizeable $KLF2^{LO}$ naïve T cell population, so the *in vivo* factors affecting KLF2 levels appear to be specifically affecting CD4+ memory-phenotype T cells and not their naïve counterparts.

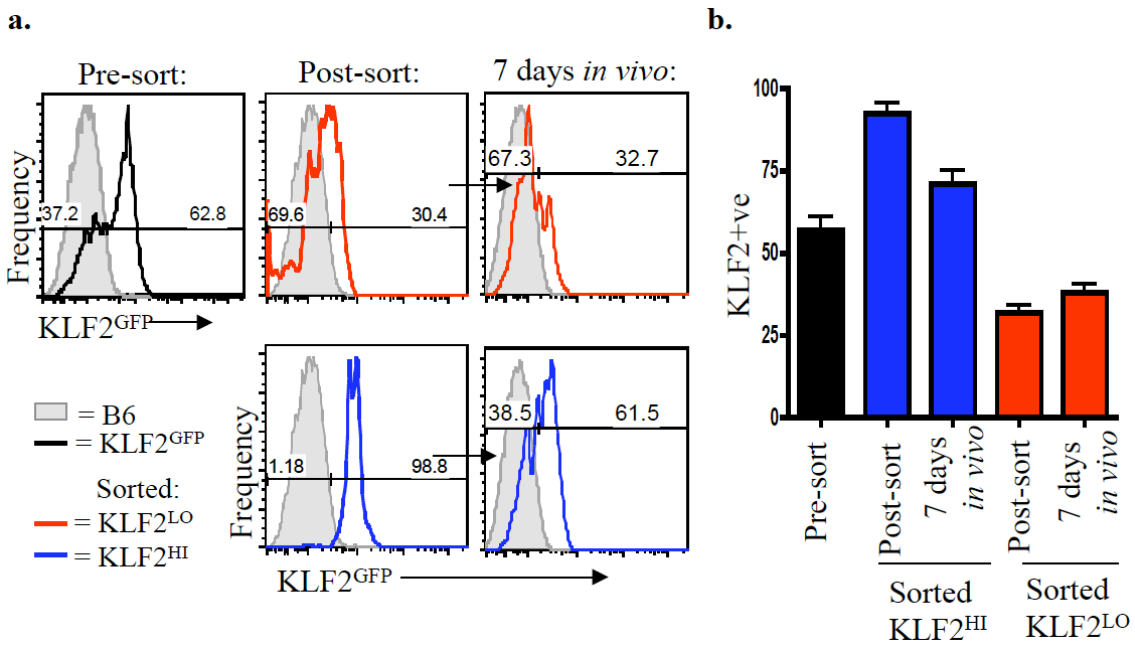

Figure 4-6. A subset of KLF2^{LO} cells arise from sorted KLF2^{HI} CD4+ memory-phenotype T cells when returned in vivo. (a-b) KLF2^{HI} (blue) and KLF2^{LO} (black) memory-phenotype CD4+ T cells were sorted from spleens and lymph nodes of steady state KLF2^{GFP} reporter mice and adoptively transferred into congenically distinct WT mice. 7 days later, KLF2^{GFP} levels were assessed. (a) KLF2^{GFP} levels of sorted KLF2^{HI} and KLF2^{LO} memory-phenotype T cells post-sort (middle) and 7 days later (right) compared with sample pre-sort (black). (b) Percent KLF2-positive of adoptively transferred sorted cells versus pre-sort sample.

KLF2 is decreased in CD4+ memory-phenotype T cells after systemic inflammation driven by TLR agonists.

While we had determined that the KLF2 status of CD4+ memory-phenotype T cells was not transient, it was still unclear what was driving low KLF2 expression in KLF2^{LO} CD4+ memory-phenotype T cells. Research has shown that treatment of the IFNα/β inducer Polyinosinic:polycytidylic acid (Poly(I:C)) causes transient upregulation of CD69[113]. Poly(I:C) is recognized by TLR3 and leads to the production of IFNα/β.

Lipopolysacharide (LPS) is another TLR agonist which activates TLR4 and converges on a similar pathway driving IFNα/β[133]. Since the $KLF2^{LO}$ CD4+ memory-phenotype T cells consistently correlate with CD69, we wanted to investigate whether these TLR stimuli also affected KLF2 levels.

$KLF2^{GFP}$ reporter or WT mice were intravenously injected with either Poly(I:C) or LPS and 6 or 24 hours later (respectively) tissues were harvested to assess $KLF2^{GFP}$ levels. In both CD4+ naïve and memory-phenotype T cells exposure to TLR agonists resulted in decreased $KLF2^{GFP}$ expression compared with control treated mice (Fig 4-7a). As expected, CD69 expression also increased with exposure to these stimulants (Fig 4-7b).

Since systemic exposure to TLR agonists can affect many cell types and lead to the production of other cytokines besides IFNα/β, we wanted to determine whether the downregulation of KLF2 was a consequence of IFNα/β exposure versus a separate factor driven by the inflammatory stimulants. To do so, we first exposed bulk $KLF2^{GFP}$ or WT splenocytes to either Poly(I:C) or IFNα/β *in vitro* and monitored $KLF2^{GFP}$ expression over time. Plate bound anti-CD3 and soluble anti-CD28 was included in additional wells as a positive control. Preliminary data suggested that the presence of either Poly(I:C) or IFNα/β resulted in similar downregulation of KLF2 over time in both CD4+ naïve and memory-phenotype T cells (Fig 4-8a). While this confirmed that IFNα/β exposure itself can affect $KLF2^{GFP}$ levels, it was still unclear whether these cytokines themselves were functioning directly on CD4+ T cells or through the production of another factor produced from a different cell type present in the *in vitro* culture.

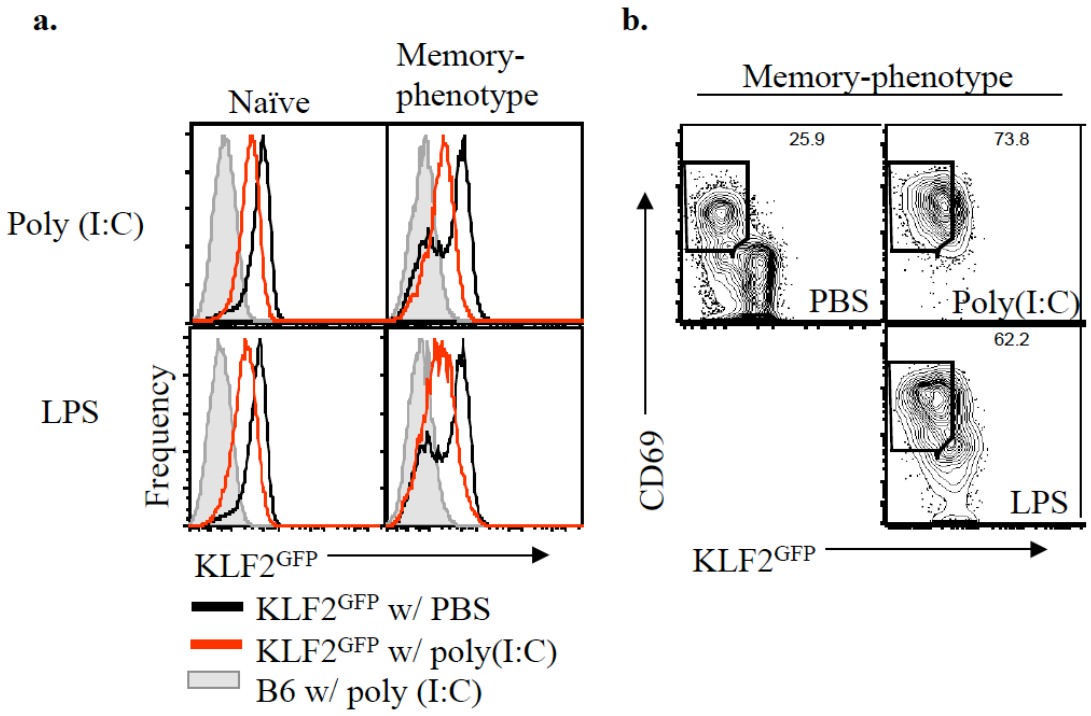

Figure 4-7. Naïve and memory-phenotype CD4+ T cells have diminished KLF2^{GFP} when exposed to TLR agonists. (a-b) KLF2^{GFP} reporter mice were treated with 10ug Poly(I:C) (top) or 50ug LPS (bottom) for 6 or 24 hours (respectively) (a). KLF2^{GFP} expression in KLF2^{GFP} (red) or WT (grey) mice receiving TLR agonist compared with KLF2^{GFP} with vehicle only (black) of naïve (left) and memory-phenotype (right) CD4+ T cells. (b) KLF2^{GFP} versus CD69 expression in memory-phenotype CD4+ T cells from KLF2^{GFP} mouse given PBS (top left), Poly(I:C) (top right) or LPS (bottom right).

Therefore, we conducted an experiment using adoptive transfer of IFNα/β receptor dominant negative (DN) cells into mice to specifically test whether responsiveness to IFNα/β itself on CD4+ T cells was necessary for the decrease in KLF2 observed during TLR agonist stimulation. Preliminary data suggested that when CD4+ T cells were unable to respond to IFNα/β in the context of systemic Poly(I:C) administration, the CD4+ T cells still resulted in decreased KLF2 expression (Fig 4-8b). This suggests that a separate factor potentially produced by another cell type's response to IFNα/β was affecting KLF2 levels in CD4+ T cells. While KLF2 was not affected in

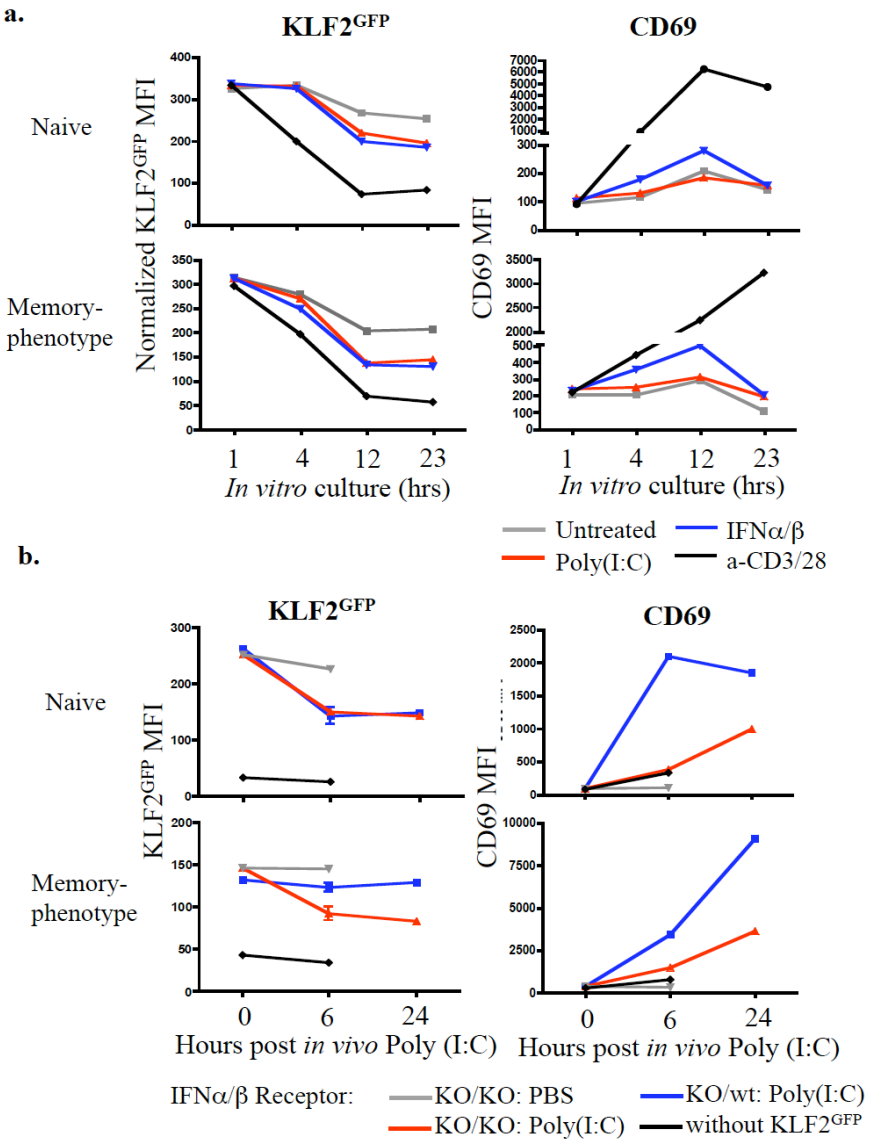

Figure 4-8. Exposure to IFNα/β and Poly(I:C) both drive down KLF2^{GFP} in CD4+ T splenocytes, yet do so independently of CD4+ T cell responsiveness to IFNα/β. (a) Splenocytes from a KLF2^{GFP} or WT mouse were exposed to 10ug Poly(I:C) (red), 50u/ml IFNα/β (blue), anti-CD3/28 (black), or untreated (grey) and monitored *in vitro* over time. Gated on CD44^{LO} (top) or CD44^{HI} (bottom) CD4+ T cells. Left is KLF2^{GFP} MFI (WT splenocyte GFP MFI subtracted) and right is CD69 MFI. (b) IFNα/β R DN KO/KO (red) or KO/WT (blue) KLF2^{GFP} splenocytes were co-transferred into a mouse and Poly(I:C) was administered as in Figure 4-7. As a control, IFNα/β R DN KO/KO KLF2^{GFP} (grey) or WT (black) were co-transferred and received vehicle only. KLF2^{GFP} and CD69 MFI levels were monitored over time in naïve (top) and memory-phenotype (bottom) CD4+ T cells.

IFNα/β receptor DN CD4+ T cells, CD69 upregulation did appear to be negatively affected when CD4+ T cells were unable to respond to IFNα/β (Fig 4-8b). While these data need to be repeated before drawing definitive conclusions, this initial experiment suggested that independent pathways were leading to CD69 upregulation versus KLF2 downregulation.

The population of KLF2^{LO} CD4+ memory-phenotype T cells found in the steady state are not specific for gut commensal microbiota

While we identified a population of KLF2^{LO} CD4+ memory-phenotype T cells in the steady state of KLF2^{GFP} reporter mice, the specificity of these cells was unknown. Since our facilities use specific-pathogen free mice, it was possible that the KLF2^{LO} CD4+ memory-phenotype T cells identified were cells specific to microorganisms found in the gut. These CD4+ T cells could then be low for KLF2 because they were responding to their specific cognate antigen found in the gut microbiota. Animals housed in a completely germ-free habitat are not naturally colonized by microorganisms and are thus termed "germ-free". Using germ-free mice, we were able to investigate whether gut commensal bacteria were the consequence of the KLF2^{LO} CD4+ T cells observed in the steady state.

Due to technical and feasibility issues, we were unable to generate germ-free KLF2^{GFP} reporter mice. However, CD69 upregulation consistently correlated with KLF2^{LO} CD4+ memory-phenotype T cells so we were able to use CD69 expression as a

surrogate for KLF2^{LO} CD4+ memory-phenotype T cells (Fig 4-9a). If the gut microbiota was driving KLF2^{LO} CD4+ T cells in the steady state of mice, we would expect to see a decrease in the percentage of CD69+ CD4+ memory-phenotype T cells in germ-free mice

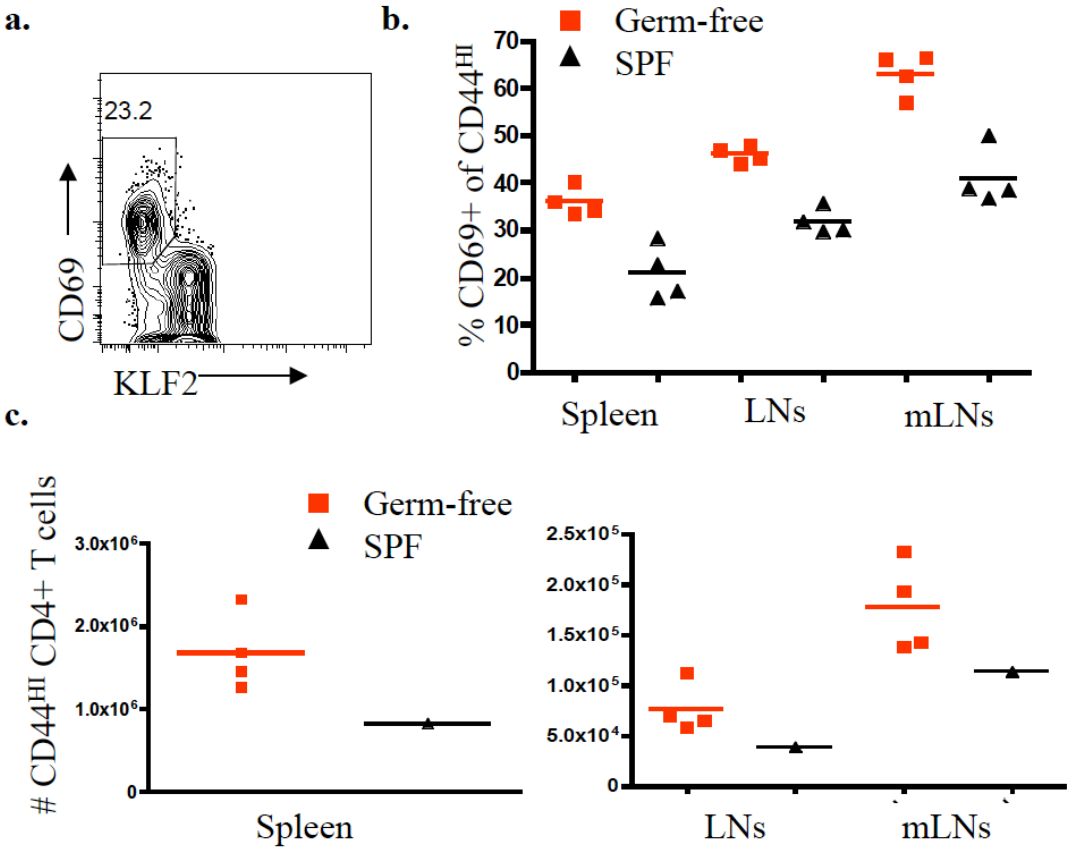

Figure 4-9. Germ-free mice have similar percentages of CD69+ CD4+ memory-phenotype T cells when compared to specific-pathogen free mice. (a) KLF2 versus CD69 expression in memory-phenotype CD4+ T cells from the spleen of a KLF2^{GFP} reporter mouse. (b) Percentage of CD69+ cells within the CD44^{HI} compartment of specific-pathogen free (black) and germ-free (red) mice found in the spleen, lymph nodes, and mesenteric lymph node. (c) Number of CD44^{HI} CD4+ T cells in germ-free (red) and SPF (black) secondary lymphoid organs.

compared to specific-pathogen free (SPF) mice; However, this was not the case (Fig 4-9b). Germ-free mice actually had slightly elevated percentages of CD69+ cells within the CD44^{HI} CD4+ T cell compartment. Since the number of CD44^{HI} CD4+ T cells

themselves were not altered (and potentially elevated) (Fig 4-9c), this preliminary data suggested commensal bacteria were not the mechanism leading to $KLF2^{LO}$ CD4+ memory-phenotype T cells in the steady state of $KLF2^{GFP}$ reporter mice.

Functionally, $KLF2^{LO}$ CD4+ memory T cells produce less IFNγ and IL-2 than $KLF2^{HI}$ CD4+ memory T cells

We next wanted to determine whether KLF2 expression correlated with functional characteristics of CD4+ memory T cells. Since cytokine production is one of the main effector functions of CD4+ T cells, we analyzed the ability of $KLF2^{LO}$ and $KLF2^{HI}$ CD4+ memory T cells to produce IFNγ and IL-2.

$KLF2^{GFP}$ reporter mice were infected with LCMV, and 30 days later CD4+ memory T cells were sorted based on KLF2 expression. Sorted populations (or the pre-sorted sample) were stimulated *ex-vivo* with GP66-81 peptide for 5 hours and cells were subsequently stained for intracellular IFNγ and IL-2. Sorted $KLF2^{LO}$ CD4+ memory T cells had diminished production of both IFNγ and IL-2 compared with sorted $KLF2^{HI}$ CD4+ memory T cells (Fig 4-10a). The percentage of IA^b:GP66-81 tetramer+ CD4+ memory T cells was similar in each sorted population, ruling out the possibility that skewed percentages of antigen-specific CD4+ T cells were affecting the interpretation of these results (Fig 4-10b). These preliminary results suggest that $KLF2^{LO}$ CD4+ memory T cells have decreased potential to produce IFNγ and IL-2.

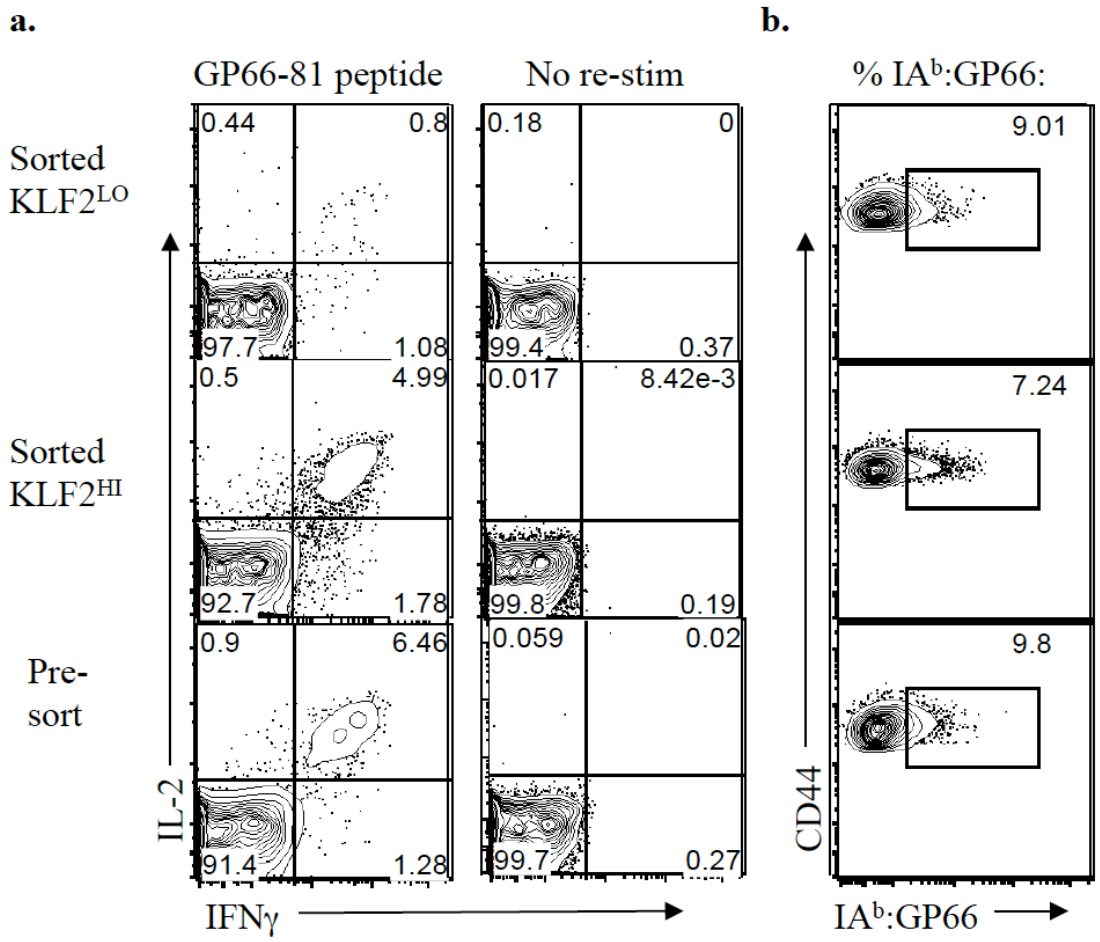

Figure 4-10. Sorted KLF2^{LO} CD4+ memory T cell have diminished IFNγ and IL-2 production compared with KFL2^{HI} CD4+ memory T cells. KLF2^{HI} and KLF2^{LO} CD4+ memory T cells were sorted from KLF2^{GFP} reporter mice >30 days post LCMV. (a) Sorted cells were cultured in vitro for 5 hours with gp61-80 peptide (10ug/ml) before intracellular staining for cytokines was performed. (b) Sorted cells were stained for IA^b:GP66-80 tetramer. Representative of 2 independent experiments.

CD4+ anergic memory-phenotype T cells are low for KLF2

The observation that KLF2^{LO} CD4+ memory T cells have diminished IFNγ and IL-2 production upon *ex vivo* stimulation could mean that KLF2^{LO} CD4+ memory T cells are anergic. Anergic T cells are defined by having a lack of an immune response based on both proliferative capacity and cytokine production of T cells[128]. Recently FR4 and CD73

have been shown to be upregulated on anergic T cells[129], so we sought to determine whether KLF2^{LO} CD4+ T cells also express these markers.

Preliminary analysis of KLF2^{GFP} reporter mice demonstrated that anergic CD4+ T cells, based on expression of FR4 and CD73, are indeed KLF2^{LO} (Fig 4-11a). However, it is worth noting that this anergic subset did not comprise the entire population of KLF2^{LO} CD4+ memory-phenotype T cells (Fig 4-11b). Therefore, while anergic CD4+ memory-phenotype T cells do fall within the KLF2^{LO} subset, they are not the sole contributor making up the KLF2^{LO} population.

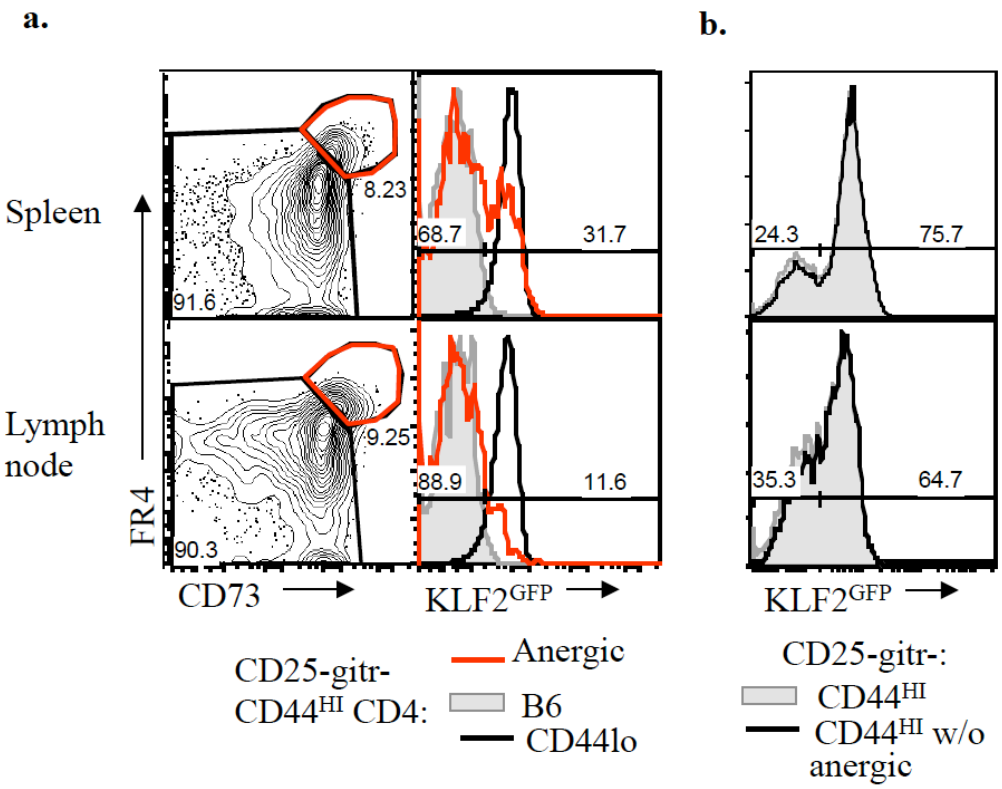

Figure 4-11. Anergic CD4+ memory-phenotype T cells have reduced KLF2^{GFP} levels, but do not comprise a majority of the KLF2^{LO} CD4+ memory-phenotype T cell compartment. (a) Gating strategy (left) and KLF2 levels (right) for anergic (red) CD4+ T cells in KLF2^{GFP} mice compared to WT (grey) or CD44^{LO} CD4+ T cells (black). (b) KLF2^{GFP} levels in CD44^{HI} (grey) vs CD44^{HI} memory-phenotype T cells with anergic cells excluded. (a-b) CD25 and gitr were used to exclude T regs from analysis.

Germinal center CD4+ T follicular helper cells also have low expression of KLF2

Since anergic CD4+ T cells could not account for all $KLF2^{LO}$ CD4+ memory-phenotype T cells in the steady state of an animal, we wanted to discern whether other defined CD4+ T cells subsets also have low KLF2 expression. Considering $KLF2^{LO}$ CD4+ memory T cells have diminished IL-2/IFNγ production and CD4+ T follicular helper cells (T_{FH}) have also been shown to have decreased production of these cytokines[134], we investigated the KLF2 status of T_{FH}.

We infected $KLF2^{GFP}$ reporter mice with LCMV and 20 days later analyzed the $KLF2^{GFP}$ expression in antigen-specific CD4+ T cells. Indeed, $CXCR5^{HI}$ germinal center T_{FH} were $KLF2^{LO}$ (Fig 4-12a). When we analyzed mRNA from sorted CD4+ memory-phenotype T cells based on KLF2 levels (as in Fig 4-3c), we also found that $KLF2^{LO}$ CD4+ memory-phenotype T cells were enriched for transcripts of the defined T_{FH} transcription factor BCL-6 as well as message for the T_{FH} -associated cytokine IL-21 (Fig 4-12b).

To strengthen this finding, we also isolated mRNA from bulk germinal center T_{FH} 8 or 30 days after LCMV infection, as well as CD4+ naïve T cells and non- T_{FH} memory T cells as controls (Fig 4-13a). RT real time PCR confirmed that germinal center T_{FH} are low for KLF2 transcripts both 8 and 30 days after LCMV when normalized to mRNA from non- T_{FH} 30 days after infection (Fig 4-13b). Likewise, mRNA for a target of KLF2 S1PR1 was also diminished in germinal center T_{FH} (Fig 4-13b). While preliminary data suggested that CD69 mRNA was not elevated in T_{FH}, further repeats of this experiment

need to be performed before drawing conclusions from these data as inconsistency between the two independent experiments performed was noted. In total, these data determine that along with anergic T cells, T_{FH} are also a subset of CD4+ memory T cells that fall within the $KLF2^{LO}$ population.

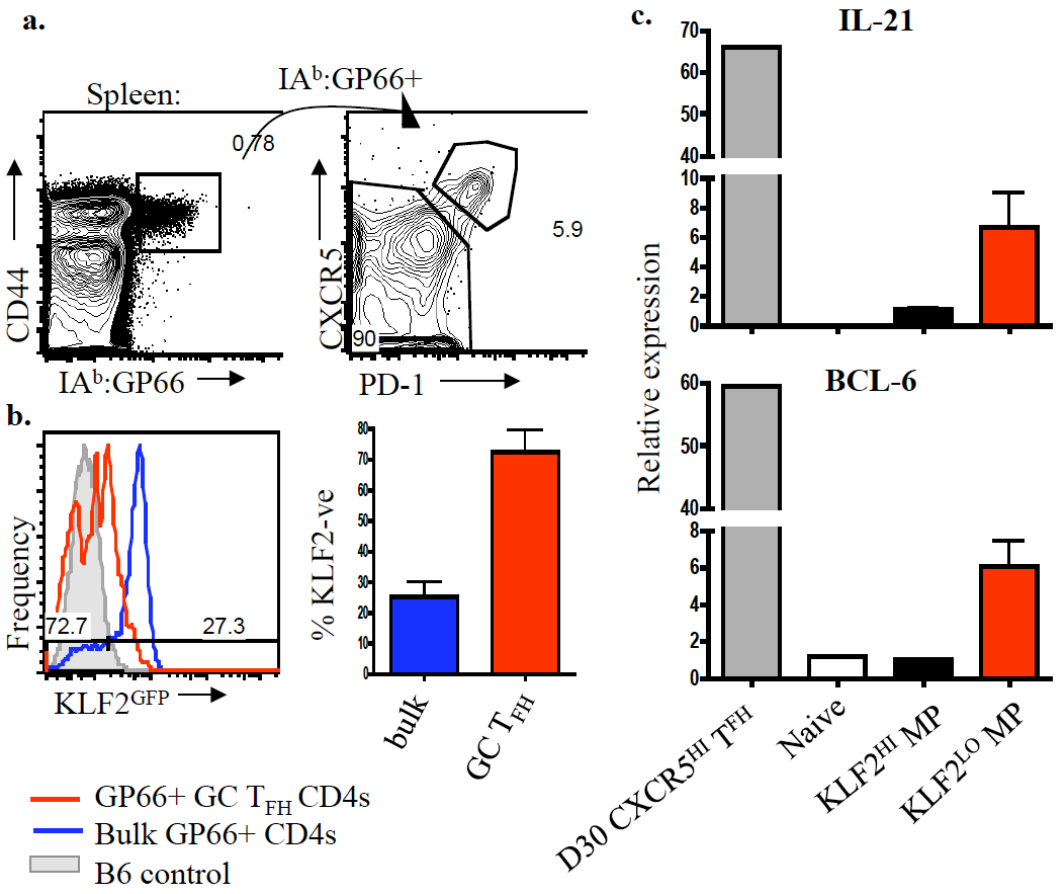

Figure 4-12. Germinal center CD4+ follicular helper T cells are $KLF2^{LO}$ and sorted $KLF2^{LO}$ CD4+ memory-phenotype T cells are enriched for T_{FH} transcripts. (a-b) $KLF2^{GFP}$ reporter mice were infected with LCMV and 20 days later analyzed for T_{FH} markers. (a) Gating strategy for responding $I:A^b$ GP66-80 tetramer+ cells (left) with the highest expression of CXCR5 and PD-1 (germinal center T_{FH}) (right). (b) $KLF2^{GFP}$ levels of bulk (blue) or GC T_{FH} (red) I:Ab GP66-80 tetramer+ cell compared to a WT B6 control (grey filled). Compiled percent KLF2-negative cells of bulk (blue) or GC T_{FH} (red) I:Ab GP66-80 tetramer+ cell is shown on the right. As described in Fig 4-3, RNA from sorted $KLF2^{HI}$ or $KLF2^{LO}$ MP CD4+ T cells was analyzed for T_{FH} markers with $KLF2^{HI}$ MP CD4+ T cells set at one.

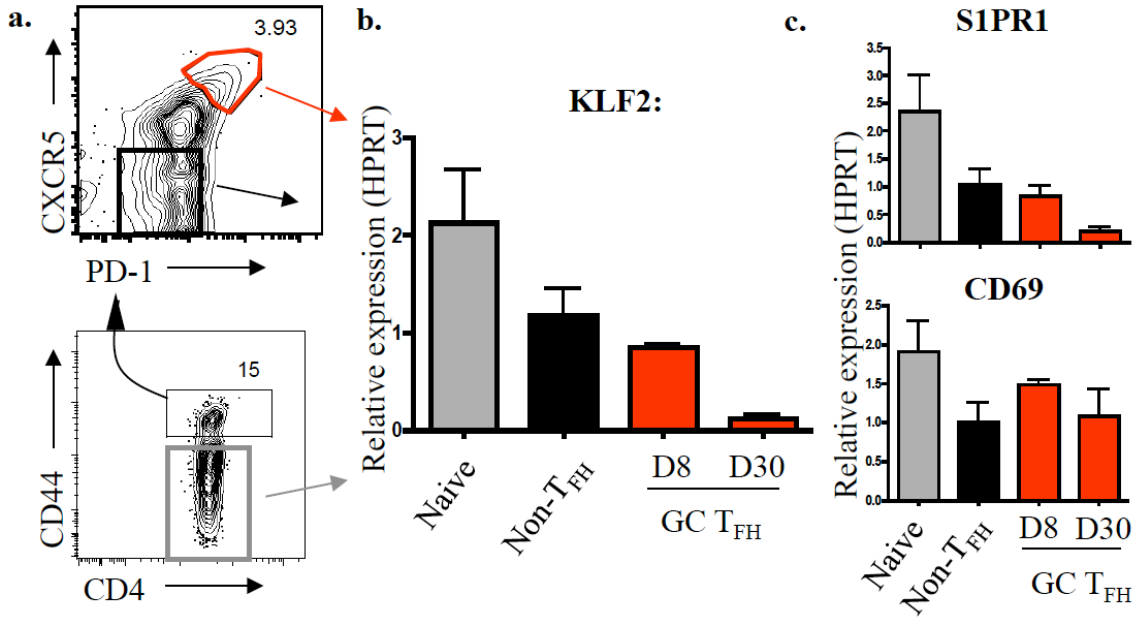

Figure 4-13. Germinal center CD4+ follicular helper T cells also have low KLF2 and S1PR1 mRNA levels. (a-c) WT mice were infected with LCMV and 8 or 30-33 days later splenocytes were sorted for $CD44^{LO}$ CD25- (naïve, grey), $CD44^{HI}$ $CXCR5^{LO}$ /PD-1^{LO} (non- T_{FH},,black), and $CD44^{HI}$ $CXCR5^{HI}$ /PD-1^{HI} (GC T_{FH}, red) populations. (a) Gating strategy for GC T_{FH} (red) and non- T_{FH} (black) (top) as well as naïve CD4s (grey, bottom). (b-c) KLF2 (b), S1PR1(c), and CD69(c) mRNA from sorted populations normalized to HPRT with non-TFH levels set as one.

$KLF2^{LO}$ CD4+ memory T cells do not egress from lymph nodes

Since germinal center T_{FH} are restricted to germinal centers and $KLF2^{LO}$ T cells would be expected to have decreased potential to leave lymph nodes, we sought to determine whether $KLF2^{LO}$ CD4+ memory T cells exhibited slower egress from lymph nodes compared with $KLF2^{HI}$ cells. To test this, we administered the lymph node entry blocking antibodies anti-αL (component of LFA-1 integrin) and anti-α4 (component of α4β7 integrin important for entry into mesenteric lymph nodes) to $KLF2^{GFP}$ reporter mice and analyzed various lymph nodes 24 hours after treatment. Blocking these

integrins inhibited T cells from tethering to the high endothelial vessels of lymph nodes, effectively eliminating the ability of T cells to enter lymph nodes through HEVs. By inhibiting the entrance of T cells into lymph nodes through the HEVs, we were able to monitor the number of CD4+ $KLF2^{LO}$ and $KLF2^{HI}$ memory T cell subsets in lymph nodes over time to determine the capacity of these populations to egress.

Blocking antibody had a pronounced decrease on the number of CD4+ naïve T cells compared to untreated controls in lymph nodes, while the number of CD4+ $CD44^{HI}$ T cells was unchanged in the bracial and axial lymph nodes (Fig 4-14a). This was not the case in the mesenteric lymph node for unknown reasons (Fig 4-14a). When subsetting CD4+ memory-phenotype T cells based on CD62L and KLF2 expression, it was determined that the number of $KLF2^{LO}$ CD4+ memory-phenotype T cells remained constant when entry blocking antibody was administered while the number of CD4+ CD62L+/ $KLF2^{HI}$ memory-phenotype T cells was slightly decreased (Fig 4-14b). Interestingly, the population of CD4+ $KLF2^{HI}$ CD62L- memory-phenotype T cells actually increased when blocking antibody was administered. While preliminary, these data suggest that, unlike naïve and CD62L+ memory-phenotype T cells, the $KLF2^{LO}$ CD4+ memory-phenotype T cells are not egressing within this timecourse.

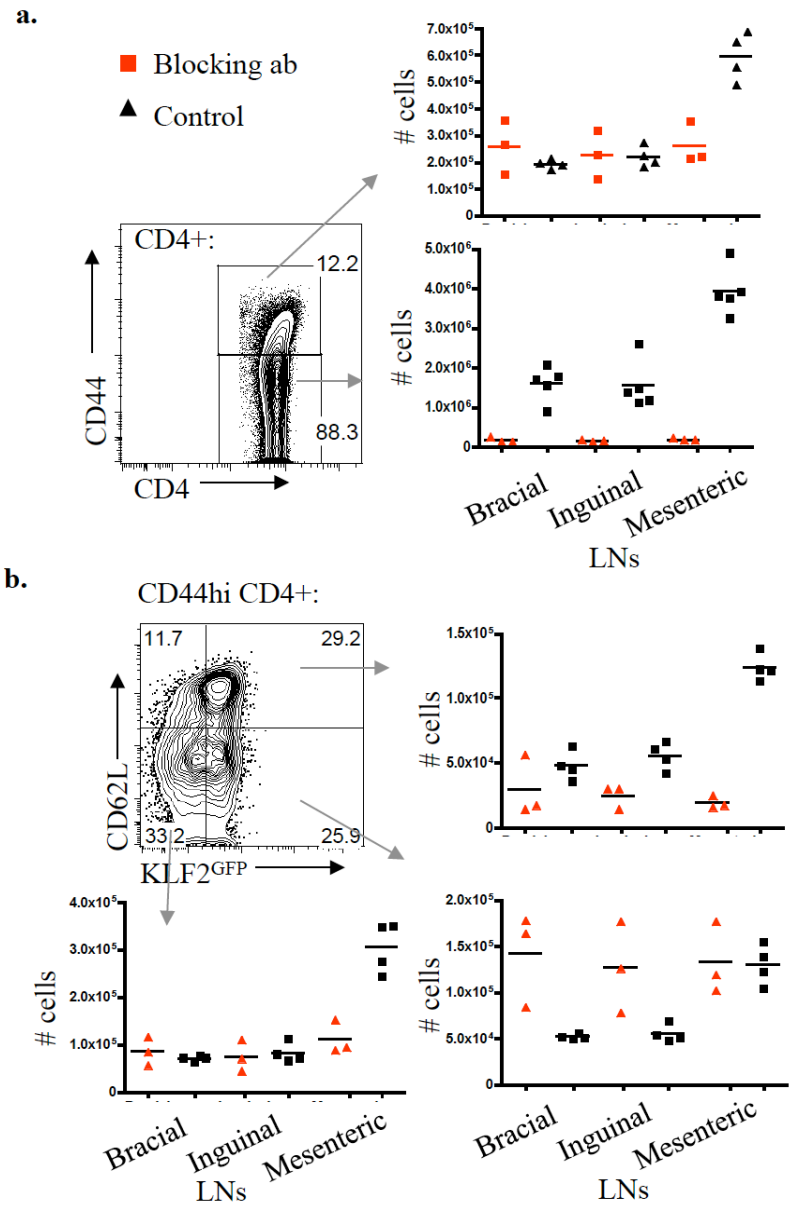

Figure 4-14. KLF2^{LO} CD4+ memory-phenotype T cells are not egressing. (a-b) 100ug of both anti-αL and anti-α4 integrin were administered IP to KLF2 reporter mice or PBS as a control. 48 hours later lymph nodes were harvested and CD4+ T cells were analyzed. (a) Number of CD44^{HI} memory-phenotype (top) or CD44^{LO} naïve (bottom) CD4+ T cells were quantified with (red) or without (black) blocking antibody. (b) Within the memory phenotype CD4+ T cell pool, CD62L+ KLF2^{HI} (top), CD62L- KLF2^{HI} (bottom right), and CD62L- KLF2^{LO} (bottom left) cell numbers were quantified with (red) and without (black) blocking antibody in each lymph node. N=3-4 from one experiment. In an additional experiment, two of the three mice receiving blocking antibody did not experience a decline in the number of CD4+ naïve T cells while the third mouse had data consistent with the results above.

Discussion

In this chapter we have defined a population of CD4+ memory T cells present in lymphoid tissue that lack the expression of the transcription factor KLF2. After investigation of a number of different variables that could contribute to the status of these cells, it appears that the $KLF2^{LO}$ CD4+ memory-phenotype T cells are comprised of various subsets of CD4+ memory T cells and not necessarily driven by one particular mechanism like we defined for the CD8+ T_{RM}. Instead of KLF2 status defining a new subset of CD4+ helper T cells, our data suggest KLF2 levels may reflect the trafficking capacity of a cell overlaying with already defined helper T cell subsets.

The majority of germinal center T_{FH} were shown to be $KLF2^{LO}$. Germinal center T_{FH} have been shown to localize to germinal centers and as such do not need to leave lymph nodes to exert their effector functions like other T cell subsets[15]. Since we demonstrated that CD4+ germinal center T_{FH} cells are KLF2 low and $KLF2^{LO}$ memory-phenotype cells are not egressing from lymph nodes, it may be that KLF2 downregulation is significant for the localization of CD4+ germinal center T_{FH} cells to germinal centers, or for allowing these cells to stay there once they have arrived. Experiments using forced KLF2 or S1PR1 could address this possibility. If cells that were forced to express KLF2 had dampened T_{FH} numbers, KLF2 would be shown to be significant for the localization and development of T_{FH}. Likewise, although perhaps less likely, knocking out KLF2 in activating CD4+ T cells and seeing whether a larger population of KLF2 T_{FH} form could also be informative.

Likewise, anergic CD4+ T cells based on FR4/CD73 expression also appeared $KLF2^{LO}$. In both T_{FH} and anergic T cells, it is likely that these cells are coming into contact with their cognate antigen:MHC complexes that may be responsible for KLF2 downregulation. In the case of anergic T cells that may be specific to self antigen, the downregulation of KLF2 may inhibit anergic T cells from migrating into the periphery and potentially causing tissue damage. While data from chapter 3 suggests downregulation of KLF2 in CD8+ T_{RM} in non-lymphoid tissues is likely driven by inflammatory cytokines, for CD4+ anergic T cells and T_{FH} KLF2 downregulation may be due to TCR engagement.

In CD8+ T_{RM}, surface expression of CD69 was likely the result of a decrease in S1PR1 levels since CD69 mRNA was equivalent between salivary glands and spleen while surface expression of CD69 was drastically different (Fig 2-2b, S2-1b). With CD4+ T cells, surface expression of CD69 on $KLF2^{LO}$ cells appears to be more complicated. In the context of systemic TLR agonism, surface CD69 expression was dependent on CD4+ T cells responding to IFNα/β, yet KLF2 downregulation was not. Likewise, during experiments addressing the stability of $KLF2^{LO}$ and $KLF2^{HI}$ CD4+ memory T cell subsets *in vitro*, KLF2 expression appeared to be relatively stable in $KLF2^{LO}$ cells while CD69 levels dropped down to baseline. These experiments start to unravel the association of surface CD69 upregulation with KLF2 downregulation in CD4+ T cells. While we never see CD69+ T cells that are not $KLF2^{LO}$ *in vivo*, *ex vivo* the inverse correlation begins to falter in certain conditions. Therefore, there may be an unknown factor present *in vivo* that is affecting CD69 upregulation that is independent of KLF2 levels leading to surface

CD69 expression. IFNα/β has been shown to transiently affect CD69 mRNA[113], so this may be a good candidate for this affect. At the same time, it may be that the factors that drive down KLF2 are not present during *in vitro* culture either. While KLF2 levels did not equilibrate *in vitro* when CD4+ memory T cells were sorted and cultured *in vitro*, there was a noticeable increase in KLF2 MFI. It may be that low levels of KLF2 may be enough to drive S1PR1 expression resulting in the hindrance of basal CD69 making it to the surface of sorted cells *in vitro*. Monitoring mRNA levels over time in CD4+ memory T cells sorted on KLF2 expression could shed light on this issue.

While Poly(I:C) transiently increases CD69 message, we did not see an increase in CD69 message when sorting $KLF2^{LO}$ memory-phenotype T cells. It is unclear what percentage of the $KLF2^{LO}$ population is driven by exposure to an IFNα/β rich environment, but this inconsistency suggests that this potential pathway leading to downregulation of KLF2 is unlikely the main driver of the $KLF2^{LO}$ subset. At this time it is unclear what factor is decreasing KLF2 in the context of systemic TLR agonism, but it does not appear to be IFNα/β specifically affecting CD4+ T cells.

This issue is particularly complicated because it is unknown what is driving low KLF2 expression in the $KLF2^{LO}$ CD4+ memory T cells. Stability and mRNA experiments suggest that the $KLF2^{LO}$ population is not transient, so it is unlikely that the KLF2 status is rapidly changing. Since the $KLF2^{LO}$ population is made up of more than one already defined subset of CD4+ T cells, it may be that different stimuli are driving the $KLF2^{LO}$ status in different CD4+ T cell subsets. Germinal center T_{FH} cells are expected to be exposed to their cognate antigen regularly during the germinal center

response[126], so it seems likely that TCR stimulation is what is driving low KLF2 expression levels in this population. While we were able to rule out the possibility that the $KLF2^{LO}$ CD4+ memory-phenotype T cells in the steady state recognized cognate antigen from commensal microbiota in the gut, $KLF2^{LO}$ CD4+ memory-phenotype T cells in the steady state of an animal may be the result of tolerized self-reactive CD4+ T cells. This would be consistent with anergic CD4+ T cells being $KLF2^{LO}$. If this were the case, these cells may be regularly encountering their cognate antigen resulting in KLF2 downregulation.

Yet similar to CD8+ T_{RM}, it is possible that a subset of cells falling into the $KLF2^{LO}$ population are the result of exposure to a stimuli separate from TCR engagement. We demonstrated that the environment produced during TLR agonist exposure is able to decrease KLF2 levels *in vivo* and *in vitro*. While preliminary data suggests direct IFNα/β responsiveness was not responsible for this, other inflammatory cytokines may be contributing. Indeed, preliminary data with IL-12/18 *in vitro* suggests these cytokines are also able to negatively affect $KLF2^{GFP}$ expression (data not shown). This is consistent with data in chapter 3 identifying inflammatory cytokines that lead to downregulation of KLF2 *in vitro*. Similarly, CD69 message is not upregulated in the bulk $KLF2^{LO}$ CD4+ memory-phenotype pool, suggesting recent TCR engagement is not the main result of KLF2 downregulation. Experiments using adoptive transfer of sorted CD4+ memory T cells based on KLF2 expression into MHCII KO mice could distinguish whether TCR engagement versus other stimuli are the main driver of KLF2 downregulation in the $KLF2^{LO}$ pool.

While it is unclear what is driving down KLF2 in the $KLF2^{LO}$ CD4+ T cells identified, administering lymph node blocking antibodies was instructive in understanding the trafficking potential of this subset. Experiments using blocking antibodies that inhibited cells from entering lymph nodes via high endothelial venules demonstrated that $KLF2^{LO}$ CD4+ memory T cells are not egressing from these organs, at least not in the timecourse analyzed and with respect to CD4+ naïve and CD62L+ memory-phenotype T cells (Fig 4-14). These preliminary data suggest that downregulation of KLF2 is significant for affecting the ability of these cells to leave the lymph node. Further research investigating the location of the $KLF2^{LO}$ CD4+ T cells using immunohistochemistry could be informative in understanding whether KLF2 levels are significant for micro-localization within lymphoid tissues.

At the same time, a population of $KLF2^{HI}$ CD62L- CD4+ memory-phenotype T cells actually increased when lymph node entry blocking antibodies were administered. While the reason for this is unclear, cells that enter lymph nodes through the afferent lymph may be able to fill up the space in lymph nodes created by the loss of naïve and CD62L+ T cells that are leaving but no longer entering the lymph node due to the administration of entry blocking antibodies. This experimental design does highlight that some cells are entering lymph nodes from alternative routes besides HEVs, which could be an interesting area of further research. The fact that CD62L negative cells are enriched in lymph nodes with blocked HEV entry suggests that this population has an enhanced capacity to enter lymph nodes in a unique pathway other than the HEVs. Follow-up

studies investigating this pathway and the CD62L- $KLF2^{HI}$ CD4+ T cell subset may be informative in understanding the trafficking patterns of CD4+ T cells.

While a few different mechanisms may lead to KLF2 downregulation in CD4+ memory T cells, including inflammatory cytokines and TCR engagement, we have shown that the result of low KLF2 expression is cellular retention in lymph nodes. This chapter identifies KLF2 as a transcription factor whose absence is significant for the trafficking potential and phenotypic characteristics of CD4+ T cells falling within already defined CD4+ T cell subsets.

Materials and methods

Mice.

C57BL/6 and CD45.1 congenic B6 mice were purchased from the National Cancer Institute and used at 6-8 weeks of age. $KLF2^{GFP}$ reporter mice were crossed to Smarta TCR transgenic mice (specific for the $I\text{-}A^b$ restricted LCMV $gp_{66\text{-}80}$ epitope and kindly provided by David Masopust's lab at the University of Minnesota) and IFNα/β receptor dominant negative mice (kindly provided by Matthew Mescher's lab at the University of Minnesota). Spleens from germ-free mice were provided by Sue Tonkonogy at the Gnotobiotic Core of the Center for Gastrointestinal Biology and Disease, College of Veterinary Medicine, North Caroline State University. For adoptive co-transfer studies, combinations of CD45.2, CD45.1 and CD45.1/CD45.2 mice were used for donor and host strains, to allow for discrimination of each donor population versus host cells. Animals were maintained under specific pathogen-free conditions at the University of Minnesota, and all experimental procedures were approved by the Institutional Animal Care and Use Committee.

Adoptive transfer and infections.

Splenocytes were prepared from $KLF2^{GFP}$ and congenic wild type smarta mice. The cell populations were mixed 1:1 and 25,000-45,000 CD4+ T cells were transferred into recipient B6 mice, which were infected the next day with $2x10^5$ PFU LCMV (Armstrong strain), via ip injection. Mice were maintained under BSL-2 housing and, at indicated times following infection, were sacrificed for analysis.

Flow cytometry and antibodies.

Single-cell suspensions were prepared and cells were resuspended at 3-6x10^7 cells/ml in FACS buffer (1% FBS, 0.1% sodium azide) and stained in 100ul. All additional fluorochome-conjugated antibodies were purchased from eBioscience, BD BioScience, R&D Systems, or BioLegend. For I-A^b:GP66-80+ tetramer staining, cells were stained at 1:100 for 1 hour at room temperature, followed by standard master mix staining on ice for 20-30minutes. For T_{FH} staining, cells were stained at 1:20 with anti-CXCR5 PE for 1 hour at room temperature during tetramer staining if applicable, spun down and subsequently stained for 20 minute on ice with the remaining antibodies. Likewise, CCR7 staining was also at 1:20 for 1 hour at room temperature. Cells were analyzed using a BD Pharmingen LSR II flow cytometer and data analyzed using FlowJo (TreeStar) software.

Quantitative RT PCR.

For CD4+ memory-phenotype RNA, spleen and lymph nodes from $KLF2^{GFP}$ reporter mice were negatively selected for CD4+ T cells using a CD4+ isolation Kit (Milenyi Biotec). CD44+ CD25- CD4+ T cells were sorted on a FACS Aria (Becton Dickinson) based on KLF2 expression into $KLF2^{HI}$ and $KLF2^{LO}$ populations. $CD44^{LO}$ naïve CD4+ T cells were also sorted for analysis.

For T_{FH} cell isolation, WT mice were infected with LCMV and 8 or 30-33 days later splenocytes were selected for CD4+ T cells using a CD4+ isolation Kit. $CD44^{LO}$

CD25- (naïve), CD25- CD44^{HI} CXCR5 ^{LO} /PD-1^{LO} (non- T_{FH}), or CD25- CD44^{HI} CXCR5 ^{HI} /PD-1^{HI} were sorted on a FACS Aria.

RNA was isolated using the RNeasy microkit (Qiagen) and reverse transcription was performed (qScript cDNA synthesis kit, Quanta Biosciences). Expression levels of genes were determined using the ABI 7700 sequence detection system and amplification was detected using the SYBR Green PCR Master Mix (Applied Biosystems). Cycle threshold values were normalized to a control gene (HPRT or GAPDH) to determine relative quantitative gene expression levels with naïve CD4+ T cells (Fig 4-3), KLF2^{HI} MP CD4+ T cells (Fig 4-12) or CD44+ CD4+ non-T_{FH} cells 30 days after LCMV (Fig 4-13) set at 1.

Gene:	Forward:	Reverse:
KLF2	ACCAACTGCGGCAAGACCTA	CATCCTTCCCAGTTGCAATGA
S1PR1	GTGTAGACCCAGAGTCCTGCG	AGCTTTTCCTTGGCTGGAGAG
CD69	TGGTCCTCATCACGTCCTTAATAA	TCCAACTTCTCGTACAAGCCTG
BCL-6	CCTGTGAAATCTGTGGCACTCG	CGCAGTTGGCTTTTGTGACG
IL-21	GCTCCACAAGATGTAAAGGGGC	GCTCCACAAGATGTAAAGGGGC
HPRT	CATTATGCCGAGGATTTGGAA	CACACAGAGGGCCACAATGT
GAPDH	TGGCCTACATGGCCTCCA	TCCCTAGGCCCCTCCTGTTAT

CD4+ memory T cell KLF2^{GFP} sort followed by *in vitro* culture or adoptive transfer *in vivo*.

For *in vitro* culture, spleen and lymph nodes from KLF2^{GFP} reporter mice infected >4 weeks earlier with LCMV were negatively selected for CD4+ T cells using a CD4+ isolation Kit (Milenyi Biotec). CD44+ CD25- CD4+ T cells were sorted on a FACS Aria (Becton Dickinson) based on KLF2 expression into KLF2^{HI} and KLF2^{LO} populations. CD44^{LO} naïve CD4+ T cells were also sorted for analysis. Aproximately 60,000 sorted

$KLF2^{HI}$, $KLF2^{LO}$, or naïve CD4+ T cells were added 1:5 (300,000 cells) with bulk congenically distinct uninfected splenocytes in 1 ml RP10/well of a 24 well tissue culture plate and cultured at 37°C. 0, 24 or 72 hours later cells were stained with I-A^b:GP66-80+ tetramer for 1 hour at room temperature followed by incubation with LIVE/DEAD Fixable Aqua Dead Cell Stain Kit (Invitrogen) for 15 min at 4°C to detect dying cells. Lastly, a cell surface antibody cocktail, including an antibody against a congenic marker to distinuish sorted cells, was stained for 20 minutes on ice.

For $KLF2^{GFP}$ sorting followed by adoptive transfer *in vivo* (Fig 4-6), sorting was on CD4+ memory-phenotype T cells from $KLF2^{GFP}$ reporter mice in the steady state instead of infected animals. Aproximately 150,000-300,000 sorted CD4+ memory-phenotype T cells were transferred into congenically distinct uninfected animals and 7 days later tissues were harvested. Cellular pull-down on anti-CD45.2 APC using a Miltenyi MACS column was performed to enrich for adoptively transferred cells before analysis.

***In vivo* and *in vitro* TLR agonist treatment.**

For Poly(I:C) *in vivo* treatment, 1mg/ml stock was heated to 50°C for 10 minutes and then allowed to cool. 10ug in PBS was injected IV into the tail vail and tissues were harvested 6 hours later. For LPS *in vivo* treatment, 50ug diluted in PBS was injected IV into the tail vail and tissues were harvested 24-25 hours later.

For the experiment using IFNα/β Receptor Dominant Negative (R DN) cells, 5x10^6 bulk lymph node cells from a IFNα/β R DN KO/KO and KO/WT $KLF2^{GFP}$ mice

were co-transferred into congenically distinct mice before Poly(I:C) adminitration. For the PBS control animal, IFNα/β R DN KO/KO cells from KLF2^{GFP} and WT mice were co-transferred as controls.

For *in vitro* culture with TLR agonists, 3x10^6 bulk splenocytes from a WT or KLF2^{GFP} mouse were cultured at 37°c with Poly(I:C) (10ug), IFNα/β (50u/ML), or anti-CD3/28 for a positive control in 1 ML RP-10 complete media in a 24 well flat bottom tissue culture plate. At various time points after culture, cells were stained with LIVE/DEAD Fixable Aqua Dead Cell Stain Kit (Invitrogen) for 15 min at 4°C to detect dying cells followed by a 15 minute surface stain before analyzing KLF2^{GFP} levels.

Sorted KLF2 populations followed by *in vitro* stimulation.

Spleens and lymph nodes from KLF2^{GFP} reporter mice infected with LCMV >30 days earlier were incubated with collagenase D (1mg/ml Roche applied science) at 37°C for 20 minutes. Negative selection for CD4+ T cells was then performed using a CD4+ isolation Kit (Milenyi Biotec) before sorting CD44^{HI} CD4+ T cells on KLF2 levels (FACS aria). Sorted samples were stained for IA^{b}:GP66-81 and the cultured *in vitro* with 10ug/ml gp61-80 peptide (or not for the no restimulation control) for 5 hours at 37°C. Cells were fixed with a fix/perm solution (eBioscience) followed by intracellular staining for IFNγ and IL-2.

Lymph node blocking antibody experiment: anti-αL and anti-α4 integrin treatment.

100ug of both anti-αL and anti-α4 integrin diluted in PBS was administered intraperitoneally to KLF2^{GFP} reporter mice (or PBS as a control) and 48 hours later inguinal, bracial, and mesenteric lymph nodes were isolated and quantified.

Chapter 5

Discussion

Conclusions

This thesis investigated heterogeneity in KLF2 expression in CD4+ and CD8+ effector and memory T cells with a focus on both lymphoid and non-lymphoid tissue. As further research defines the location of T cell subsets and the significance of cells being present at that location[63, 71, 73, 135-137], it is becoming clear that the integration of T cell migration and function is important for understanding the capacity a memory T cell has in contributing to the immune response against subsequent infections. Data in this thesis identifies KLF2 downregulation as significant for inhibiting T cell egress from both lymphoid and non-lymphoid tissue.

We identified two distinct T cell populations that had diminished KLF2 levels: CD8+ T_{RM} in non-lymphoid tissue (Fig 2-1) and CD4+ germinal center T follicular helper cells (Fig 4-12). For CD8+ T_{RM}, we demonstrated that inflammatory cytokines predominantly located in non-lymphoid tissue could downregulate KLF2 levels. This suggests local cytokine milieus can govern the downregulation of KLF2 in T cells leading to tissue residency. At the same time, TCR stimulation was shown to not be the universal mechanism of KLF2 downregulation in CD8+ T_{RM} establishing in all non-lymphoid tissue.

The mechanism causing the appearance of $KLF2^{LO}$ CD4+ memory T cells in lymphoid tissue is more complex and potentially more complicated. Due to the increased likelihood of both anergic and T_{FH} cells coming into contact with their cognate antigen, it is unclear whether cytokine exposure, TCR engagement, or another factor is leading to downregulation of KLF2 in CD4+ T cells. Further studies focusing on determining how

each of these factors are involved, including use of MHCII KO mice and potentially cytokine deficient mice, could shed light on how signals affect KLF2 and subsequent T cell trafficking in different CD4+ T cell subsets.

For CD8+ T cells, we showed that inflammatory cytokines can downregulate KLF2 through the P13K/AKT pathway. Many different cytokines may converge on the P13K/AKT pathway, allowing for the possibility of extensive cytokine diversity in different non-lymphoid tissues leading to similar downregulation of KLF2. Since each non-lymphoid tissue microenvironment is unique, the fact that downregulation of KLF2 functions through this pathway provides a common mechanism for the establishment of T_{RM} in diverse cytokine microenvironments. While CD103 upregulation has been shown to be important for CD8+ T cell retention in the gut[93], CD103 is not upregulated in many non-lymphoid tissues inhibiting the likelihood of this retention mechanism broadly applying to all non-lymphoid tissue. The fact that KLF2 is uniformly downregulated in the parenchyma of all non-lymphoid tissue provides a universal mechanism for the establishment of T_{RM} in non-lymphoid tissue. Since identification of transcription factors being involved in defining other T cell subset has been informative in previous research[110-112], the significance of low KLF2 expression in T_{RM} outlined in this thesis may similarly be important for further distinction of the T_{RM} pool.

For CD8+ T_{RM}, we were able to show the functional significant of KLF2 and S1PR1 downregulation for the establishment of T_{RM}. It will be informative to test whether KLF2 downregulation in CD4+ germinal center T_{FH} is also significant for the localization of this CD4+ T cell subset. Since a defining factor of germinal center T_{FH} is

their localization in the germinal center, identifying the factors leading to decreased egress of this population is important. While upregulation of CXCR5 has been shown to be important for the localization of T_{FH} [138-140], it may be that downregulation of KLF2 and S1PR1 is also important for allowing CD4+ T cells to remain in the lymph node and be positioned to develop into a germinal center T_{FH}.

When this project began, it was known that S1PR1 was essential for T cell egress from lymphoid tissue[38, 96], but its role in non-lymphoid tissue had not been extensively addressed. This thesis shows that transcriptional downregulation of S1PR1 by KLF2 was significant for the establishment of T_{RM} in non-lymphoid tissue. Surface CD69 is universally present on T_{RM} isolated from non-lymphoid tissue[93]. Due to the functional antagonism between CD69 and S1PR1[113], the mechanism that leads to dampened T_{RM} formation when forcing S1PR1 is not yet fully understood. It is possible that either 1. increased surface CD69 provides a retention signal allowing T_{RM} to stay embedded in non-lymphoid tissues or 2. S1PR1 provides an egress signal and therefore lack of surface S1PR1 results in the decreased ability of a T cell to egress from non-lymphoid tissues.

Either of these possibilities would result in diminished T_{RM} formation when forcing S1PR1, the former resulting in decreased surface CD69 due to competitive interaction with abundant S1PR1. If possibility number one is the accurate mechanism for T_{RM} retention, then the stimuli driving surface CD69 is relevant. Since CD69 message has been shown to be transiently increased in T cells during exposure to TLR agonists[113], it is possible that the mechanism driving increased surface CD69 is IFNα/β (or another, yet defined, cytokine) exposure leading to increased CD69 message. This would make

the downregulation of KLF2 inconsequential during the initial priming of T_{RM}, since lowered S1PR1 mRNA levels would not be needed if CD69 itself is upregulated.

However, in the context of CD8+ T_{RM}, this is not the case because while surface expression of CD69 was drastically different between the salivary glands and spleen (Fig S2-1b), CD69 message was unaltered (Fig 2-2b). Therefore, it is unlikely that retention of T_{RM} is due to increased surface CD69 driven by transcriptional upregulation of CD69 mRNA. It is still possible that increased surface CD69 is the result of decreased S1PR1. Further studies using CD69 deficient cells could distinguish whether CD69 is functioning as a retention mechanism versus S1PR1 as an egress signal in non-lymphoid tissue. If $CD69^{-/-}$ CD8+ T cells do not experience dampened T_{RM} formation compared with WT controls, one would have direct evidence of CD69 not being a significant retention mechanism for T_{RM}. At the same time, trafficking of $CD69^{-/-}$ T cells to non-lymphoid tissue may result in decreased T_{RM} residency due to any basal S1PR1 being present on the surface of a cell and subsequently leading to enhanced egress. Therefore, careful experimental designs are needed to parcel out the distinction between CD69 as a retention signal and S1PR1 as an egress signal in future studies.

Based on extensive research looking at S1PR1's role in T cell egress from lymphoid tissues[38, 96], it seems likely that the second listed possibility of diminished S1PR1 leading to decreased egress is the mechanism of T_{RM} retention. As proposed in chapter three, decreased KLF2 levels, potentially caused by inflammatory cytokine exposure and converging on the P13K/AKT pathway, could decrease S1PR1 and extinguish the egress signal allowing a cell to leave non-lymphoid tissue (Fig 3-14). In

this model, increased surface CD69 levels would be a result of basal CD69 making it to the surface of the cell due to the absence of its functional competitor S1PR1.

KLF2 levels drop very rapidly in responding CD8+ T cells migrating into the parenchyma of non-lymphoid tissue during viral infection (Fig 2-3). In fact, as soon as we could detect responding effector CD8+ T cells showing up in non-lymphoid tissue, KLF2 protein was already dropping. As highlighted in chapter two, this is the time when T_{RM} are forming as shown by the peak of T_{RM} happening 8 days after LCMV-armstrong infection (Fig 2-3d). Therefore, the rapid downregulation of KLF2 appears to be important for the initial arrest of CD8+ T cells in non-lymphoid tissue. At the same time, it may be that other retention mechanisms are involved in keeping T_{RM} embedded in non-lymphoid tissues after the initial T cell cessation caused by the lack of S1PR1. The chemokine receptor CCR7 has been shown to be important for T cell egress from non-lymphoid tissue as well[45, 46], so the downregulation of CCR7 may also be involved in inhibiting the exit of T_{RM} from non-lymphoid tissues. CD103 has already been mentioned as a retention signal in the gut[93], and other molecules may be identified that also contribute to T_{RM} retention.

It is unclear what mechanism is keeping KLF2 levels low after initial T_{RM} establishment. During infection, multiple inflammatory cytokines are upregulated in non-lymphoid tissue that could be involved in the initial downregulation of KLF2. After an infection is cleared, it may be that other cytokines maintain low KLF2 levels. This thesis focused primarily on the early establishment of T_{RM}, however further studies using

inducible models of S1PR1 or KLF2 could be informative in understanding the maintenance of T_{RM} residency.

In CD8+ T_{RM}, it appeared that KLF2 downregulation leading to the decrease in S1PR1 was the main driven of surface CD69 expression. With CD4+ T cells, CD69 surface expression on $KLF2^{LO}$ cells appears more complex. While CD69 message was unaltered in bulk CD4+ $KLF2^{LO}$ memory-phenotype T cells, it may be that a small percentage of cells falling in this subset were actually receiving TCR engagement and would be expected to have elevated CD69 message. Additional studies focusing on particular subsets falling in the $KLF2^{LO}$ pool could be informative in understanding what is driving low KLF2 expression in the heterogeneous $KLF2^{LO}$ CD4+ T cell pool.

This thesis focused on the downregulation of physiological levels of KLF2. To investigate the importance of this in CD8+ T_{RM}, we chose to force a target of KLF2, S1PR1, instead of forcing KLF2 itself. The reason for this was due to the fact that ectopic KLF2 overexpression forces cells out of the cell cycle[82, 83]. Therefore, with proliferation defects potentially prevalent in the experimental design, the interpretation of experiments using forced KLF2 could be difficult. Likewise, experiments using inducible knockout of KLF2 also have complications due to the necessity of S1PR1 for egress from lymphoid tissue. However, developing inducible models to force or knockout KLF2 could be informative, particularly in CD4+ T cell subsets. Inducibly knocking out or overexpressing KLF2 and analyzing it's affect on germinal center T_{FH} for instance, could establish whether KLF2 expression was significant for the localization of this subset.

Understanding how T cells remain in non-lymphoid tissue (in the case of T_{RM}) or in lymphoid tissue (particularly T_{FH}) is a significant step toward being able to develop therapeutics to target and enhance these populations. This thesis identified KLF2 and S1PR1 downregulation as significant for the establishment of T_{RM}. Our data suggest that induced downregulation of KLF2 or S1PR1 could be used as a method to efficiently enhance the formation of T_{RM} during vaccination. Further understanding of the retention mechanisms of T_{RM} and T_{FH} and how KLF2 and S1PR1 are involved could lead to new approaches to boost these populations.

Bibliography

1. Janeway, C., Vol. Seventh edition. (ed. P.T.a.M.W. Kenneth Murphy) (Garland Science, 2008).
2. Schenten, D. & Medzhitov, R. The control of adaptive immune responses by the innate immune system. *Adv Immunol* **109**, 87-124 (2011).
3. Medzhitov, R. Toll-like receptors and innate immunity. *Nat Rev Immunol* **1**, 135-145 (2001).
4. Janeway, C.A., Jr. & Medzhitov, R. Innate immune recognition. *Annu Rev Immunol* **20**, 197-216 (2002).
5. Islam, S.A. & Luster, A.D. T cell homing to epithelial barriers in allergic disease. *Nat Med* **18**, 705-715 (2012).
6. DiLillo, D.J., Horikawa, M. & Tedder, T.F. B-lymphocyte effector functions in health and disease. *Immunol Res* **49**, 281-292 (2011).
7. Sallusto, F., Geginat, J. & Lanzavecchia, A. Central memory and effector memory T cell subsets: function, generation, and maintenance. *Annu Rev Immunol* **22**, 745-763 (2004).
8. Treanor, B. B-cell receptor: from resting state to activate. *Immunology* **136**, 21-27 (2012).
9. Wang, L.D. & Clark, M.R. B-cell antigen-receptor signalling in lymphocyte development. *Immunology* **110**, 411-420 (2003).
10. McHeyzer-Williams, M.G. B cells as effectors. *Curr Opin Immunol* **15**, 354-361 (2003).
11. Guermonprez, P., Valladeau, J., Zitvogel, L., Thery, C. & Amigorena, S. Antigen presentation and T cell stimulation by dendritic cells. *Annu Rev Immunol* **20**, 621-667 (2002).
12. Rock, K.L. & Goldberg, A.L. Degradation of cell proteins and the generation of MHC class I-presented peptides. *Annu Rev Immunol* **17**, 739-779 (1999).
13. Nishana, M. & Raghavan, S.C. Role of recombination activating genes in the generation of antigen receptor diversity and beyond. *Immunology* **137**, 271-281 (2012).
14. Watts, C. Capture and processing of exogenous antigens for presentation on MHC molecules. *Annu Rev Immunol* **15**, 821-850 (1997).
15. Ma, C.S., Deenick, E.K., Batten, M. & Tangye, S.G. The origins, function, and regulation of T follicular helper cells. *J Exp Med* **209**, 1241-1253 (2012).
16. Rock, K.L., Farfan-Arribas, D.J. & Shen, L. Proteases in MHC class I presentation and cross-presentation. *J Immunol* **184**, 9-15 (2010).
17. Seder, R.A. & Ahmed, R. Similarities and differences in CD4+ and CD8+ effector and memory T cell generation. *Nat Immunol* **4**, 835-842 (2003).
18. Mescher, M.F. *et al.* Signals required for programming effector and memory development by CD8+ T cells. *Immunol Rev* **211**, 81-92 (2006).
19. June, C.H., Ledbetter, J.A., Gillespie, M.M., Lindsten, T. & Thompson, C.B. T-cell proliferation involving the CD28 pathway is associated with cyclosporine-resistant interleukin 2 gene expression. *Mol Cell Biol* **7**, 4472-4481 (1987).

20. Chen, L. & Flies, D.B. Molecular mechanisms of T cell co-stimulation and co-inhibition. *Nat Rev Immunol* **13**, 227-242 (2013).
21. Sharpe, A.H. Mechanisms of costimulation. *Immunol Rev* **229**, 5-11 (2009).
22. Curtsinger, J.M. *et al.* Inflammatory cytokines provide a third signal for activation of naive CD4+ and CD8+ T cells. *J Immunol* **162**, 3256-3262 (1999).
23. Bachmann, M.F. & Kopf, M. Balancing protective immunity and immunopathology. *Curr Opin Immunol* **14**, 413-419 (2002).
24. Obar, J.J., Khanna, K.M. & Lefrancois, L. Endogenous naive CD8+ T cell precursor frequency regulates primary and memory responses to infection. *Immunity* **28**, 859-869 (2008).
25. Moon, J.J. *et al.* Naive CD4(+) T cell frequency varies for different epitopes and predicts repertoire diversity and response magnitude. *Immunity* **27**, 203-213 (2007).
26. Bajenoff, M. *et al.* Highways, byways and breadcrumbs: directing lymphocyte traffic in the lymph node. *Trends Immunol* **28**, 346-352 (2007).
27. Itano, A.A. & Jenkins, M.K. Antigen presentation to naive CD4 T cells in the lymph node. *Nat Immunol* **4**, 733-739 (2003).
28. Gowans, J.L. The effect of the continuous re-infusion of lymph and lymphocytes on the output of lymphocytes from the thoracic duct of unanaesthetized rats. *Br J Exp Pathol* **38**, 67-78 (1957).
29. Rosen, S.D., Singer, M.S., Yednock, T.A. & Stoolman, L.M. Involvement of sialic acid on endothelial cells in organ-specific lymphocyte recirculation. *Science* **228**, 1005-1007 (1985).
30. Gallatin, W.M., Weissman, I.L. & Butcher, E.C. A cell-surface molecule involved in organ-specific homing of lymphocytes. *Nature* **304**, 30-34 (1983).
31. Xu, J., Grewal, I.S., Geba, G.P. & Flavell, R.A. Impaired primary T cell responses in L-selectin-deficient mice. *J Exp Med* **183**, 589-598 (1996).
32. Catalina, M.D. *et al.* The route of antigen entry determines the requirement for L-selectin during immune responses. *J Exp Med* **184**, 2341-2351 (1996).
33. Gunn, M.D. *et al.* A chemokine expressed in lymphoid high endothelial venules promotes the adhesion and chemotaxis of naive T lymphocytes. *Proc Natl Acad Sci U S A* **95**, 258-263 (1998).
34. Denucci, C.C., Mitchell, J.S. & Shimizu, Y. Integrin function in T-cell homing to lymphoid and nonlymphoid sites: getting there and staying there. *Crit Rev Immunol* **29**, 87-109 (2009).
35. Bargatze, R.F., Jutila, M.A. & Butcher, E.C. Distinct roles of L-selectin and integrins alpha 4 beta 7 and LFA-1 in lymphocyte homing to Peyer's patch-HEV in situ: the multistep model confirmed and refined. *Immunity* **3**, 99-108 (1995).
36. von Andrian, U.H. & Mempel, T.R. Homing and cellular traffic in lymph nodes. *Nat Rev Immunol* **3**, 867-878 (2003).
37. Pham, T.H. *et al.* Lymphatic endothelial cell sphingosine kinase activity is required for lymphocyte egress and lymphatic patterning. *J Exp Med* **207**, 17-27 (2010).

38. Matloubian, M. *et al.* Lymphocyte egress from thymus and peripheral lymphoid organs is dependent on S1P receptor 1. *Nature* **427**, 355-360 (2004).
39. Pappu, R. *et al.* Promotion of lymphocyte egress into blood and lymph by distinct sources of sphingosine-1-phosphate. *Science* **316**, 295-298 (2007).
40. Schwab, S.R. *et al.* Lymphocyte sequestration through S1P lyase inhibition and disruption of S1P gradients. *Science* **309**, 1735-1739 (2005).
41. Mandala, S. *et al.* Alteration of lymphocyte trafficking by sphingosine-1-phosphate receptor agonists. *Science* **296**, 346-349 (2002).
42. Luo, Z.J., Tanaka, T., Kimura, F. & Miyasaka, M. Analysis of the mode of action of a novel immunosuppressant FTY720 in mice. *Immunopharmacology* **41**, 199-207 (1999).
43. Tilney, N.L. Patterns of lymphatic drainage in the adult laboratory rat. *J Anat* **109**, 369-383 (1971).
44. Braun, A. *et al.* Afferent lymph-derived T cells and DCs use different chemokine receptor CCR7-dependent routes for entry into the lymph node and intranodal migration. *Nat Immunol* **12**, 879-887 (2011).
45. Bromley, S.K., Thomas, S.Y. & Luster, A.D. Chemokine receptor CCR7 guides T cell exit from peripheral tissues and entry into afferent lymphatics. *Nat Immunol* **6**, 895-901 (2005).
46. Debes, G.F. *et al.* Chemokine receptor CCR7 required for T lymphocyte exit from peripheral tissues. *Nat Immunol* **6**, 889-894 (2005).
47. McLachlan, J.B. *et al.* Mast cell-derived tumor necrosis factor induces hypertrophy of draining lymph nodes during infection. *Nat Immunol* **4**, 1199-1205 (2003).
48. Palframan, R.T. *et al.* Inflammatory chemokine transport and presentation in HEV: a remote control mechanism for monocyte recruitment to lymph nodes in inflamed tissues. *J Exp Med* **194**, 1361-1373 (2001).
49. Kunkel, E.J. & Butcher, E.C. Chemokines and the tissue-specific migration of lymphocytes. *Immunity* **16**, 1-4 (2002).
50. von Andrian, U.H. & Mackay, C.R. T-cell function and migration. Two sides of the same coin. *N Engl J Med* **343**, 1020-1034 (2000).
51. Reiss, Y., Proudfoot, A.E., Power, C.A., Campbell, J.J. & Butcher, E.C. CC chemokine receptor (CCR)4 and the CCR10 ligand cutaneous T cell-attracting chemokine (CTACK) in lymphocyte trafficking to inflamed skin. *J Exp Med* **194**, 1541-1547 (2001).
52. Hansson, M., Nygren, P.A. & Stahl, S. Design and production of recombinant subunit vaccines. *Biotechnol Appl Biochem* **32 (Pt 2)**, 95-107 (2000).
53. Mackay, C.R., Marston, W.L. & Dudler, L. Naive and memory T cells show distinct pathways of lymphocyte recirculation. *J Exp Med* **171**, 801-817 (1990).
54. Gebhardt, T., Mueller, S.N., Heath, W.R. & Carbone, F.R. Peripheral tissue surveillance and residency by memory T cells. *Trends Immunol* **34**, 27-32 (2013).
55. Woodland, D.L. & Kohlmeier, J.E. Migration, maintenance and recall of memory T cells in peripheral tissues. *Nat Rev Immunol* **9**, 153-161 (2009).

56. Klonowski, K.D. *et al.* Dynamics of blood-borne CD8 memory T cell migration in vivo. *Immunity* **20**, 551-562 (2004).
57. Sallusto, F., Lenig, D., Forster, R., Lipp, M. & Lanzavecchia, A. Two subsets of memory T lymphocytes with distinct homing potentials and effector functions. *Nature* **401**, 708-712 (1999).
58. Hikono, H. *et al.* Activation phenotype, rather than central- or effector-memory phenotype, predicts the recall efficacy of memory CD8+ T cells. *J Exp Med* **204**, 1625-1636 (2007).
59. Masopust, D., Vezys, V., Wherry, E.J., Barber, D.L. & Ahmed, R. Cutting edge: gut microenvironment promotes differentiation of a unique memory CD8 T cell population. *J Immunol* **176**, 2079-2083 (2006).
60. Chang, J.T. *et al.* Asymmetric T lymphocyte division in the initiation of adaptive immune responses. *Science* **315**, 1687-1691 (2007).
61. Harrington, L.E., Janowski, K.M., Oliver, J.R., Zajac, A.J. & Weaver, C.T. Memory CD4 T cells emerge from effector T-cell progenitors. *Nature* **452**, 356-360 (2008).
62. Stemberger, C. *et al.* A single naive CD8+ T cell precursor can develop into diverse effector and memory subsets. *Immunity* **27**, 985-997 (2007).
63. Masopust, D. & Schenkel, J.M. The integration of T cell migration, differentiation and function. *Nat Rev Immunol* **13**, 309-320 (2013).
64. Jameson, S.C. & Masopust, D. Diversity in T cell memory: an embarrassment of riches. *Immunity* **31**, 859-871 (2009).
65. Joshi, N.S. *et al.* Inflammation directs memory precursor and short-lived effector CD8(+) T cell fates via the graded expression of T-bet transcription factor. *Immunity* **27**, 281-295 (2007).
66. Mueller, S.N., Gebhardt, T., Carbone, F.R. & Heath, W.R. Memory T cell subsets, migration patterns, and tissue residence. *Annu Rev Immunol* **31**, 137-161 (2013).
67. Masopust, D. *et al.* Dynamic T cell migration program provides resident memory within intestinal epithelium. *J Exp Med* **207**, 553-564 (2010).
68. Wakim, L.M., Woodward-Davis, A. & Bevan, M.J. Memory T cells persisting within the brain after local infection show functional adaptations to their tissue of residence. *Proc Natl Acad Sci U S A* **107**, 17872-17879 (2010).
69. Hofmann, M. & Pircher, H. E-cadherin promotes accumulation of a unique memory CD8 T-cell population in murine salivary glands. *Proc Natl Acad Sci U S A* **108**, 16741-16746 (2011).
70. Gebhardt, T. *et al.* Memory T cells in nonlymphoid tissue that provide enhanced local immunity during infection with herpes simplex virus. *Nat Immunol* **10**, 524-530 (2009).
71. Jiang, X. *et al.* Skin infection generates non-migratory memory CD8+ T(RM) cells providing global skin immunity. *Nature* **483**, 227-231 (2012).
72. Mackay, L.K. *et al.* Long-lived epithelial immunity by tissue-resident memory T (TRM) cells in the absence of persisting local antigen presentation. *Proc Natl Acad Sci U S A* **109**, 7037-7042 (2012).

73. Schenkel, J.M., Fraser, K.A., Vezys, V. & Masopust, D. Sensing and alarm function of resident memory CD8(+) T cells. *Nat Immunol* **14**, 509-513 (2013).
74. Suzuki, T., Aizawa, K., Matsumura, T. & Nagai, R. Vascular implications of the Kruppel-like family of transcription factors. *Arterioscler Thromb Vasc Biol* **25**, 1135-1141 (2005).
75. Anderson, K.P., Kern, C.B., Crable, S.C. & Lingrel, J.B. Isolation of a gene encoding a functional zinc finger protein homologous to erythroid Kruppel-like factor: identification of a new multigene family. *Mol Cell Biol* **15**, 5957-5965 (1995).
76. Kuo, C.T., Veselits, M.L. & Leiden, J.M. LKLF: A transcriptional regulator of single-positive T cell quiescence and survival. *Science* **277**, 1986-1990 (1997).
77. Carlson, C.M. *et al.* Kruppel-like factor 2 regulates thymocyte and T-cell migration. *Nature* **442**, 299-302 (2006).
78. Rosen, H., Alfonso, C., Surh, C.D. & McHeyzer-Williams, M.G. Rapid induction of medullary thymocyte phenotypic maturation and egress inhibition by nanomolar sphingosine 1-phosphate receptor agonist. *Proc Natl Acad Sci U S A* **100**, 10907-10912 (2003).
79. Bai, A., Hu, H., Yeung, M. & Chen, J. Kruppel-like factor 2 controls T cell trafficking by activating L-selectin (CD62L) and sphingosine-1-phosphate receptor 1 transcription. *J Immunol* **178**, 7632-7639 (2007).
80. Sebzda, E., Zou, Z., Lee, J.S., Wang, T. & Kahn, M.L. Transcription factor KLF2 regulates the migration of naive T cells by restricting chemokine receptor expression patterns. *Nat Immunol* **9**, 292-300 (2008).
81. Weinreich, M.A. *et al.* KLF2 transcription-factor deficiency in T cells results in unrestrained cytokine production and upregulation of bystander chemokine receptors. *Immunity* **31**, 122-130 (2009).
82. Wu, J. & Lingrel, J.B. KLF2 inhibits Jurkat T leukemia cell growth via upregulation of cyclin-dependent kinase inhibitor p21WAF1/CIP1. *Oncogene* **23**, 8088-8096 (2004).
83. Buckley, A.F., Kuo, C.T. & Leiden, J.M. Transcription factor LKLF is sufficient to program T cell quiescence via a c-Myc--dependent pathway. *Nat Immunol* **2**, 698-704 (2001).
84. Takada, K. *et al.* Kruppel-like factor 2 is required for trafficking but not quiescence in postactivated T cells. *J Immunol* **186**, 775-783 (2011).
85. Schober, S.L. *et al.* Expression of the transcription factor lung Kruppel-like factor is regulated by cytokines and correlates with survival of memory T cells in vitro and in vivo. *J Immunol* **163**, 3662-3667 (1999).
86. Grayson, J.M., Murali-Krishna, K., Altman, J.D. & Ahmed, R. Gene expression in antigen-specific CD8+ T cells during viral infection. *J Immunol* **166**, 795-799 (2001).
87. Endrizzi, B.T. & Jameson, S.C. Differential role for IL-7 in inducing lung Kruppel-like factor (Kruppel-like factor 2) expression by naive versus activated T cells. *Int Immunol* **15**, 1341-1348 (2003).

88. Sinclair, L.V. *et al.* Phosphatidylinositol-3-OH kinase and nutrient-sensing mTOR pathways control T lymphocyte trafficking. *Nat Immunol* **9**, 513-521 (2008).
89. Kerdiles, Y.M. *et al.* Foxo1 links homing and survival of naive T cells by regulating L-selectin, CCR7 and interleukin 7 receptor. *Nat Immunol* **10**, 176-184 (2009).
90. Tzivion, G., Dobson, M. & Ramakrishnan, G. FoxO transcription factors; Regulation by AKT and 14-3-3 proteins. *Biochim Biophys Acta* **1813**, 1938-1945 (2011).
91. Fabre, S. *et al.* FOXO1 regulates L-Selectin and a network of human T cell homing molecules downstream of phosphatidylinositol 3-kinase. *J Immunol* **181**, 2980-2989 (2008).
92. Catalfamo, M. & Henkart, P.A. Perforin and the granule exocytosis cytotoxicity pathway. *Curr Opin Immunol* **15**, 522-527 (2003).
93. Casey, K.A. *et al.* Antigen-independent differentiation and maintenance of effector-like resident memory T cells in tissues. *J Immunol* **188**, 4866-4875 (2012).
94. Anderson, K.G. *et al.* Cutting edge: intravascular staining redefines lung CD8 T cell responses. *J Immunol* **189**, 2702-2706 (2012).
95. Bankovich, A.J., Shiow, L.R. & Cyster, J.G. CD69 suppresses sphingosine 1-phosophate receptor-1 (S1P1) function through interaction with membrane helix 4. *J Biol Chem* **285**, 22328-22337 (2010).
96. Cyster, J.G. & Schwab, S.R. Sphingosine-1-phosphate and lymphocyte egress from lymphoid organs. *Annu Rev Immunol* **30**, 69-94 (2012).
97. Rivera, J., Proia, R.L. & Olivera, A. The alliance of sphingosine-1-phosphate and its receptors in immunity. *Nat Rev Immunol* **8**, 753-763 (2008).
98. Liu, L. *et al.* Epidermal injury and infection during poxvirus immunization is crucial for the generation of highly protective T cell-mediated immunity. *Nat Med* **16**, 224-227 (2010).
99. Bevan, M.J. Memory T cells as an occupying force. *Eur J Immunol* **41**, 1192-1195 (2011).
100. Sheridan, B.S. & Lefrancois, L. Regional and mucosal memory T cells. *Nat Immunol* **12**, 485-491 (2011).
101. Ariotti, S., Haanen, J.B. & Schumacher, T.N. Behavior and function of tissue-resident memory T cells. *Adv Immunol* **114**, 203-216 (2012).
102. Masopust, D. & Picker, L.J. Hidden memories: frontline memory T cells and early pathogen interception. *J Immunol* **188**, 5811-5817 (2012).
103. Yusuf, I. & Fruman, D.A. Regulation of quiescence in lymphocytes. *Trends Immunol* **24**, 380-386 (2003).
104. Graler, M.H., Huang, M.C., Watson, S. & Goetzl, E.J. Immunological effects of transgenic constitutive expression of the type 1 sphingosine 1-phosphate receptor by mouse lymphocytes. *J Immunol* **174**, 1997-2003 (2005).
105. Moran, A.E. *et al.* T cell receptor signal strength in Treg and iNKT cell development demonstrated by a novel fluorescent reporter mouse. *J Exp Med* **208**, 1279-1289 (2011).

106. Zhang, Y.E. Non-Smad pathways in TGF-beta signaling. *Cell Res* **19**, 128-139 (2009).
107. Plas, D.R. & Thompson, C.B. Akt activation promotes degradation of tuberin and FOXO3a via the proteasome. *J Biol Chem* **278**, 12361-12366 (2003).
108. Miyazawa, K., Shinozaki, M., Hara, T., Furuya, T. & Miyazono, K. Two major Smad pathways in TGF-beta superfamily signalling. *Genes Cells* **7**, 1191-1204 (2002).
109. Tomura, M. *et al.* Monitoring cellular movement in vivo with photoconvertible fluorescence protein "Kaede" transgenic mice. *Proc Natl Acad Sci U S A* **105**, 10871-10876 (2008).
110. Ohkura, N., Kitagawa, Y. & Sakaguchi, S. Development and maintenance of regulatory T cells. *Immunity* **38**, 414-423 (2013).
111. Zhu, J. & Paul, W.E. Peripheral CD4+ T-cell differentiation regulated by networks of cytokines and transcription factors. *Immunol Rev* **238**, 247-262 (2010).
112. Rutishauser, R.L. & Kaech, S.M. Generating diversity: transcriptional regulation of effector and memory CD8 T-cell differentiation. *Immunol Rev* **235**, 219-233 (2010).
113. Shiow, L.R. *et al.* CD69 acts downstream of interferon-alpha/beta to inhibit S1P1 and lymphocyte egress from lymphoid organs. *Nature* **440**, 540-544 (2006).
114. Casey, K.A. *et al.* Antigen-independent differentiation and maintenance of effector-like resident memory T cells in tissues. *Journal of immunology* **188**, 4866-4875 (2012).
115. Sallusto, F. & Lanzavecchia, A. Heterogeneity of CD4+ memory T cells: functional modules for tailored immunity. *Eur J Immunol* **39**, 2076-2082 (2009).
116. Mosmann, T.R., Cherwinski, H., Bond, M.W., Giedlin, M.A. & Coffman, R.L. Two types of murine helper T cell clone. I. Definition according to profiles of lymphokine activities and secreted proteins. *J Immunol* **136**, 2348-2357 (1986).
117. Martinez, F.O., Sica, A., Mantovani, A. & Locati, M. Macrophage activation and polarization. *Front Biosci* **13**, 453-461 (2008).
118. Stout, R.D. & Bottomly, K. Antigen-specific activation of effector macrophages by IFN-gamma producing (TH1) T cell clones. Failure of IL-4-producing (TH2) T cell clones to activate effector function in macrophages. *J Immunol* **142**, 760-765 (1989).
119. Okoye, I.S. & Wilson, M.S. CD4+ T helper 2 cells--microbial triggers, differentiation requirements and effector functions. *Immunology* **134**, 368-377 (2011).
120. Korn, T., Bettelli, E., Oukka, M. & Kuchroo, V.K. IL-17 and Th17 Cells. *Annu Rev Immunol* **27**, 485-517 (2009).
121. Josefowicz, S.Z., Lu, L.F. & Rudensky, A.Y. Regulatory T cells: mechanisms of differentiation and function. *Annu Rev Immunol* **30**, 531-564 (2012).
122. Zhou, L., Chong, M.M. & Littman, D.R. Plasticity of CD4+ T cell lineage differentiation. *Immunity* **30**, 646-655 (2009).

123. Johnston, R.J. *et al.* Bcl6 and Blimp-1 are reciprocal and antagonistic regulators of T follicular helper cell differentiation. *Science* **325**, 1006-1010 (2009).
124. Nurieva, R.I. *et al.* Bcl6 mediates the development of T follicular helper cells. *Science* **325**, 1001-1005 (2009).
125. Yu, D. *et al.* The transcriptional repressor Bcl-6 directs T follicular helper cell lineage commitment. *Immunity* **31**, 457-468 (2009).
126. Crotty, S. Follicular helper CD4 T cells (TFH). *Annu Rev Immunol* **29**, 621-663 (2011).
127. Nakayamada, S., Takahashi, H., Kanno, Y. & O'Shea, J.J. Helper T cell diversity and plasticity. *Curr Opin Immunol* **24**, 297-302 (2012).
128. Schwartz, R.H. T cell anergy. *Annu Rev Immunol* **21**, 305-334 (2003).
129. Martinez, R.J. *et al.* Arthritogenic self-reactive CD4+ T cells acquire an FR4hiCD73hi anergic state in the presence of Foxp3+ regulatory T cells. *J Immunol* **188**, 170-181 (2012).
130. Hara, T., Jung, L.K., Bjorndahl, J.M. & Fu, S.M. Human T cell activation. III. Rapid induction of a phosphorylated 28 kD/32 kD disulfide-linked early activation antigen (EA 1) by 12-o-tetradecanoyl phorbol-13-acetate, mitogens, and antigens. *J Exp Med* **164**, 1988-2005 (1986).
131. Cosulich, M.E., Rubartelli, A., Risso, A., Cozzolino, F. & Bargellesi, A. Functional characterization of an antigen involved in an early step of T-cell activation. *Proc Natl Acad Sci U S A* **84**, 4205-4209 (1987).
132. Marzio, R., Mauel, J. & Betz-Corradin, S. CD69 and regulation of the immune function. *Immunopharmacol Immunotoxicol* **21**, 565-582 (1999).
133. Raetz, C.R. & Whitfield, C. Lipopolysaccharide endotoxins. *Annu Rev Biochem* **71**, 635-700 (2002).
134. King, C., Tangye, S.G. & Mackay, C.R. T follicular helper (TFH) cells in normal and dysregulated immune responses. *Annu Rev Immunol* **26**, 741-766 (2008).
135. Marelli-Berg, F.M., Cannella, L., Dazzi, F. & Mirenda, V. The highway code of T cell trafficking. *J Pathol* **214**, 179-189 (2008).
136. Marsal, J. & Agace, W.W. Targeting T-cell migration in inflammatory bowel disease. *J Intern Med* **272**, 411-429 (2012).
137. Cauley, L.S. & Lefrancois, L. Guarding the perimeter: protection of the mucosa by tissue-resident memory T cells. *Mucosal Immunol* **6**, 14-23 (2013).
138. Kim, C.H. *et al.* Subspecialization of CXCR5+ T cells: B helper activity is focused in a germinal center-localized subset of CXCR5+ T cells. *J Exp Med* **193**, 1373-1381 (2001).
139. Schaerli, P. *et al.* CXC chemokine receptor 5 expression defines follicular homing T cells with B cell helper function. *J Exp Med* **192**, 1553-1562 (2000).
140. Breitfeld, D. *et al.* Follicular B helper T cells express CXC chemokine receptor 5, localize to B cell follicles, and support immunoglobulin production. *J Exp Med* **192**, 1545-1552 (2000).